

**Human enteroids as a model for infectious disease**

Mayumi Kate Holly

A dissertation

submitted in partial fulfillment of the  
requirements for the degree of

Doctor of Philosophy

University of Washington

2019

Reading Committee:

Jason G. Smith, Chair

Lucas Hoffman

Kelly D. Smith

Program Authorized to Offer Degree:

Microbiology

©Copyright 2019

Mayumi Kate Holly

University of Washington

**Abstract**

Human enteroids as a model for infectious disease

Mayumi Kate Holly

Chair of the Supervisory Committee:

Associate Professor Jason G. Smith

Department of Microbiology

The human gastrointestinal (GI) tract is a major site of host-pathogen interactions. As such, many human pathogens have evolved to either use the GI tract as a portal of entry to gain access to distal sites in the body or cause acute disease within the GI tract. For many years we lacked a suitable cell culture system for modeling the epithelial cellularity of the human GI tract, thus our understanding of how the human intestinal epithelium responds to infection has been limited by previous models. Recently, a new system for culturing untransformed intestinal epithelial cells was developed, termed enteroids. Human enteroids are a powerful tool for understanding the complex interactions between human intestinal epithelial cells and enteric pathogens. We used human enteroids to investigate infection of intestinal epithelial cells by two important human pathogens, human adenovirus (HAdV) and *Salmonella enterica* subspecies *enterica* serovar Typhimurium (*S. Typhimurium*). Enteric HAdV are notoriously difficult to

culture *in vitro* despite being excreted in high numbers from infected individuals. We found that both prototype strains and clinical isolates of enteric and nonenteric HAdVs productively replicate in human enteroids. Additionally, we show that HAdV-5p, a respiratory pathogen, and HAdV-41p, an enteric pathogen, are both sensitive to type I and III interferons in human enteroid monolayers but not A549 cells, a transformed cell line commonly employed in adenovirology. And, HAdV-5p but not HAdV-41p was potently neutralized by the enteric human alpha-defensin HD5. Unique to enteroids is the diversity of intestinal epithelial cell types found in the gut, thus enteroids can reveal novel aspects of HAdV tropism. Intriguingly, HAdV-5p, but not HAdV-41p, preferentially infected goblet cells. These studies highlight new facets of HAdV biology that are uniquely revealed by primary intestinal epithelial cell culture.

To extend our studies on innate immune sensing in untransformed intestinal epithelial cells, we chose to study *S. Typhimurium*, another enteric pathogen. *S. Typhimurium* has been studied extensively in transformed cell lines, immune cells, and mice, but there is a dearth of knowledge on how *S. Typhimurium* infects and is sensed by human intestinal epithelial cells. We showed that *S. Typhimurium* elicits rapid and robust IL-18 secretion from untransformed intestinal epithelial cells compared to C2Bbe1 cells, a common transformed cell line derived from colorectal adenocarcinoma. Interestingly, IL-18 secretion is dependent on caspase-4, but not caspase-1 or caspase-5. Additionally, lack of caspase-4 in human enteroid monolayers resulted in increased intracellular colony forming units and increased numbers of intracellular bacteria per cell. These data indicate that caspase-4 is critical caspase for sensing and responding to *S. Typhimurium* infection, and plays a vital role in restricting intracellular bacterial numbers. Taken together, human enteroids uncovered novel and interesting aspects of enteric pathogen biology and intestinal epithelial innate immune responses.

## TABLE OF CONTENTS

|   |           |
|---|-----------|
| <b>LIST OF FIGURES .....</b>  | <b>6</b>  |
| <b>CHAPTER 1: INTRODUCTION.....</b>   | <b>9</b>  |
| <b>THE GASTROINTESTINAL TRACT.....</b>  | <b>9</b>  |
| <b>HOST DEFENSES IN THE GASTROINTESTINAL TRACT.....</b>   | <b>13</b> |
| <i>Physical barriers to infection.....</i>  | <i>13</i> |
| <i>Antimicrobial Peptides and Proteins.....</i>   | <i>13</i> |
| <i>Immune cell surveillance.....</i>  | <i>15</i> |
| <i>Intestinal Epithelial Defenses.....</i>  | <i>16</i> |
| <i>Microbiome and Colonization Resistance.....</i>  | <i>19</i> |
| <b>MODELS FOR STUDYING HOST-PATHOGEN INTERACTIONS IN THE GI TRACT.....</b>  | <b>22</b> |
| <b>CHAPTER 2: CHARACTERIZATION OF HUMAN ENTEROIDS.....</b>  | <b>24</b> |
| <b>INTRODUCTION.....</b>  | <b>24</b> |
| <b>RESULTS .....</b>  | <b>25</b> |
| <i>Human enteroids express markers of differentiated cell types.....</i>  | <i>25</i> |
| <b>DISCUSSION.....</b>  | <b>29</b> |
| <b>CHAPTER 3: ADENOVIRUS REPLICATION IN HUMAN ENTEROIDS.....</b>  | <b>30</b> |
| <b>INTRODUCTION.....</b>  | <b>30</b> |
| <b>RESULTS .....</b>  | <b>31</b> |
| <i>Infection and replication of prototype HAdV strains in cell lines.....</i>   | <i>31</i> |
| <i>Replication of prototype HAdV strains in human ileal enteroids.....</i>  | <i>36</i> |
| <i>Human enteroids support the replication of clinical isolates of human adenoviruses.....</i>                                    | <i>38</i> |
| <i>Interferon attenuates HAdV replication in enteroids.....</i>   | <i>40</i> |
| <i>HAdV-41p is resistant to the neutralizing activity of human enteric <math>\alpha</math>-defensin HD5.....</i>                  | <i>44</i> |
| <i>HAdV-5p preferentially infects Goblet cells over other non-Goblet cell types in human enteroids.....</i>                       | <i>44</i> |
| <b>DISCUSSION.....</b>  | <b>46</b> |
| <b>CHAPTER 4: SALMONELLA INDUCED INFLAMMASOME ACTIVATION IN HUMAN ENTEROIDS .....</b>   | <b>51</b> |
| <b>INTRODUCTION.....</b>  | <b>51</b> |
| <b>RESULTS .....</b>  | <b>60</b> |
| <i>Human enteroids express components of inflammasomes.....</i>   | <i>60</i> |
| <i>S. Typhimurium infection of human enteroids elicits robust and rapid IL-18 secretion.....</i>                                  | <i>62</i> |
| <i>S. Typhimurium-induced IL-18 secretion can be partially inhibited by peptide inhibitors of pro-inflammatory caspases.....</i>  | <i>65</i> |
| .....   | <i>67</i> |
| <i>IL-18 secretion by human epithelial cells in response to Salmonella Typhimurium is dependent on CASP4 activity.....</i>        | <i>69</i> |
| <i>Salmonella Typhimurium induced IL-8 expression is unaffected by CASP4 deficiency.....</i>                                      | <i>70</i> |
| <i>Salmonella Typhimurium replicates to higher intracellular levels in CASP4 deficient enteroids than WT human enteroids.....</i> | <i>74</i> |

|  |            |
|--|------------|
| <i>S. Typhimurium</i> hyper-replication is absent in untransformed intestinal epithelial cells....                   | 76         |
| <i>CASP4</i> restricts <i>S. Typhimurium</i> from replicating to high numbers in untransformed epithelial cells..... | 78         |
| <b>DISCUSSION.....</b>   | <b>81</b>  |
| <b>CHAPTER 5: SIGNIFICANCE AND FUTURE PERSPECTIVE .....</b>  | <b>90</b>  |
| <b>HUMAN ENTEROIDS AS A PLATFORM FOR STUDYING ENTERIC PATHOGENS .....</b>  | <b>90</b>  |
| <b>FUTURE PERSPECTIVES .....</b>   | <b>92</b>  |
| <b>SUPPLEMENT 1: PANETH CELLS .....</b>  | <b>96</b>  |
| <b>LOCATION AND SECRETORY FUNCTION OF PANETH CELLS .....</b>   | <b>96</b>  |
| <b>MODELS FOR STUDYING PANETH CELLS .....</b>  | <b>97</b>  |
| <b>INDUCING PANETH CELLS IN HUMAN ENTEROIDS .....</b>  | <b>99</b>  |
| <i>Expression of Wnt3 in human enteroids .....</i>   | <i>99</i>  |
| <i>Expression of Mist1 in human enteroids.....</i>   | <i>101</i> |
| <b>CHAPTER 6: MATERIALS AND METHODS .....</b>  | <b>105</b> |
| <b>COPYRIGHT PERMISSIONS .....</b>   | <b>121</b> |
| <b>BIBLIOGRAPHY .....</b>  | <b>123</b> |

## LIST OF FIGURES

|   |     |
|---|-----|
| FIGURE 1 SMALL INTESTINAL EPITHELIUM.....   | 12  |
| FIGURE 2 HUMAN INTESTINAL ENTEROIDS CONTAIN DIFFERENTIATED EPITHELIAL CELL TYPES FOUND IN THE SMALL INTESTINE.....                | 28  |
| FIGURE 3 INFECTION OF CELL LINES.....   | 33  |
| FIGURE 4 REPLICATION IN 293 $\beta$ 5 CELLS.....  | 35  |
| FIGURE 5 HAdVs REPLICATE IN ILEAL ENTEROIDS.....  | 37  |
| FIGURE 6 CLINICAL ISOLATES OF HAdVs REPLICATE IN UNDIFFERENTIATED ILEAL ENTEROIDS.....  | 39  |
| FIGURE 7 INTERFERON PRETREATMENT INHIBITS REPLICATION OF HAdV IN DIFFERENTIATED HUMAN ENTEROID MONOLAYERS BUT NOT A549 CELLS..... | 43  |
| FIGURE 8 HAdV-5p, BUT NOT HAdV-41p, IS NEUTRALIZED BY HD5 AND PREFERENTIALLY INFECTS GOBLET CELLS.....                            | 45  |
| FIGURE 9 INFLAMMASOME ACTIVATION.....   | 56  |
| FIGURE 10 HUMAN ENTEROIDS EXPRESS COMPONENTS OF INFLAMMASOMES.....  | 61  |
| FIGURE 11 S. TYPHIMURIUM REPLICATES IN AND INDUCES IL-18 SECRETION FROM INTESTINAL EPITHELIAL CELLS.....                          | 64  |
| FIGURE 12 IL-18 SECRETION IS DEPENDENT ON PRO-INFLAMMATORY CASPASE ACTIVITY.....  | 68  |
| FIGURE 13 IL-18 SECRETION IS DEPENDENT ON CASP4.....  | 73  |
| FIGURE 14 S. TYPHIMURIUM REPLICATES TO HIGHER INTRACELLULAR CFUs IN CASP4 KO ENTEROID MONOLAYERS.....                             | 75  |
| FIGURE 15 HYPER-REPLICATION IS ABSENT IN UNTRANSFORMED INTESTINAL EPITHELIAL CELLS.....   | 77  |
| FIGURE 16 CASP4 RESTRICTS INTRACELLULAR REPLICATION.....  | 80  |
| FIGURE 17 EXPRESSION OF MIST1 OR Wnt3 IS NOT SUFFICIENT TO INDUCE PANETH CELL DIFFERENTIATION                                     | 104 |

## ACKNOWLEDGEMENTS

Many people have contributed to this work through scientific expertise, encouragement, and support

I would like to thank Jason Smith for his mentorship and guidance throughout graduate school. I am immensely grateful for your help in making me a better scientist.

Members of my thesis committee: Luke Hoffman, Jenny Hyde, Nina Salama, and Kelly Smith. I would especially like to thank Luke Hoffman and Kelly Smith for being on my reading committee.

Members of the Smith lab, including Youngmee Sul, Karina Diaz, Mayim Wiens, and Sarah Wilson for their scientific discussions, support, both scientific as well as personal, and many happy hours after work.

Jenny Hyde and members of the Hyde lab for their suggestions during our joint lab meeting.

Leigh Knodler, Bruce Vallance, and Vivian Lee for reagents and technical expertise in *Salmonella* culture and infection models.

Mary Estes, Xi-Lei Zheng, and Victoria Tenge for reagents and technical expertise in enteroid culture.

Kaitlyn LaCourse and Phil Burke for being the best friends I could ever hope to have in my life.

Garrett Dean for being my adventurous life partner and encouraging me to get out of lab and have some fun.

The Lynn and Mike Garvey Imaging Core for providing access and technical expertise for confocal microscopy.

The University of Washington Department of Microbiology for the Neal Groman Award, Stanley Falkow Award, and the Helen Riaboff Whiteley Fellowship.

This work was supported in part by T32 GM007270

## **DEDICATION**

This thesis is dedicated to my parents, Julie and Rick, who have supported me through every step of my journey and have continuously encouraged my curiosity. And, to my sister, Lauren, for showing me just how much one can accomplish.

## **Chapter 1: Introduction**

### **The gastrointestinal tract**

The gastrointestinal (GI) tract is a complex organ system composed of the esophagus, stomach, small intestine, cecum, colon, and rectum. Each of these regions is morphologically and functionally discrete from the rest, and each organ is comprised of a unique composition of epithelial cells and antimicrobial defenses. Specifically, the small intestine and the colon perform separate operations during digestion, absorption of nutrients and absorption of water and consolidation of feces, respectively [1]. These different functions are reflected in their distinct architecture. The small intestine is subdivided into three segments termed the jejunum, duodenum, and ileum based on architecture and gene expression [2, 3]. Although these subdivisions have distinct structural features they are universally characterized by large absorptive villi that project into the lumen to increase surface area for absorption of nutrients from foods digested in the stomach (Fig 1) [2, 4]. These large villi are interspersed by invaginations in the intestinal wall called intestinal crypts (Fig 1). In contrast, the colon has no villi and is characterized by intestinal crypts connected by large flat luminal spaces [1].

Intestinal epithelial cells, which compose the intestinal epithelium lining the interior of both the small intestine and colon, are derived from intestinal stem cells located in the base of the intestinal crypts. Intestinal crypts contain two classes of multipotent intestinal stem cells:  $Lgr5^+$  crypt base columnar cells (CBCs) and +4 label retaining cells (LRCs) (Fig 1) [5].  $Lgr5^+$  CBCs undergo symmetrical division and stochastically become another CBC or a transit amplifying cell [6]. Of the subset of CBC daughter cells that become transit amplifying cells, some will differentiate into Paneth cells (only found in the small intestine) and remain in the crypt base. The remainder of the transit amplifying cells will migrate out of the stem cell compartment and

differentiate into one of the other intestinal epithelial cell types, including enterocytes, enteroendocrine cells, goblet cells, and tuft cells. Recent studies have shown that the +4 LRCs are transit amplifying cells that are precursors of Paneth cells and enteroendocrine cells [7]. This population is not well-defined by markers (*Bmi1*, *mTert*, *Hopx*, and *Lrig1*), because expression of these markers is not exclusive to the crypt base [8]. However, lineage tracing experiments, as well as studies on sensitivity to radiation treatment, have identified a population of cells at approximately the +4 position that retain label for a prolonged period of time, are actively cycling, and are sensitive to radiation damage. Thus, under normal conditions, Paneth cells and enteroendocrine cells differentiate from CBCs via the +4 LRCs; however, there is evidence for plasticity in the intestinal compartment whereby the +4 LRCs and even more committed lineages such as enterocytes can revert to a more stem cell state when the CBCs are lost due to damage [7, 9]. Inflammation and physical damage can also stimulate an expansion of the Paneth cell compartment [10, 11]. (Adapted from [12])

The intestinal epithelium is composed of a wide variety of intestinal epithelial cell types (Fig 1) that have distinct functions in both homeostasis as well as host-defense. Paneth cells secrete antimicrobial peptides and provide necessary signals for maintenance of the stem cell niche (as discussed above). Goblet cells secrete mucus to form the mucus layer in both the small intestine and colon. Tuft cells, which are present at mucosal surfaces inside and outside of the GI tract, only constitute approximately 0.4-2% of all intestinal epithelial cells, but are important in microbial sensing [13]. Additionally, Tuft cells can be divided into two transcriptionally distinct subtypes: Tuft-1 which express a neuronal signature and Tuft-2 which are characterized by eicosanoid biosynthesis expression [14]. Enteroendocrine cells are part of the same secretory lineage as goblet and tuft cells [4]. These cells secrete hormones and, like tuft cells, are

subdivided into separate classes based on the specific repertoire of hormones expressed.

Interestingly, these cells are susceptible to infection by rotavirus [15]. Finally, absorptive

enterocytes are the predominant cell type in the gut. Enterocytes absorb nutrients, electrolytes

and water from the lumen of the intestine [16].

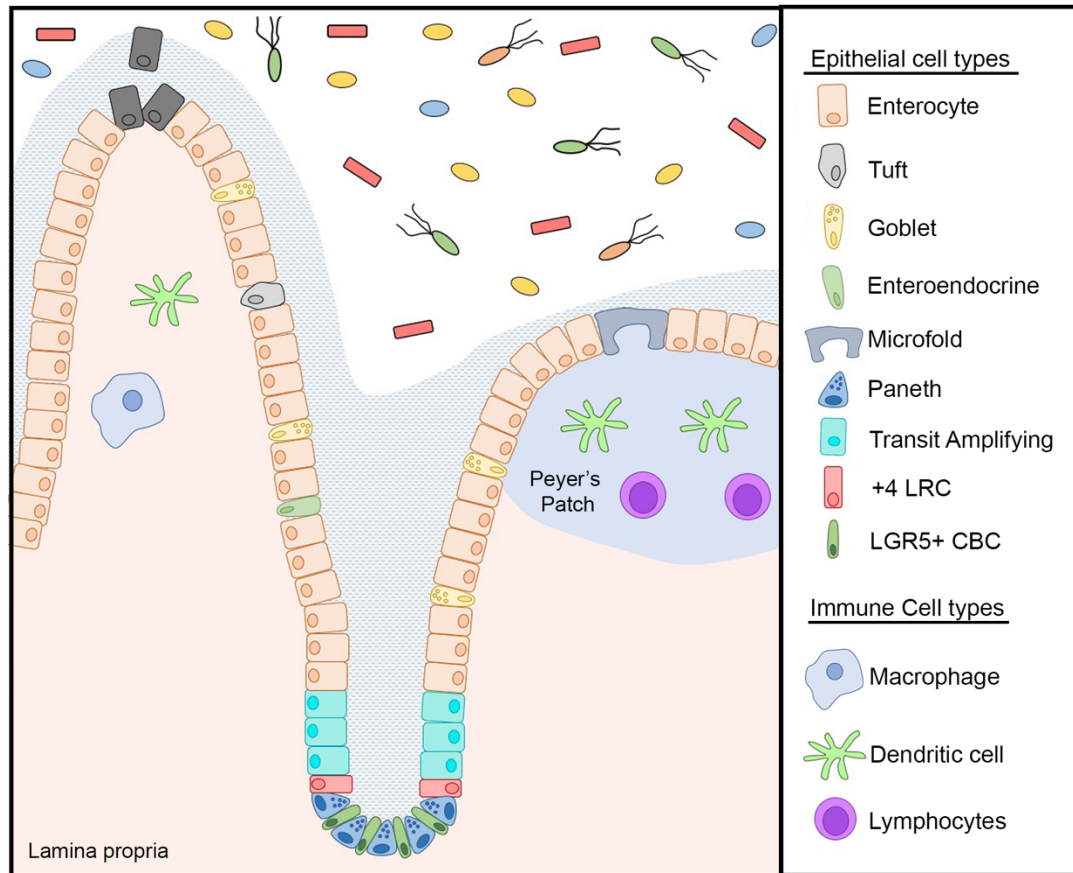


**Figure 1 Small intestinal epithelium.**

The small intestinal epithelium is composed of several different types of intestinal epithelial cells that form a barrier between the outside environment and the interior of the body. All intestinal epithelial cells are derived from LGR5+ stem cells in the crypt base. Daughter cells from the LGR5+ stem cells become transit amplifying cells and continue to differentiate as they move up the crypt-villus axis. Ultimately, mature intestinal epithelial cells are extruded from the villus tip. The intestinal epithelium is overlaid with a mucus layer produced by goblet cells in the intestinal epithelium. This mucus layer serves to protect the epithelium from the enteric microbiome.

## **Host defenses in the gastrointestinal tract**

### Physical barriers to infection

The intestinal epithelia in the small intestine and colon are overlaid by a mucus layer composed of mucins. Mucins are glycoproteins characterized by proline, threonine, and serine rich domains, which are adorned with *O*-linked glycans [17]. Mucins are divided into two different categories: transmembrane mucins and gel-forming mucins. The transmembrane mucins are predominantly expressed on the apical surface of enterocytes and make up the epithelial glycocalyx [18]. The exact function of transmembrane mucins is unknown, but likely contributes to preventing bacteria from interacting with the enterocyte cell surface. Gel-forming mucins are produced by goblet cells in the small intestine and colon. The small intestinal mucus layer formed by the gel-forming mucins is relatively porous and is attached loosely to epithelial cells [17]. A porous mucus layer is disadvantageous since it allows bacteria and other particulate matter to reach the intestinal epithelium but is a functional necessity as it permits for efficient absorption of nutrients [17]. The lack of mucus density is compensated for by the presence of antimicrobial peptides and proteins (discussed below). In contrast, the colon is coated by a thick layer of mucus that is divided into two sections [17]. The inner mucus layer is composed of dense layers of gel-forming mucus that are attached to the intestinal epithelium. The density of this layer restricts microbial access to the epithelium. Processing of this inner mucus layer by luminal proteases generates the looser outer mucus layer that functions in fecal compaction.

### Antimicrobial Peptides and Proteins

Antimicrobial peptides and proteins are abundantly expressed by the intestinal epithelium and protect the intestinal epithelium from bacterial, viral, and fungal infections. Human  $\beta$  defensins (HBDs) are small, cationic and amphipathic peptides that are broadly antibacterial. Only a fraction of the HBDs have been examined at the protein or transcriptional level [19, 20]. Although there are many reports of HBD transcripts in various tissues, in general, expression is restricted to keratinocytes of skin and epithelial cells of the genitourinary, gastrointestinal, and respiratory tracts [20, 21] [22]. HBD1 is constitutively expressed by most epithelial cells in the small intestine and colon, whereas HBD2 expression is induced and only detectable during infection or inflammation of the gut [21, 22]. Because the induction of HBD expression is driven by signaling pathways including innate immune sensors (e.g., TLRs), the differential expression of these sensors in tissues (e.g., lung versus gut) results in tissue-specific upregulation by particular ligands [22]. Both HBD1 and HBD2 are primarily active against Gram-negative bacteria, with limited activity against Gram-positive bacteria [21]. RegIII $\beta$  and RegIII $\gamma$  (HIP/PAP in humans) are antibacterial C-type lectins that target peptidoglycan of Gram-positive bacteria [23, 24].  $\alpha$ 1-antitrypsin is a serine protease inhibitor with some antimicrobial activity including inhibition of hemolysis by enteropathogenic *Escherichia coli* and *Cryptosporidium parvum* infection [19]. (Adapted from [12, 25])

Several types of antimicrobial peptides and proteins are packaged into and secreted via Paneth cell granules including enteric  $\alpha$ -defensins, lysozyme, secretory phospholipase A2 (sPLA<sub>2</sub>), angiogenin-4 (Ang4), RegIII $\gamma$ , and  $\alpha$ 1-antitrypsin. Collectively, these molecules have broad antimicrobial activity against a wide range of organisms. Enteric  $\alpha$ -defensins are the most abundant secreted product [26, 27]. Additionally, of the antimicrobial products packaged into Paneth cell granules, only  $\alpha$ -defensins have known anti-viral activity, which has been recently

reviewed [28, 29].  $\alpha$ -defensins are small, cationic, and amphipathic peptides with two  $\beta$ -sheets stabilized by three disulfide bonds [28, 30, 31]. Humans encode genes for two  $\alpha$ -defensins, human defensin 5 (HD5), and human defensin 6 (HD6), whereas mice encode over 25 different enteric  $\alpha$ -defensin genes, although only a subset is expressed abundantly in any given mouse strain [32]. The broad antimicrobial activity of HD5, including potent antiviral activity, is well documented [28, 29, 33, 34], while HD6 has a unique mode of action and functions by trapping bacteria and fungi [35]. (Adapted from [12])

The other antimicrobial constituents of the Paneth cell granules are not known to be active against viruses. Lysozyme is an enzyme that cleaves peptidoglycan in the cell walls of bacteria [5]. Mice encode two genes for lysozyme; one is expressed in Paneth cells and the other is expressed in macrophages [36]. In contrast, humans encode only one lysozyme gene that is expressed in both Paneth cells and macrophages. Human and mouse sPLA<sub>2</sub> catalyzes the hydrolysis of phospholipids and is bactericidal for Gram-positive, but not Gram-negative, bacteria [37, 38]. Mouse Ang4 is a bactericidal member of the RNase superfamily with activity against both Gram-positive and Gram-negative bacteria, although the human ortholog angiogenin is not localized to Paneth cells [39]. A naturally occurring peptide derived from this protein also has anti-HIV activity [40]. Paneth cells are the sole epithelial source within the intestine of  $\alpha$ -defensins [41], lysozyme [42], sPLA<sub>2</sub> [43], and Ang4 [39], but RegIII $\gamma$ , RegIII $\beta$ , and  $\alpha$ 1-antitrypsin are expressed by other epithelial cell types [44, 45]. (Adapted from [12])

### Immune cell surveillance

The lamina propria below the intestinal epithelium is occupied by resident immune cells. Cross-talk between the intestinal epithelium and resident immune cells occurs through a variety

of mechanisms. Gut associated lymphoid tissues (GALT) populates both the small intestine and colon of humans [46]. Within the small intestine, Peyer's patches form part of the GALT and are composed of aggregates of lymphoid follicles that underlie the follicle associated epithelium (FAE) [47]. This FAE is composed of microfold (M) cells (Fig 1), specialized intestinal epithelial cells, that transcytose particulate matter from the lumen to antigen presenting cells below. Peyer's patches always have germinal centers, demonstrating that the resident immune cells are constantly stimulated. This process can activate immune cells in the lamina propria if any danger associated molecular patterns are sensed. However, some pathogens, such as *Salmonella* and *Shigella*, have co-opted this homeostatic process to gain access to the basolateral side of the intestinal epithelium and resident immune cells [48, 49].

CD11c<sup>+</sup> dendritic cells can send up a transepithelial dendrites (TED) to sample the luminal contents. TEDs are rare under homeostatic condition but are evident upon infection or TLR stimulation, suggesting TEDs primarily function in response to infection rather than development of oral tolerance [50]. Similar to M cell transcytosis, TEDs can be a mechanism through which pathogens reach the lamina propria. *In vitro* dendritic cells can transcytose *Salmonella enterica* subspecies enterica serovar Typhimurium (*S. Typhimurium*) cross an epithelial monolayer [51]. Moreover, TEDs were present as soon as 30 min post-*S. Typhimurium* infection of ligated small intestinal loops [51]. How much TEDs contribute to restricting or facilitating pathogenic infection is unclear. Whether TEDs occur in the general dendritic cell population or is a specific subset is currently a matter of debate.

### Intestinal Epithelial Defenses

Many of the intestinal epithelial cells also function in host defense. Paneth cells (Fig 1) in the small intestine secrete antimicrobial peptides and proteins, such as defensins and lysozyme, which modulate the enteric microbiome composition as well as prevent bacterial and viral infection (discussed in depth above) [12]. Outside of their role in secretion of antimicrobial peptides, Paneth cells also play a key role in host defense by sensing microorganisms. There are numerous innate immune sensing pathways including inflammasomes, RIG-I-like receptors, and toll-like receptors (TLRs) [52]. The importance of TLR-mediated sensing of bacteria by Paneth cells has been specifically addressed. MyD88 is a signaling adaptor protein involved in transducing signals from TLRs, IL-1 receptor, and IL-18 receptor. Deletion of *MyD88* or expression of a dominant negative allele of *MyD88* results in decreased production of RegIII $\gamma$ , RELM $\beta$ , and RegIII $\beta$  by the intestinal epithelium and increased susceptibility to STm [53, 54]. *MyD88* expression was selectively reconstituted in Paneth cells of *MyD88*<sup>-/-</sup> mice through use of the Paneth cell-specific cryptdin-2 (CR2) promoter [53]. CR2-MyD88 transgenic mice infected with STm had fewer bacteria in their mesenteric lymph node compared to infected *MyD88*<sup>-/-</sup> mice, suggesting that Paneth cell intrinsic sensing and function is sufficient to restore the mucosal barrier. Interestingly, STm infection did not increase expression of the *MyD88*-dependent gene program in conventional mice, indicating that the microbiome stimulates Paneth cells to express antimicrobial genes. (Adapted from [12])

Although it was originally thought that goblet cells functioned only in physical defense of the intestine through production of the mucus layer, it has recently been appreciated that they have an additional role in modulation of the immune system. Under steady-state conditions goblet cells can expel their mucus granules via compound exocytosis, which is separable from regulated secretion of the granules [50]. The goblet cells then form goblet cell associated antigen

passages (GAPs) [50]. These GAPs perform endocytic functions by taking up particles from the lumen and transporting them to antigen presenting cells in the lamina propria. Both goblet cells and GAPs are necessary for development of tolerance to bacterial antigens in mice prior to weaning. These results suggest that GAPs are potentially involved in oral tolerance, which as yet unproven. GAPs, like M cells, have the potential to be co-opted by invading pathogens. While GAP formation is reduced during *S. Typhimurium* infection of mice, *S. Typhimurium* could localize to the remaining GAPs [55]. Interestingly, *S. Typhimurium* dissemination was enhanced when colonic GAP formation was induced [55]. Thus, goblet cells play essential roles in maintenance of the mucosal barrier, development of oral tolerance, and protection of the lamina propria from *S. Typhimurium* infection.

Tuft cells occupy only a fraction of the intestinal epithelial cell population [13] yet fulfill a vital role in response to parasitic infections [14]. Tuft cell modulation of the immune system occurs via group 2 innate lymphoid cells (ILC2s) in the lamina propria [14]. ILC2s function to integrate a diverse set of signals and alert the immune system upon disruption of homeostasis. Tuft cells activate ILC2s by producing IL-25. IL-25-activated ILC2s then secrete IL-13 which skews intestinal epithelial differentiation towards the tuft cell lineage, leading to tuft cell hyperplasia. Stimulation of tuft cells to initiate this feed-forward loop with ILC2s occurs through a unique mechanism. Unlike many cells which use toll-like receptor signaling to sense pathogens, Tuft cells have evolved to chemosense helminths and protists via taste receptor transduction [14]. Tuft cells do not express any of the canonical taste receptors yet express all of the other signal transduction components. Succinate receptor 1 (SUCNR1), which is expressed on tuft cells in the small intestine, has recently been identified as a receptor that induces tuft cell hyperplasia. Succinate is often produced by enteric pathogens that thrive in nutrient rich, but

oxygen poor environments. Thus, tuft cells have evolved to sense enteric pathogens via their unique chemotransduction pathways. Interestingly, although tuft cells play critical part in helminth infections, they were recently identified as the reservoirs for chronic murine norovirus infection in mice [56]. Although constituting but a fraction of the total intestinal epithelial cells, tuft cells play complex and diverse roles in epithelial homeostasis.

### Microbiome and Colonization Resistance

The intestinal microbiome is a complex milieu of bacteria, viruses, and protists. In recent years the intestinal microbiome has been intensively scrutinized to understand the interplay between shifts in the microbiome and disease. Our understanding of the role that the microbiome plays in disease susceptibility, development, and progression is in its infancy. It is clear that the microbiome can be host-protective. Many factors contribute to the composition of the microbiome, including host genetics, diet, drugs, and antimicrobial peptides and proteins, which are discussed below [57-59].

Diet can directly modulate the enteric microbiome. Consumption of particular nutrients can act as energy sources for members of the intestinal microbiome [57]. Expansion of particular genera of commensal bacteria can prevent invasion by pathogenic bacteria through competition for consumption of key nutrients or expression of antibacterial proteins [57 {Sorbara, 2019 #595}]. Additionally, diet can indirectly modify the microbiome through effects on gut health. Intraepithelial lymphocyte numbers, tight junctions, and goblet cell and Paneth cell function are all potentially impaired by the absence of key nutrients leading to modulation of the gut microbiome [57].

It has been known for a long time that antibiotic treatment of humans and other animals disrupts the microbiome. Humans treated with antibiotics are at risk of developing severe gastrointestinal infections from *Clostridium difficile*, *S. Typhimurium*, and *Shigella*. However, other drugs likely impact the microbiome. The microbiome can metabolize drugs and affect their absorption, potency, and toxicity [60]. These studies have strongly focused on how the microbiome affects the efficacy of the drug on mammalian disease, with little care for how these drugs are in turn modulating the population of the intestinal microbiome. A recent study found that non-antibiotic drugs from a wide-variety of different drug classes affected the growth of commensal bacteria *in vitro* [58]. Key producers of short chain fatty acids, which have roles in colonization resistance [61], immune tolerance [62], and potentially development of obesity, type 2 diabetes, and non-alcoholic fatty liver disease [63], were particularly sensitive to the non-antibiotic drugs tested [58]. Thus, human targeted drugs and antibiotics have profound effects on the gut microbiome that could impair colonization resistance.

Genetically susceptible mice orally infected with *S. Typhimurium* do not develop spontaneous enteritis but become chronically infected at distal sites [64]. This disease is reminiscent of *Salmonella enterica* subspecies *enterica* serovar Typhi (*S. Typhi*) infection of humans rather than acute gastroenteritis caused by *S. Typhimurium*. Disruption of the intestinal microbiome by antibiotic pretreatment makes mice susceptible to oral *S. Typhimurium* infection. Antibiotic pretreated mice infected with *S. Typhimurium* develop inflammation in both their cecum and colon. This broad-spectrum antibiotic treatment depleted butyrate-producing *Clostridia* in the gut [61]. Butyrate is oxidized by colonocytes to carbon dioxide, creating a hypoxic environment in the lumen that disfavors aerobic bacteria. Reduction in butyrate leads to increased oxygenation of the lumen and aerobic outgrowth of *S. Typhimurium*. Many more

examples of the commensal microbiome competing with pathogens to prevent colonization exist including, acidification of the environment and production of bacterial toxins (e.g. bacteriocins) [65], however these mechanisms will not be discussed further.

Paneth cell derived antimicrobial products directly affect the enteric microbiome. Two mouse models have been critical in understanding the impact of  $\alpha$ -defensins in particular on the composition of the host microbiome: *Mmp7*<sup>-/-</sup> mice and *DEFA5* transgenic mice [59]. MMP7 is produced by mouse Paneth cells and converts pro-defensins into mature enteric  $\alpha$ -defensins [66]. Thus, the *Mmp7*<sup>-/-</sup> mouse is a functional  $\alpha$ -defensin knockout in the ileum, although this is an imperfect model, because mature  $\alpha$ -defensins that result from processing by other luminal proteases can be recovered in the caecum and colon [67]. *DEFA5* transgenic mice express HD5 at levels comparable to native mouse enteric  $\alpha$ -defensins under the control of the human *DEFA5* promoter, which restricts expression to Paneth cells [68]. *Mmp7*<sup>-/-</sup> mice have an altered microbiome relative to wild-type littermate control mice with an increase in Firmicutes species and a decrease in Bacteroidetes species in the ileum [59, 69]. In contrast, *DEFA5* transgenic mice had a reciprocal change with a decrease in Firmicutes and an increase in Bacteroidetes. Interestingly, while *Mmp7*<sup>-/-</sup> mice were colonized by segmented filamentous bacteria (SFB), *DEFA5* transgenic mice lacked a detectable SFB population. Moreover, *DEFA5* transgenic mice and wild-type mice with low levels of SFB have fewer CD4<sup>+</sup> T cells expressing IL-17A than *Mmp7*<sup>-/-</sup> or wild-type mice with high levels of SFB. (Adapted from [12])

The mechanism of SFB modulating T cell development in the gut has been partially elucidated. Upon SFB-intestinal epithelial cell contact, which only occurs in the ileum, type 3 innate lymphoid cells secrete IL-22, which stimulates production of epithelial serum amyloid A proteins 1 and 2 (SAA1/2) from intestinal epithelial cells [70]. It is important to note that

SAA1/2 production could be due to SFB contact with intestinal epithelial cells or a combination of SFB contact and IL-22 signaling. SAA1/2 could then act directly upon Th17 cells. Thus, SFB colonization impacts Th17 effector functions in the GI tract, shaping not only the composition of the microbiome but also potentially the functionality of the GALT [59, 70, 71]. (Adapted from [12])

### **Models for studying host-pathogen interactions in the GI tract**

The GI tract represents the first line of defense against ingested pathogens and is, thus, a major site of host-pathogen interactions. Epithelial cells, which line the interior of the organs in the GI tract, are the first cellular barrier to infection. Intestinal epithelial cells in particular have been notoriously difficult to culture *in vitro*. Due to this fact, many studies have relied on short-lived intestinal explants, transformed cell lines derived from cancer, and mice to study host-pathogen interactions in the GI tract [72 {Randall, 2011 #588}]. While these models have provided invaluable information, they do not accurately represent the epithelial cellularity of the human GI tract.

Intestinal explants are segments of the intestine or purified intestinal crypts that can be cultured *in vitro* for short periods of time [33, 73]. Since this model is derived from tissue from patients or mice, they represent a source of primary, untransformed cells. However, intestinal explant and crypt cultures are not stable and can only be maintained for a short period of time. Although tissue derived from some parts of the GI tract can be cultured for almost 2 weeks, small intestinal tissue culture is limited to 24-48 h [73]. Similarly, purified small intestinal crypts for studying the activity of defensins [33] are rapidly undergoing cell death, thereby confounding any results.

To overcome the challenges of isolating primary intestinal epithelial cells, many researches have relied on transformed cell lines. However, transformed cells derived from cancer are phenotypically different from primary, untransformed cells [74], resulting in many caveats for these studies. Several human cell lines are commonly used to model host-pathogen interactions in the gut including Caco-2, C2Bbe1, HT-29, and T-87, which are all derived from colorectal cancers [75, 76]. Notably, no cell line derived from the human small intestine is in widespread use. The lack of a small intestinal cell line has resulted in a dearth of knowledge of how human small intestinal epithelial cells respond to infection. This is of particular note since the intestine is divided into five morphologically distinct segments that express different markers of differentiation and display distinct architecture [4]. Furthermore, it is difficult to extrapolate information gained from studies of colorectal cancer cells to different regions of the GI tract, since each region can be susceptible to different pathogens, have varied pathogen loads, and exhibit divergent host cell signaling and cytokine secretion.

Unlike cell lines, mice allow observation of more complex aspects of host-pathogen interactions in the gut. Additionally, mice are a genetically tractable model with the availability of many different knockout mouse lines for investigating the relative importance of different genes on infection. However, mice and humans differ significantly in a variety of ways including overall size, expression of innate immune genes, susceptibility to pathogens, microbiome composition, diet, metabolic rate, length of their GI tract, and adaptation different environmental conditions [64, 77-80]. Confounding many studies in mice is the resistance of mice to many relevant human pathogens via the natural route of infection [81] leading to use of high pathogen doses, alternative routes of infection or other mechanisms to promote susceptibility. For example, *S. Typhimurium* causes self-limiting diarrhea in humans, but in mice causes a

disseminated disease similar to typhoid unless the microbiome is disrupted by antibiotic treatment [64]. Therefore, findings in mice do not always recapitulate what occurs in humans, and it is important to have a system that more accurately models the human GI tract.

Until recently, with the exception of limited studies of short-lived intestinal explants or crypt preparations, intestinal epithelial cells could only be studied *in vivo* due to a lack of a long-term culture system. In 2009, pioneering work by the Clevers group established a new model for culturing primary intestinal epithelial cells *in vitro*, termed enteroids [82], which are discussed in depth in Chapter 2. An additional method to culture untransformed intestinal epithelial cells is accomplished through differentiation of induced pluripotent stem cells (iPSC) into 3D structures that contain intestinal epithelial cells [83]. These iPSC derived structures are termed organoids, whereas those derived from adult intestinal epithelial cells are referred to as enteroids [84]. Distinct from enteroids which show similar expression profiles to fresh crypts [85], human intestinal organoids are more similar to fetal adult small intestinal tissue [86]. Moreover, human intestinal organoids are composed of both the intestinal epithelium and outer layer of mesenchymal cells [83]. Both human enteroids and human intestinal organoids have been used to study host-pathogen interactions [15, 87-91].

## **Chapter 2: Characterization of human enteroids**

### **Introduction**

Human enteroids are three-dimensional structures that consist of primary, untransformed intestinal epithelial cells and recapitulate much of the cellularity of the GI tract [92, 93].

Intestinal crypts, which contain the intestinal stem cells, are isolated from the intestine and cultured *in vitro* in an extracellular matrix. The intestinal crypts self-organize to form a sealed structure. The interior of the enteroid is topologically equivalent to then interior of the intestine.

Although they are untransformed, enteroids can be genetically manipulated, maintained in culture for extended periods of time, and cryopreserved to establish a repository [93, 94]. The enteroids are differentiated into mature epithelial cell types found in the gut and maintain characteristics unique to the tissue from which they are derived [3, 85, 93]. (Adapted from [87])

## Results

### Human enteroids express markers of differentiated cell types

Human enteroid cultures were established from normal human deidentified ileal tissue obtained from surgical resections. Enteroids were propagated in a largely undifferentiated state in medium containing specific growth factors and small molecules; however, to recapitulate the cellular composition of the mature intestinal epithelium, the medium formulation was modified to promote differentiation. Since human small intestinal enteroid culture is not standardized, we characterized differentiation under our culture conditions, which were derived from published protocols [92, 93, 95]. We observed consistent upregulation of markers for mature enterocytes (solute carrier family 10 member 2, encoded by *SLC10A2*) and goblet cells (trefoil factor 3, *TFF3*) after 5 days in differentiation medium compared to undifferentiated enteroids in multiple independent cultures from two separate donors, HIE5 (Fig. 2A) and HIE3 (Fig. 2B).

Upregulation of the enteroendocrine cell marker chromogranin B (*CHGB*) was more consistent in samples from one donor than the other. Expression of a Paneth cell-specific gene (human defensin 5, *DEFA5*) was undetectable in all samples on day 1 and detected in only 3 of 6 replicates on day 5 for human ileal enteroid 5 (HIE5) but in all 4 replicates for human ileal enteroid 3 (HIE3) (Fig. 2A and B). It is unclear why there is variability in *CHGB* and *DEFA5* expression within and between cultures of human enteroids. (Adapted from [87])

Human enteroids contain morphologically distinct intestinal epithelial cell types

As has been observed by others [15], the enteroids within a single sample exhibited heterogeneous morphology with approximately 40% of differentiated human enteroids forming budding structures (Fig. 1D, top) reminiscent of the crypt-villus axis of the small intestine, while the other 60% formed small, dense cystic structures without overt budding (Fig. 1D, bottom). A single-cell-thick epithelium with polarized nuclei was apparent by hematoxylin and eosin (H&E) staining in all cases (Fig. 1E). Mature, functional goblet cells were identified as cells with large cytoplasmic vacuoles by H&E (Fig. 1E) or were positive for periodic acid-Schiff (PAS) staining in enteroids with both morphologies (Fig. 1F). PAS-positive debris was also found in the lumen, indicating goblet cell secretion. Notably absent in these cultures were cells with the distinct morphology of Paneth cells, even in samples where expression of the Paneth cell-specific gene *DEFA5* was robust. (Adapted from [87])

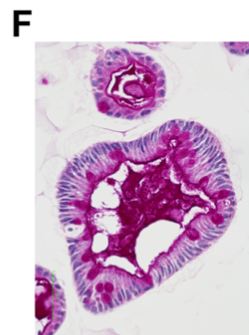
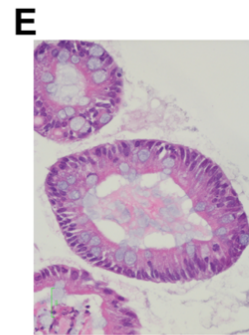
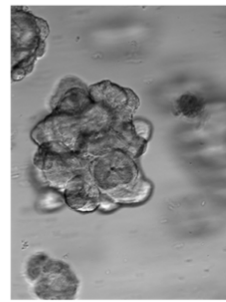
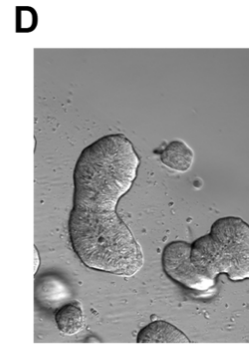
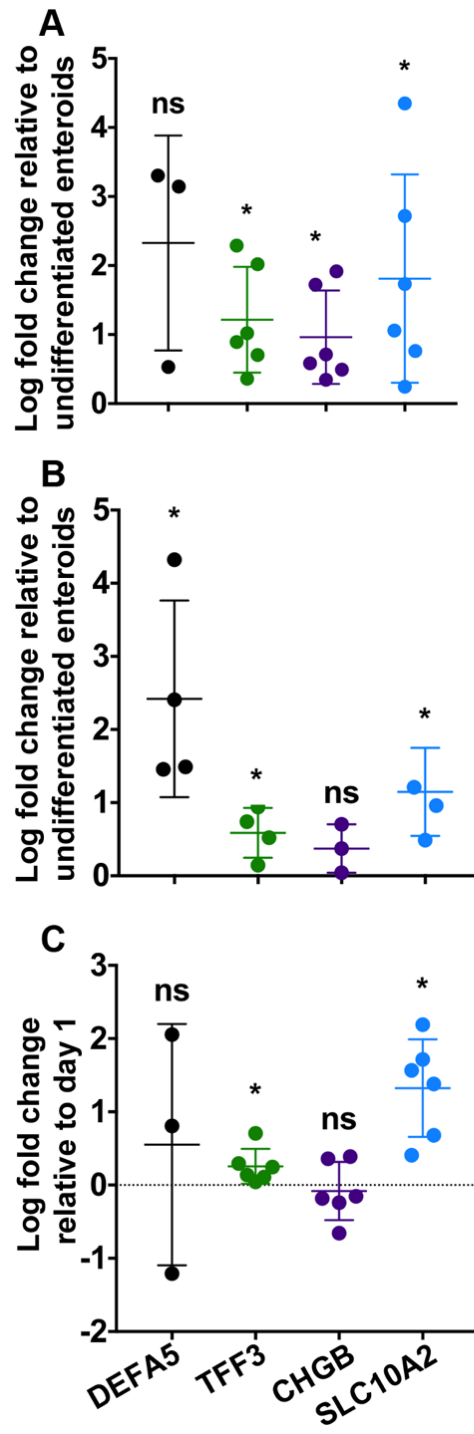


**Figure 2 Human intestinal enteroids contain differentiated epithelial cell types found in the small intestine**

Expression of human defensin 5 (*DEFA5*, Paneth cells), trefoil factor 3 (*TFF3*, goblet cells), chromogranin B (*CHGB*, enteroendocrine cells), and a bile acid transporter (*SLC10A2*, enterocytes) in differentiated HIE5 (A), differentiated HIE3 (B), and differentiated monolayers derived from HIE5 (C). For panels A and B, log fold increase in gene expression was calculated by comparing gene expression on day 5 to undifferentiated enteroids. For panel C, log fold increase in gene expression was calculated by comparing gene expression on day 5 to day 0 post-plating. Each dot is an independent biological replicate. Note that although all 4 of the samples in panel B had detectable *DEFA5* expression, this was true for only 3 of 6 samples in panel A and 2 of 6 samples in panel C. Individual replicates are plotted with the mean values  $\pm$  standard deviations (SD) for each gene. (D) Bright-field images of differentiated enteroids representative of morphology with (top) and without (bottom) budding (4X objective). (E and F) Representative images of hematoxylin and eosin-stained (E) and periodic acid-Schiff-stained (F) differentiated human ileal enteroids (40X objective). For panels A to C, data were analyzed using a one-sample *t* test, \*,  $P < 0.05$ ; ns, not significant.

## Discussion

Human enteroids provide a unique opportunity to investigate host-pathogen interactions in an *in vitro* system that more accurately represents the cellularity of the GI tract. They are composed of untransformed cells, which have intact signal transduction pathways, and contain a mixture of mature, differentiated intestinal epithelial cell types [92]. Both of these features are absent from standard cell lines. Our medium conditions for culturing human enteroids combine elements from several previously published formulations [92, 93, 95]. Human enteroids differentiated under our conditions contain upregulated transcriptional markers of enterocytes, enteroendocrine cells, and goblet cells and distinct morphology of a polarized epithelium with functional goblet cells. However, expression of both the Paneth cell marker *DEFA5* and the enteroendocrine cell marker *CHGB* were the most variable. Previous reports by others [15] have shown enteroendocrine cells, indicating that they are likely present in enteroids. It is unclear why expression of *CHGB* is variable, however it could be explained by low percentages within in the enteroid populations. Although we have also tried a variety of different published medium compositions, we have only rarely identified Paneth cell morphology by histology even in samples with robust *DEFA5* expression. Because Wnt-dependent expression of *DEFA5* is separable from the gene program required for Paneth cell morphology [26, 96, 97], it is likely that the culture of human enteroids lacks a key component required for Paneth cell morphology. This has also been noted by others [98]. Nonetheless, we have validated suitable conditions for stable culture, prolonged passage, and differentiation of human enteroids. (Adapted from [87])

## **Introduction**

Human adenoviruses (HAdV) are a family of DNA viruses that are important human pathogens, causing a wide variety of diseases, including respiratory infections, conjunctivitis, cystitis, and gastroenteritis [99]. Much of our understanding of adenovirus replication and host interaction is due to studies of human adenovirus 5 (HAdV-5), a serotype of species C (HAdV-C). However, HAdV-F serotypes (HAdV-40 and -41), which are common causes of childhood gastroenteritis [100], differ significantly from HAdV-C [101, 102]. They encode two different fiber proteins (long and short) [103], and their penton base proteins lack the canonical RGD sequence used by all other known HAdV serotypes for binding to integrin coreceptors [104]. The importance of these unique features for cell entry and pathogenesis is unresolved, largely due to an inability to grow either prototype strains or clinical isolates of HAdV-F serotypes to high titers in standard transformed cell lines or non-intestinal primary cells [102, 105, 106]. (Adapted from [87])

HAdV-F species are naturally tropic for the gastrointestinal (GI) tract [107]. More broadly, the GI tract is a site of infection and replication leading to intermittent shedding and persistence of HAdV serotypes that cause disease at other sites (e.g., the respiratory tract) or have no known disease association [100, 108, 109]. In this regard, virus watch programs in Seattle and New York during the 1960s documented fecal shedding of respiratory serotypes of HAdV that were known at that time, including HAdV-1, -2, -3, and -5 [108, 109]. HAdV-C and -D are also frequently isolated from fecal samples of HIV patients [110], and HAdV-D has been found at high prevalence in diarrheal samples from children [110-112]. Thus, in addition to HAdV-A and -F, which have strong causative associations with childhood diarrhea [111], even

serotypes more commonly associated with respiratory and ocular infections can be fecal-orally transmitted and in some cases can cause diarrhea in young children [100, 111]. More recently, several species of HAdVs have been shown to persist in the lamina propria of the small intestine and colon and, upon immunosuppression, reactivate to infect the intestinal epithelium, likely from the basolateral surface [107]. Furthermore, the capacity of HAdV-B and -E serotypes, which are frequent causes of acute respiratory disease in military recruits, to replicate in the intestine was exploited as a vaccine strategy [113]. These studies highlight the importance of the GI tract for HAdV replication and transmission. A significant short-coming in the field of adenovirology has been the lack of a physiologically relevant cell culture system for studying HAdV infection of the gut *in vitro*. Human enteroids have been used to study replication of other enteric viruses [15, 88, 114], but until now no reports of HAdV replication in human enteroids has been published. Here we demonstrate that human enteroids are a suitable system for supporting replication of HAdV and reveal novel aspects of HAdV infection of intestinal epithelial cells. (Adapted from [87])

## **Results**

### Infection and replication of prototype HAdV strains in cell lines

Reports of enteric HAdV-F replication in transformed cells are inconsistent [102, 105, 106, 115, 116]. We therefore compared the replications of the prototype strains HAdV-41p (HAdV-F), HAdV-5p (HAdV-C), and HAdV-16p (HAdV-B) in two standard cell lines, A549 cells (lung carcinoma) and 293 (embryonic kidney), to determine whether the culture defect for HAdV-F was at the level of initial infection, replication, or both. Note that the 293 cells used here (293 $\beta$ 5) overexpress integrin  $\beta$ 5, rendering the cells more adherent. Moreover, integrin  $\beta$ 5 are co-receptors for HAdV infection [117]. HAdV-5p and HAdV-16p are associated primarily

with respiratory disease and use coxsackievirus and adenovirus receptor (CAR) and CD46, respectively, as primary receptors [118, 119]. Infected cells were quantified by immunofluorescence for hexon, a major capsid protein, production 24 h post-infection. In 293 $\beta$ 5 cells, HAdV-5p was the most infectious, followed by HAdV-16p and HAdV-41p, which were equivalent (Fig. 3A). In A549 cells, HAdV-41p infection was substantially more limited than infection by the respiratory viruses, and HAdV-5p was  $\sim$ 3-fold more infectious than HAdV-16p (Fig. 3B). We also evaluated HAdV-41p infection on 293 cells with an attenuated interferon response due to the expression of the V protein of simian virus 5 (293-SV5/V). Despite being developed to facilitate the propagation of HAdV-F serotypes [120], 293-SV5/V cells were not more permissive than 293 $\beta$ 5 cells (Fig. 3C). (Adapted from [87])

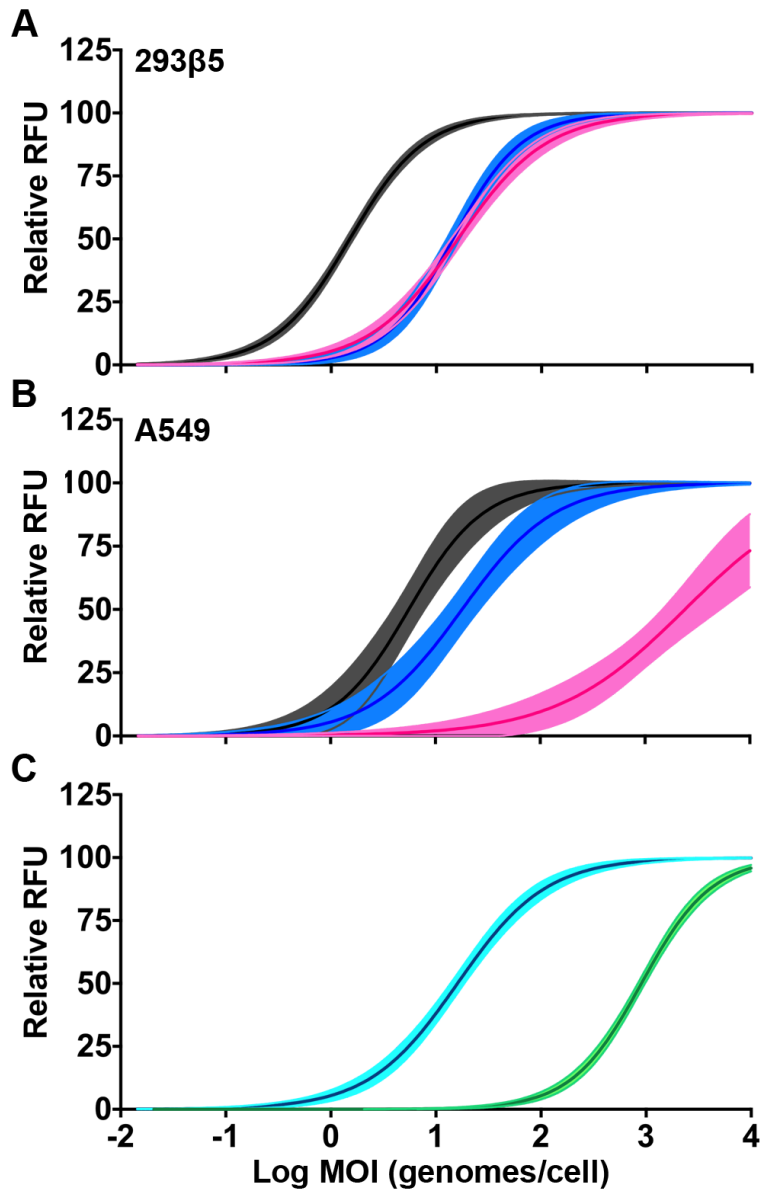


### Figure 3 Infection of cell lines

(A and B) 293β5 cells (A) and A549 cells (B) were infected with serial dilutions of HAdV-5p (black), HAdV-16p (blue), and HAdV-41p (pink). (C) 293β5 (cyan) and 293-SV5/V (green) cells were infected with serial dilutions of HAdV-41p. Lines were fitted to the mean values for three biological replicates; 95% confidence intervals of the nonlinear regression are shaded.

We next compared replication of the three HAdV serotypes in the most permissive cell line, 293β5. Parallel cultures of cells were infected and incubated at 4°C for 45 min. The inoculum was then replaced with fresh medium, and samples were shifted to 37°C. The multiplicity of infection (MOI; 5 to 10 genomes/cell) was equivalent among serotypes in a given experiment but varied slightly between experiments. Total viral genomes in the cells and supernatant were quantified every 24 h for 5 days by quantitative real-time PCR (qPCR). We used the same primer pair, which is specific for a region of *hexon* conserved in all three serotypes, to facilitate direct comparison. All three serotypes amplified rapidly within 24 h. HAdV-5p replication then proceeded at a slower, constant rate through 5 days post-infection (Fig. 4A), while that of HAdV-16p reached a plateau on day 1 (Fig. 4B) and that of HAdV-41p reached a plateau on day 2 (Fig. 4C) post-infection. The fold increase in HAdV-41p replication was higher than for HAdV-16p but lower than for HAdV-5p (Fig. 4D). Taken together, our experiments demonstrate that 293β5 cells are more easily infected than other cell lines and support genome amplification of all HAdV serotypes tested. (Adapted from [87])

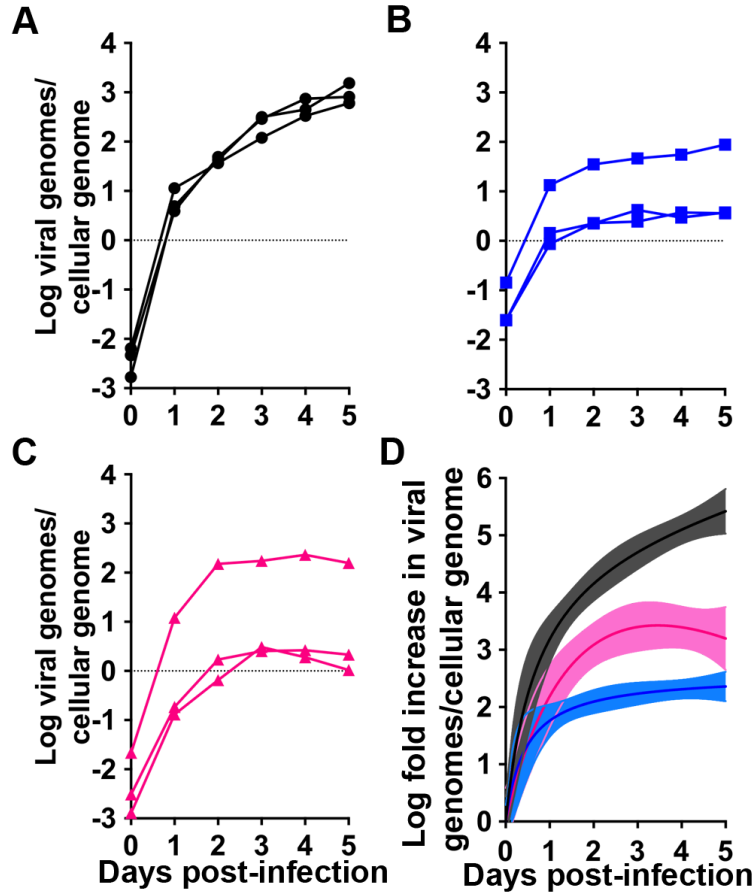


#### Figure 4 Replication in 293 $\beta$ 5 cells

(A to C) HAdV-5p (black) (A), HAdV-16p (blue) (B), and HAdV-41p (pink) (C) replication in 293 $\beta$ 5 cells infected at an MOI of 5 to 10 genomes/cell. Data are in viral genomes per cellular genome, and lines connect data points from individual replicates ( $n = 3$ ). (D) Transformation of the data in panels A to C to fold increases relative to day 0. Coloring is consistent with panels A to C. Lines were fitted to the mean values for the mean values for the three biological replicates; 95% confidence intervals of the nonlinear regression are shaded.

### Replication of prototype HAdV strains in human ileal enteroids

Unlike transformed cell lines, human enteroids are composed of primary cells. Because they are more easily cultured, we first infected undifferentiated enteroids with HAdV-5p, HAdV-16p, and HAdV-41p at the same MOI (3,000 genomes/cell). Samples taken 2 h post-infection (day 0) indicated that the numbers of cell-associated genomes for HAdV-5p and HAdV-41p were lower than that for HAdV-16p but equivalent to each other. Similar to their replication kinetics in 293 $\beta$ 5 cells, HAdV-5p (Fig. 5A and D) and HAdV-16p (Fig. 5B and D) amplified rapidly within 24 h and then continued to replicate at a slower, constant rate. HAdV-41p replication was characterized by a gradual increase in genomes over 5 days (Fig. 5C and D). The fold increase in viral genomes/cellular genome for HAdV-41p was less than HAdV-5p and -16p, which were similar (Fig. 5D). Therefore, all three HAdVs replicated in undifferentiated enteroids. (Adapted from [87])

We next infected differentiated enteroids, which contain mature intestinal epithelial cell types (Fig. 2A and E), with HAdV-41p. Replication in differentiated enteroids was similar to that in undifferentiated enteroids (Fig. 5C). Thus, both differentiated and undifferentiated enteroids express the HAdV-41 receptor and can support replication. (Adapted from [87])

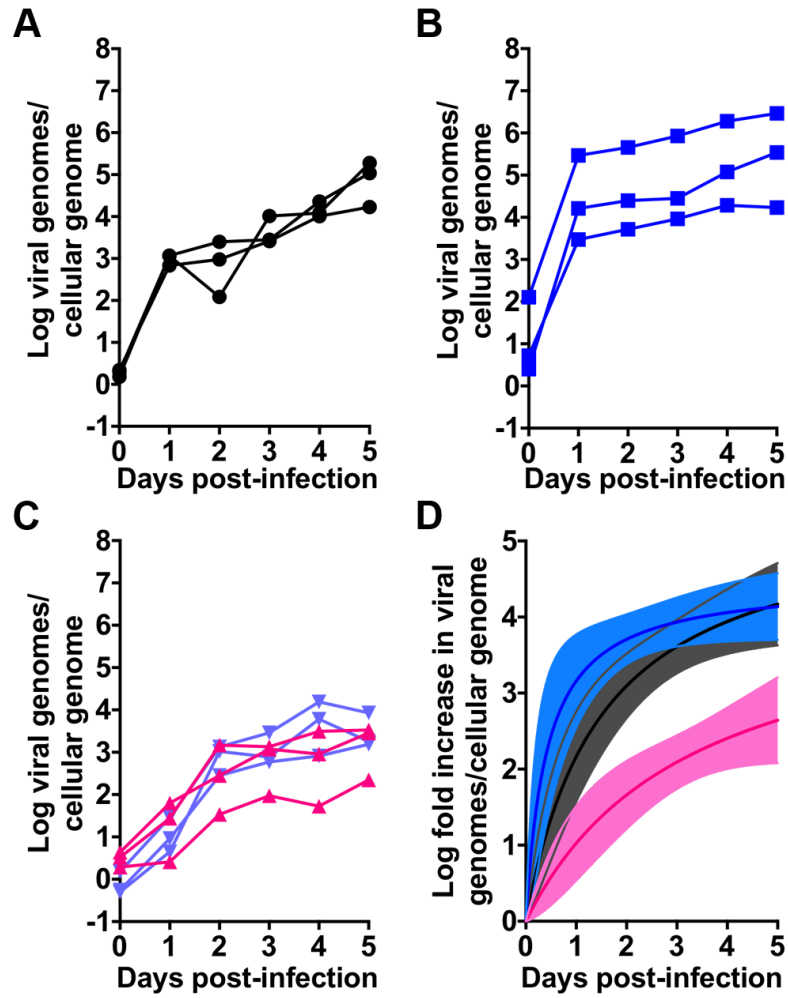


**Figure 5 HAdVs replicate in ileal enteroids.**

(A to C) HAdV-5p (black) (A), HAdV-16p (blue) (B), and HAdV-41p (pink) (C) replication in human enteroids. Data are viral genomes per cellular genome, and lines connect data points from individual replicates ( $n = 3$ ). Coloring is consistent with Fig. 3. All data are from undifferentiated enteroids except for the purple lines in panel C, which are from differentiated enteroids. (D) Transformation of HAdV replication in undifferentiated enteroids from panels A to C to fold increase relative to day 0. Coloring is consistent with panels A to C. Lines were fitted to the mean values for the three biological replicates; 95% confidence intervals of the nonlinear regression are shaded.

### Human enteroids support the replication of clinical isolates of human adenoviruses

Many enteric viruses, including HAdV, are difficult to culture from clinical samples, and prior publications have reported conflicting results of HAdV-F replication and cytopathic effects (CPE) in primary cells [102, 105, 115, 116]. Thus, we sought to determine whether human enteroids could support the growth of clinical isolates of HAdV-F. We obtained samples of HAdV-41 from the Centers for Disease Control and Prevention (CDC) and from the New York State Department of Health (NYSDOH) that were minimally passaged on transformed cells. We used undifferentiated human enteroids for these studies, because they can be cultured indefinitely. All four HAdV-41 isolates amplified over two passages (Fig. 6). We observed a 10-fold to 1,000-fold increase in genomes per cell over a span of 2 to 3 weeks. Cultures were terminated when complete CPE was observed, and our ability to passage the virus demonstrates that infectious particles were produced. We were unable to obtain clinical samples of HAdV-40, but HAdV-40p also replicated. Similarly, we cultured an HAdV-A serotype (HAdV-12p) that was originally isolated from stool (Fig. 5). In contrast to clinical isolates of enteric HAdVs, a clinical isolate of respiratory HAdV-C (HAdV-2, V-2375-18) amplified rapidly in undifferentiated enteroids to high titers within 5 days. We verified the identity of the clinical isolates obtained from external sources by HAdV fiber PCR [121]. For all clinical isolates, the virus that amplified in the enteroids matched the serotype detected in the source material (Fig. 6). These experiments show that enteroids are a suitable system for culturing prototype and clinical isolates of HAdVs, including those that are the etiologic agents of respiratory and gastrointestinal disease. (Adapted from [87])

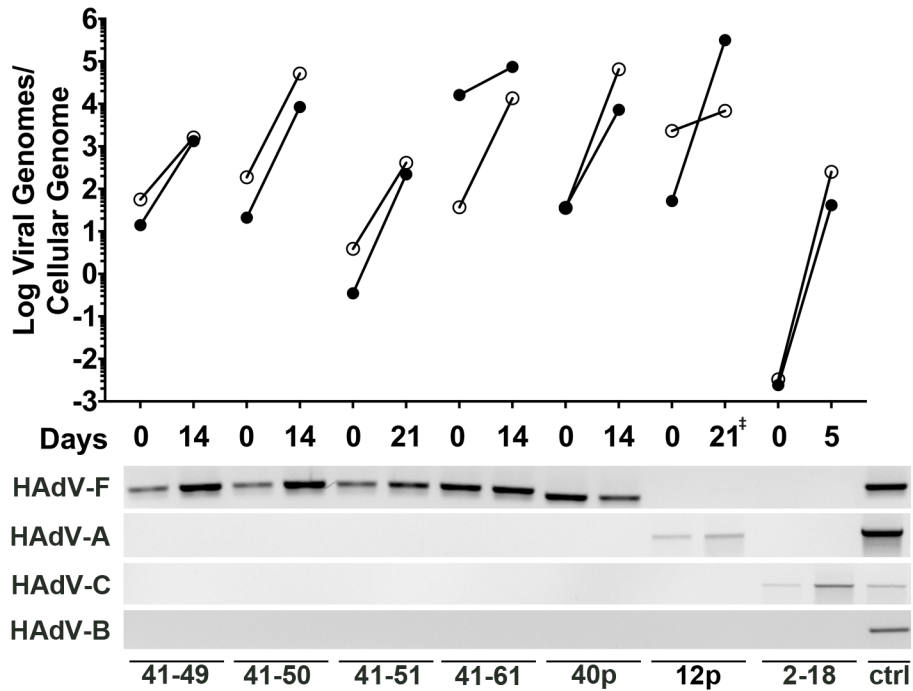


**Figure 6 Clinical isolates of HAdVs replicate in undifferentiated ileal enteroids.**

Undifferentiated human ileal enteroids were infected basolaterally with lysates of each clinical isolate or prototype strain, which are labeled with the serotype and the last two digits of the isolate designation. Data are viral genomes per cellular genome, and lines connect data points from individual passages (top panel). Closed symbols are for viral passage 1 and open symbols for viral passage 2. Time to 80% CPE for each virus was approximately the same for both passages, except for HAdV-12p, for which passage 1 took 21 days while passage 2 took 9 days (‡). Species identification of the inoculum and at the end of passage 2 was determined for each strain by endpoint PCR using species-specific fiber primers (bottom panel). The positive control (ctrl) contained a mixture of HAdV-5p, HAdV-12p, HAdV-16p, HAdV-40p, and HAdV-41p DNA.

### Interferon attenuates HAdV replication in enteroids

HAdVs contain multiple mechanisms to prevent interferon (IFN) induction [99]. Once induced, replication of respiratory serotypes is sensitive to IFN; however, efficient inhibition is apparent only in primary cells [122]. We investigated the impact of IFN pretreatment on HAdV-F replication in primary intestinal epithelial cells, which has not previously been investigated. For these experiments, we created monolayers composed of differentiated human enteroid cells. We chose to use human enteroid monolayers as opposed to 3D enteroids for three reasons: 1) human enteroid monolayers are 2D monolayers and allow direct comparison with cell lines, 2) human enteroid monolayers are polarized allowing for apical infection [88], and 3) infection of 3D human enteroids requires sheering of the enteroid which could potentially lead to an immune response as part of the wound healing process [123]. Like the differentiated enteroids, the enteroid monolayers contained cells with upregulated expression of genes associated with differentiation (Fig. 2C). Moreover, enteroid monolayers have been shown to be polarized and express tight-junction proteins [88, 93]. Monolayers were pretreated with 1,000 IU/ml IFN- $\beta$  or 500 ng/ml IFN- $\lambda$ 3 for 24 h and then infected with HAdV-5p for 24 h or HAdV-41p for 48 h. In uninfected cells, the interferon-stimulated genes (ISGs) *OAS1* and *ISG54* were upregulated at this time point (Fig. 7F). We found that IFN- $\lambda$ 3 and IFN- $\beta$  inhibited both HAdV-5p replication (105% and 86%, respectively) (Fig. 7A) at 24 h and HAdV-41p replication (110% and 82%, respectively) (Fig. 6B) at 48 h postinfection. There was no induction of ISGs upon infection of these cells in the absence of IFN pretreatment (Fig. 7E). Interestingly, neither IFN- $\beta$  nor IFN- $\lambda$ 3 pretreatment of A549 cells inhibited HAdV-5p infection at 24 h (Fig. 7C) despite comparable ISG upregulation (Fig. 7F). For HAdV-41p, although a low level of replication was detectable

only in the untreated well at 24 h postinfection, both treatments were equivalent to control at 48 h postinfection (Fig. 7D). Thus, like primary airway cells [122], untransformed intestinal epithelial cells adopt an IFN-induced antiviral state capable of limiting HAdV infection. Importantly, the inability of IFN pretreatment to inhibit HAdV replication in A549 cells is not due to an absolute inability to respond to IFN. (Adapted from [87])

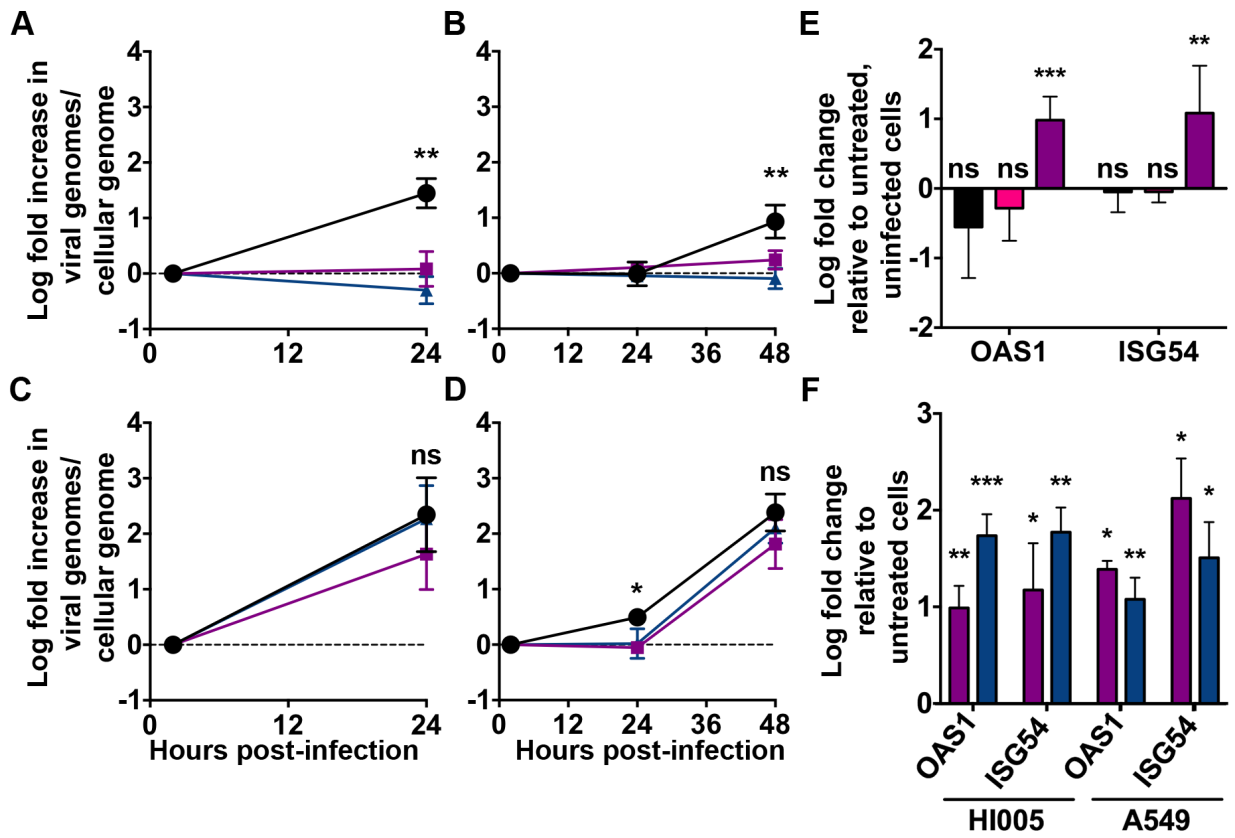


**Figure 7 Interferon pretreatment inhibits replication of HAdV in differentiated human enteroid monolayers but not A549 cells.**

Human enteroid monolayers and A549 cells were pretreated with 1,000 IU/ml of IFN- $\beta$  (purple) or 500 ng/ml IFN- $\lambda$ 3 (blue) for 24 h or left untreated (black). (A and B) Enteroid monolayers were infected with HAdV-5p at an MOI of 15 (A) or HAdV-41p at an MOI of 6 (B) to achieve similar levels of infection. (C and D) By the same rationale, A549 cells were infected with HAdV-5p at an MOI of 0.5 (C) or HAdV-41p at an MOI of 80 (D). Data are fold changes in viral genomes per cellular genome relative to day 0, and lines connect the mean values  $\pm$  SD for each time point ( $n = 3$  for each condition). (E) Enteroid monolayers were infected with HAdV-5p at an MOI of 30 (black) or HAdV-41p at an MOI of 200 (pink) or treated with 1,000 IU/ml of IFN- $\beta$  (purple) for 24 h. Data are the means  $\pm$  SD of the fold changes in gene expression relative to untreated, uninfected cells ( $n = 3$  for each condition). (F) Enteroid monolayers and A549 cells were treated with 1,000 IU/ml of IFN- $\beta$  (purple) or 500 ng/ml IFN- $\lambda$ 3 (blue) for 24 h. Data are the means  $\pm$  SD of the fold changes in gene expression relative to untreated, uninfected cells ( $n < 3$  for each condition). For panels A to D, significance in comparing untreated to IFN treated at each time point: \*,  $P < 0.05$ ; \*\*,  $P < 0.01$ ; ns, not significant. For panels E and F, data were analyzed using a one-sample  $t$  test: \*,  $P < 0.05$ ; \*\*,  $P < 0.01$ , \*\*\*,  $P < 0.001$ ; ns, not significant.

### HAdV-41p is resistant to the neutralizing activity of human enteric $\alpha$ -defensin HD5

Enteric human defensins are secreted by Paneth cells in the small intestine [6]. HD5 has been shown to both inhibit and enhance HAdV infection *in vitro* in a serotype-dependent manner [124, 125]. Furthermore, enteric defensins have been shown to play complex roles during mouse AdV infection of mice [126, 127]. HAdV-5p infection is potently inhibited and HAdV-41p infection moderately enhanced by HD5 on A549 cells [124]. Since these experiments were performed on transformed cells, we next sought to assess whether HD5 exhibited the same activities on infection of primary intestinal epithelial cells, which for HAdV-5p and HAdV-41p can be infected at a lower MOI. Human enteroid monolayers were infected with HAdV-5p and HAdV-41p in the presence or absence of 15  $\mu$ M HD5. Consistent with previous experiments using A549 cells, HAdV-5p infection of human enteroid monolayers was neutralized ( $90.1\% \pm 9.6\%$ ) by HD5 (Fig. 8A), while HAdV-41p infection was largely resistant but not enhanced (Fig. 8A). (Adapted from [87])

### HAdV-5p preferentially infects Goblet cells over other non-Goblet cell types in human enteroids

As part of these experiments, we also examined the tropism of HAdV-5p and HAdV-41p for goblet cells (GC), since recent studies of enterovirus replication in human enteroids revealed preferential infection of enteroendocrine cells by echovirus 11 coupled with a lack of goblet cell infection [114]. We co-stained the infected enteroid monolayers for MUC2, a marker of goblet cells, and hexon. While goblet cells comprised only 0.5 to 1.5% of the cells in the monolayer,  $18.9\% \pm 8.3\%$  of MUC2-positive goblet cells were infected with HAdV-5p compared to  $4.4\% \pm 3.1\%$  of the MUC2-negative cells (Fig. 8B). In contrast, HAdV-41 infected the two populations equally ( $3.9\% \pm 1.2\%$  versus  $3.1\% \pm 3.0\%$ ). Thus, HAdV-5p but not HAdV-41p preferentially infects goblet cells. And, although the MUC2-positive population is small, this preference was

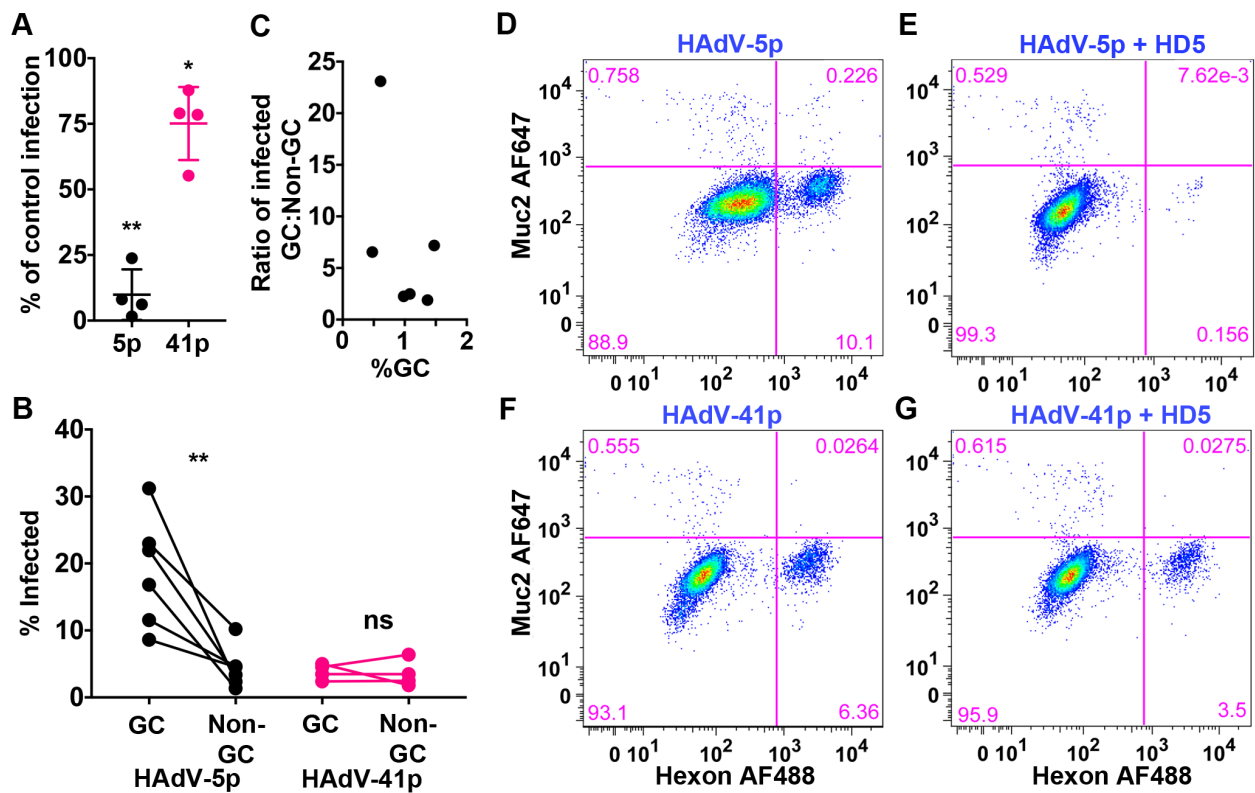


**Figure 8 HAdV-5p, but not HAdV-41p, is neutralized by HD5 and preferentially infects goblet cells.**

(A) Human enteroid monolayers were infected at MOIs of 30 and 200 for HAdV-5p and HAdV-41p, respectively, in the presence or absence of 15  $\mu$ M HD5. Infected cells were enumerated by flow cytometry at 48 h post-infection. Data are from four individual replicates graphed as the percentage of HAdV infection in the presence of HD5 compared to infection in the absence of HD5. Bars are means  $\pm$  SD. (B) HAdV-5p- and HAdV-41p-infected cells from the samples in panel A were analyzed for the percentage of MUC2<sup>+</sup> goblet cells (GC) and MUC2<sup>-</sup> nongoblet cells (non-GC) that were infected in the absence of HD5. (C) Data from panel A analyzed as the ratio of HAdV-5p infected GC to non-GC as a function of %GCs. (D to G) Representative flow cytometry plots. For panel A, the percentages of cells infected under each condition were compared. For panel B, the percentages of infected GC and non-GC were compared by ratio paired *t* tests. \*, *P* < 0.05; ns, not significant.

observed over a range of GC population sizes (Fig. 8C). To our knowledge, this is the first reported preference of HAdV for a specific cell type in the GI tract. (Adapted from [87])

## **Discussion**

Our experiments add HAdVs to the set of viruses that can be cultured in human enteroids, which also includes rotavirus, norovirus, and enterovirus [15, 88, 128]. Thus, enteroids have the potential to be a unified platform for amplifying human enteric viruses from clinical samples. HAdV-41p replicates to a similar extent in differentiated and undifferentiated enteroids; however, differentiated enteroids are less suitable for culturing slowly replicating viruses because of their limited life span (~10 days) and inability to be passaged. In contrast, undifferentiated enteroids can be passaged for an indefinite period, allowing time for viral amplification. Although human rotaviruses can replicate in both undifferentiated and differentiated human enteroids [15, 128], human rotavirus infection was significantly increased in differentiated enteroids [15]. Human norovirus replicates in enteroid monolayers [88], and human echovirus 11 replicates in differentiated human enteroids [114]. It is currently unknown whether these viruses can replicate in undifferentiated enteroids. Since rotavirus and norovirus replication efficiency is greatly impacted by the secretor status of the enteroids [15, 88], the differentiation state of the enteroids might affect the secretor phenotype. Furthermore, norovirus replication is enhanced by bile acid in human enteroid monolayers, but not standard cell lines [88]. Thus, when isolating enteric viruses from clinical samples, the potential virus species should dictate the differentiation state of the human enteroids. The generally greater replication rate of RNA viruses is also an advantage, although the one respiratory isolate (HAdV-2) that we tested also replicated rapidly. The reason for the slow replication kinetics of HAdV-F is unclear, but it has also been observed in cell lines [105, 106, 129] and may reflect some unique aspect of

enteric HAdV biology that remains to be elucidated. Since all of the inocula were lysates and the titer of the HAdV-2 V-2375-18 lysate was 2.5 log lower than the lowest HAdV-41 clinical isolate titer, low MOI or other characteristics of the inoculum are unlikely to explain the discrepancy in replication kinetics. Nonetheless, human enteroids are a remarkable system for supporting replication of human enteric viruses. Moreover, other primary human cell types (embryonic kidney cells, lung fibroblasts, and skin fibroblasts) have been tested for their capacity to support HAdV-F replication [102, 105, 115], but results have been inconsistent. Additionally, most of these primary cells were derived from locations not normally infected by enteric viruses, further complicating their utility in understanding HAdV-F biology. Interestingly, previous attempts to culture HAdV-F in fetal intestinal organ cultures did not result in infectious virus [130]. Thus, human enteroids are the only viable system for studying HAdV-F interactions with mature primary intestinal epithelial cells. (Adapted from [87])

As identified previously [102, 105, 106], there were differences in HAdV-41p infection and replication among transformed cell lines. Moreover, different groups have reported different results with the same cell lines, and sublines of the same cells have various abilities to support enteric adenovirus replication [105]. Despite considerable investigation, the factors contributing to these differences are not well defined. We found that HAdV-41p can infect 293 $\beta$ 5 and A549 lung cells, but infection was inferior to both respiratory serotypes in A549 lung cells but only to HAdV-5p in 293 $\beta$ 5 cells. The disparity in HAdV-41p infection of A549 and 293 $\beta$ 5 might reflect several different factors. First, the presence of the HAdV-5 E1 region in 293 $\beta$ 5 has been implicated as potentially complementing HAdV-F replication [101, 105, 131]. And, E1B gene products of HAdV-2, -5, and -12 rescue HAdV-40 replication in a previously nonpermissive cell line [101, 131]. Another potential explanation is the presence of a more intact innate immune

response in A549 than in 293 $\beta$ 5 cells. In our experiments, HAdV-41p appears to be no more sensitive than HAdV-5p to inhibition by IFN (Fig. 6); however, others have noted that HAdV-41 infection is blocked by IFN under conditions permissive for HAdV-2 replication [132]. Caveats of these studies include a poorly characterized mixture of IFN- $\beta$  and IFN- $\lambda$  derived from Namalwa cells (a B lymphoblast cell line) infected with Sendai virus and infection of cells thought to be conjunctival cells but later shown to be HeLa [132]. Nonetheless, in one study, prior infection with HAdV-2 rescued HAdV-41 from IFN, suggesting that HAdV-2 potentially inhibited the antiviral state [132]. Finally, these differences could reflect tissue tropism and receptor usage. HAdV-F serotypes have two fibers, long and short [103], which likely bind to distinct receptors. They also lack an RGD sequence in their penton base proteins (replaced by RGA and GDD in HAdV-40 and -41, respectively), which is present in all other known HAdVs and mediates internalization via integrin coreceptors [104]. Although purified HAdV-41 long fiber binds to CAR [133], this may not equate with receptor usage, as has been observed for other HAdVs [134]. Thus, the receptors for both enteric HAdV long and short fibers remain unproven or unknown. Given that infection by the CAR-utilizing HAdV-5p is only ~4-fold better on 293 $\beta$ 5 than A549 cells while that of HAdV-41p is improved more substantially (~150-fold), a simple model whereby the tropism of both viruses is dictated by CAR interactions alone is not supported. Elucidation of the receptors for enteric HAdV fibers and the need, if any, for a coreceptor is more easily performed in a genetically tractable system (e.g., 293 cells) but should be verified in human enteroids. Although human enteroids can be genetically engineered [135], they are not amenable to high-throughput screening techniques. More than receptor usage dictates tropism of HAdVs *in vivo* and their association with specific diseases. Experiments in

more physiologic systems like enteroids provide a platform to examine the role of additional host factors in tropism. (Adapted from [87])

Recently, an unexpected tropism of echovirus 11 for enteroendocrine cells but not goblet cells was revealed in enteroids [114]. In contrast, enterovirus 71 was shown to infect goblet cells in human enteroids [136]. These data indicate that different enteric viruses can exhibit divergent preferential target cells. Surprisingly, we found that HAdV-5p but not HAdV-41p disproportionately infected goblet cells versus nongoblet cells. Nongoblet cells in these cultures include enterocytes, enteroendocrine cells, stem cells, and partially differentiated intermediates (e.g., transit-amplifying cells) based on gene expression but were not parsed further. A previous study of an enteric mouse adenovirus revealed no preference for a particular cell type in the small intestine [137], although to our knowledge this hasn't been examined in humans. Since goblet cells are also found in the airway, it will be interesting to determine the interactions that contribute to this tropism and if it extends to other mucosal surfaces or other respiratory serotypes. These results illustrate the power of the more-physiologic enteroid system to address fundamental aspects of virology that cannot be modeled in transformed cells. (Adapted from [87])

A salient aspect of primary cell systems like human enteroids is the presence of intact signal transduction pathways of innate immunity, such as those leading to IFN production. Recent studies of HAdV-5p infection of primary bronchial epithelial cells (32) led us to investigate the impact of IFN on HAdV-5p and HAdV-41p replication. Like for airway cells, we were unable to detect IFN production in response to HAdV infection by changes in gene expression. This has also been observed in other cell types (45). However, we found that either IFN- $\beta$  or IFN- $\lambda$ 3 pretreatment was sufficient to inhibit both HAdV-5p and HAdV-41p

replication in human enteroid monolayers but not A549 cells, despite the capacity of A549 cells to respond to type I and type III IFN by other measures (50, 51). (Adapted from [87])

Type III IFN (IFN- $\lambda$ s) plays an important role in controlling viral infection of intestinal epithelial cells, whereas type I IFN (IFN- $\beta$ ) is more important for lamina propria cells [138, 139]. We observed comparable inhibition of HAdV by IFN- $\lambda$ 3 and IFN- $\beta$ , while IFN- $\beta$  inhibited human rotavirus replication in human enteroids to a greater extent than IFN- $\lambda$ 1 and IFN- $\lambda$ 3 [140]. This discrepancy in the antiviral effects of IFN- $\beta$  could reflect differences in the antagonism of IFN signaling by the two viruses, their respective replication cycles, or the enteroid platforms used: three-dimensional (3D) enteroids versus enteroid monolayer. That concentrations of IFN sufficient to inhibit replication in primary intestinal epithelial cells were insufficient to suppress HAdV replication in transformed cells underscores the importance of using relevant primary cells to study viral infection and host response. (Adapted from [87])

There are many questions in enteric adenovirology that might be addressed in the enteroid system. First, the route of respiratory HAdVs seeding the GI tract is unclear. They could apically infect the intestinal epithelium through the fecal-oral route, or transient viremia could seed the intestinal epithelium basolaterally. An apical versus basolateral preference, even if the receptor(s) remain unknown, could be addressed in transwell assays of polarized enteroid monolayers. In a similar vein, an expanded analysis of the tropism of clinical and prototype isolates of HAdVs for specific cell types is warranted. Finally, the cause for the slow replication kinetics of clinical enteric isolates could be pursued and would help in the development of cell culture systems more permissive to the isolation of enteric viruses from patient samples. Isolation and culture of more clinical isolates of enteric HAdVs can further our understanding of their biology and provide information on how to effectively treat infection. Moreover, by

studying HAdV replication in a more physiologically relevant system, we can begin to understand the molecular mechanisms driving reactivation of adenovirus, viral modulation of host responses, and innate immune responses to viral infection in the gastrointestinal tract. Elucidation of these processes can lead to development of protocols and therapeutics to ameliorate reactivation of HAdV and subsequent viremia following immune suppression. (Adapted from [87])

#### **Chapter 4: *Salmonella* induced inflammasome activation in human enteroids**

##### **Introduction**

*Salmonella* species are Gram-negative, flagellated, rod-shaped bacteria that are transmitted via the fecal-oral route and are major human pathogens [141-144]. The nomenclature of *Salmonella* is quite complex. Within *Salmonella* are two species, *Salmonella bongori* and *Salmonella enterica* [142]. *S. bongori* contains only one subspecies and will not be discussed further. In contrast, *S. enterica* contains six different subspecies with over 2500 different serovars divided among them. *S. enterica* subspecies *enterica* contains several major human pathogens that cause distinct diseases, gastroenteritis and Typhoid fever. *S. enterica* subspecies *enterica* serovar Typhi and Paratyphi are the only two serovars that cause Typhoid fever. Many serovars are capable of causing gastroenteritis, but this chapter will focus on *Salmonella enteric* subspecies *enterica* Typhimurium (*S. Typhimurium*). *S. Typhimurium* induced gastroenteritis is characterized by acute mucosal inflammation with neutrophil influx of the ileum and colon. Onset of symptoms typically occurs within one day post-infection. *S. Typhimurium* infects the intestinal tract, typically after consumption of contaminated food or water. As such, the first cellular barrier to *S. Typhimurium* infection of the host is the intestinal epithelium, which lines the interior of the intestine. However, the existing knowledge concerning the complex interaction

between *S. Typhimurium* and the human intestinal epithelium has been limited due to the absence of cell culture system for untransformed intestinal epithelial cells for many years. Thus, many questions remain regarding host sensing of and response to *S. Typhimurium* infection of the human intestinal epithelial cells.

*S. Typhimurium* can cross the intestinal epithelium through several distinct mechanisms: 1) directly invade the intestinal epithelial cells, primarily mature enterocytes, 2) transcytosis via specialized epithelial cells termed microfold (M)cells, which function to sample the luminal contents and transcytose antigens to basolateral immune cells, 3) transcytosis in between intestinal epithelial cells, and 4) sampling by dendritic cell extension of intraepithelial dendrites to sample the luminal contents. Following translocation to the basolateral surface, *S. Typhimurium* is engulfed by macrophages in the lamina propria [145]. Within the macrophage *S. Typhimurium* modifies the cytosolic vacuole into a *Salmonella* containing vacuole (SCV) to create an intracellular niche. *S. Typhimurium* can replicate within the SCV and disseminate through macrophage movement to distal sites [110]. Alternatively, *S. Typhimurium*-infected macrophages may initiate pyroptosis, an inflammatory form of cell death, which releases proinflammatory cytokines interleukin-1 $\beta$  (IL-1 $\beta$ ) and IL-18 [146, 147]. These inflammatory mediators function to alert the immune system to the invading pathogen [147, 148]. In addition, intestinal epithelial cell-derived IL-8 recruits neutrophils [149] to the primary site of infection, a hallmark of *S. Typhimurium* induced gastroenteritis is that contributes to the inflammatory response [72, 142]. *S. Typhimurium* thrives in this inflammatory environment and outcompetes the commensal microbes [150]. Thus, *S. Typhimurium* infection results in an acute inflammatory disease that generally resolves in a few days.

Of the modes of transcytosis discussed above, invasion of intestinal epithelial cells is the focus of this chapter. *S. Typhimurium* attaches to intestinal epithelial cells via adhesins. Using the type three secretion system-1 (T3SS-1), *S. Typhimurium* invades intestinal epithelial cells and enters a cytosolic vacuole. For *S. Typhimurium* several outcomes are possible following invasion. First, *S. Typhimurium* can modify the SCV in a T3SS-2-dependent manner, thus protecting its intracellular niche as it transits from the apical to basolateral surface for release into the lamina propria [151]. Second, the SCV can fuse with lysosomal vacuoles and result in bacterial degradation [152]. Third, *S. Typhimurium* can escape the vacuole early on in infection using the T3SS-1, allowing *S. Typhimurium* access to the cytosol [153, 154]. Lastly, the host autophagy pathway can degrade *S. Typhimurium* [152]. Vacuolar *S. Typhimurium* replicate to low levels and are protected from detection by cytosolic pathogen recognition receptors (PRRs) [145, 153], but are still at risk of being sensed by endosomal/vacuolar recognition systems such as autophagy [155]. In contrast, cytosolic *S. Typhimurium* are vulnerable to detection by cytosolic PRRs, such as inflammasomes [154].

The cytosol is surveilled by two major families of PRRs, retinoic acid inducible gene I (RIG-I)-like receptors (RLRs) and nucleotide binding domain oligomerization domain (NOD)-like receptors (NLRs). RLRs sense double stranded RNA (dsRNA) present during viral infection and will not be discussed further [156]. NLRs activate inflammasomes in response to a variety of signals such as bacterial derived products, viral replication, and sterile stresses [157]. Canonical inflammasomes are activated by NLRs recognizing their cognate ligands resulting in oligomerization and recruitment of an adapter protein [157] (Fig. 9A). The adapter protein then recruits an inflammatory caspase, caspase-1 (CASP1). CASP1 processes IL-1 $\beta$  and IL-18 and promotes cell death [157]. Cell death in the context of canonical inflammasomes is thought to be

mediated by caspase-8, a known effector of apoptotic cell death [157, 158], or through cleavage of gasdermin D (GSDMD), which forms pores in the plasma membrane (Fig. 9A) [159]. The canonical inflammasome activated by *S. Typhimurium* infection involves NLR family pyrin domain containing 3 (NLRP3, sensor), PYD and CARD domain containing (PYCARD, adaptor) and CASP1 (effector) or NLR family apoptosis inhibitor protein (NAIP, sensor), NLR family CARD domain containing 4 (NLRC4, adaptor), and CASP1 (effector). The ligand for NLRP3 activation is unknown, whereas human NAIP can be activated by flagellin and a component of the T3SS apparatus [160-162].

Humans encode two other proinflammatory caspases, caspase-4 (CASP4) and caspase-5 (CASP5), and mice encode caspase-11 (CASP11), which have recently been identified as important effectors of intracellular immune responses [163-165]. However, these caspases function in a noncanonical inflammasome pathway, whereby they do not depend on an NLR protein sensing its stimulus. Instead murine CASP11 and human CASP4 and CASP5 directly bind cytosolic lipopolysaccharide (LPS) and become activated via autoproteolysis (Fig. 9B). Activated CASP4 facilitates secretion of IL-1 $\alpha$  through as yet unidentified mechanism (Fig. 9B) [166]. Noncanonical inflammasome induced cell death is effected through cleavage of GSDMD by CASP11 in mice or CASP4 in humans (Fig. 9B) [167, 168]. Upon cleavage the N-terminal domain of GSDMD is released and oligomerizes in the plasma membrane to form pores leading to loss of membrane integrity and contributing to cell death [159]. CASP11 Cleavage of GSDMD is thought to recruit the noncanonical inflammasome leading to CASP1 activation (Fig. 9B) [167]. Activated CASP1 can then cleave pro-IL-1 $\beta$  and pro-IL-18 to their mature forms [169].

Results found with CASP11 are often extrapolated to CASP4/5 and vice versa. While overexpression of human *CASP4* could complement mouse *Casp11*<sup>-/-</sup> bone marrow-derived macrophages (BMDMs) for LPS-induced pyroptosis [164], it has recently been demonstrated that CASP4 is able to sense a broader range of LPS than murine CASP11 [170]. Additionally, the regulation of *CASP4*, *CASP5*, and *Casp11* differs. In mouse BMDMs, *Casp11* and *Il-1b* expression must be primed by stimulating the cells with LPS. Human *CASP4* is constitutively expressed in the human intestinal epithelium and human epithelial cell lines [154]. While CASP11 is able to promote cell death in mouse BMDMs in response to *S. Typhimurium* infection, the dependence of cell death induction on CASP4 or CASP5 in human immune cells is comparatively under studied [165, 166, 170, 171].

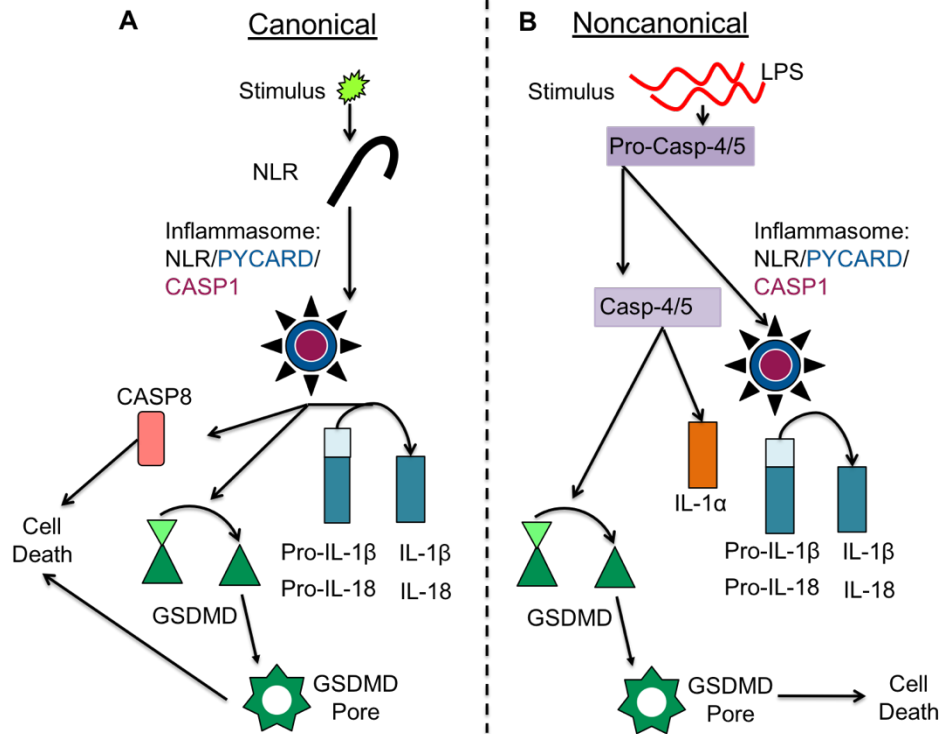


### Figure 9 Inflammasome Activation

A) The canonical inflammasome is activated by a stimulus that induces oligomerization of NLR proteins. NLR proteins recruit adapter proteins (PYCARD) that contain domains for interaction with the pro-inflammatory caspase, caspase-1 (CASP1). CASP1 undergoes proximity-dependent proteolysis to its mature, active form. Active CASP1 processes pro-IL-18 and pro-IL-1 $\beta$  to their mature forms. Additionally, CASP1 is capable of cleaving GSDMD leading to the release of the active N-terminal domain that oligomerizes into a pore that inserts into membranes. GSDMD pores reduce membrane integrity and contribute to cell death.

B) The noncanonical inflammasome is activated by binding of LPS to CASP4 or CASP5. Upon binding CASP4/5 undergoes proteolysis to its mature, active form. CASP4/5 activation leads to release of IL-1 $\alpha$  and cleavage of GSDMD. The noncanonical inflammasome can recruit the canonical inflammasome leading to production of IL-18 and IL-1 $\beta$ .

In the context of *S. Typhimurium* infection of intestinal epithelial cells, inflammasome activation results in cell death and extrusion of intestinal epithelial cells from the intestinal epithelium [153, 154, 172]. Epithelial cell extrusion is both a mechanism to protect the epithelium by removal of infected cells and a mode of transmission for *S. Typhimurium*. Under homeostatic conditions intestinal epithelial cells are extruded from the epithelium either through initiation of apoptosis or crowding [173]. During infection epithelial cells are removed via pro-inflammatory process [158, 172, 174]. Extrusion of infected cells is a mechanism to protect adjacent uninfected cells from the pathogen. However, ejection of infected intestinal epithelial cells can also expel invasion-primed *S. Typhimurium* back into the luminal space where *S. Typhimurium* can infect new intestinal epithelial cells. The exact mechanism of intestinal epithelial cell extrusion during infection is a matter of debate. C2Bbe1 cells infected with *S. Typhimurium* are extruded from the epithelial monolayer in a CASP4 dependent mechanism [154]. It has been shown in mice that intestinal epithelial cell extrusion is dependent on the NAIP/NLRC4/CASP1 inflammasome [172]. Interestingly, the extruded cells maintained membrane integrity indicating they were ejected prior to complete pyroptosis. A more recent study found that treatment of mouse enteroids with a purified NAIP ligand, *Legionella* flagellin in conjunction with protective antigen, resulted in extrusion of intestinal epithelial cells without concomitant loss of membrane integrity [158]. Although loss of membrane integrity was dependent on CASP1, it was not required for epithelial cell extrusion. The discrepancy in caspase dependency and loss in membrane integrity is likely due to several factors including: *in vivo* vs *in vitro*, mouse vs human, and whole bacteria vs purified ligands. Although inflammasomes have been extensively studied in murine macrophages and to a lesser extent in

human macrophages, epithelial cells and immune cells differ in a variety ways making it difficult to extrapolate data from one system to another. It remains to be determined which pathways are critical for restricting intracellular *S. Typhimurium* replication and initiating intestinal epithelial cell extrusion in the human intestinal epithelium.

Current models used for investigating the role of inflammasomes and other immune responses during *S. Typhimurium* infection suffer from use of models that do not fully recapitulate human intestinal epithelial cells. These models either rely on animals in which the infection occurs in a different anatomical location than in humans or human tumor cell lines that have not been demonstrated to faithfully recapitulate the biology of primary human intestinal epithelial cells [153, 154, 172]. Investigations using the streptomycin pretreated mouse model have identified NAIP1-6, NLRC4, and CASP1 as essential for restricting intraepithelial replication of *S. Typhimurium* at early time points post-infection (12-36 h) [172]. Deletion of all six NAIPs (*Naip1-6<sup>-/-</sup>*) led to increased intraepithelial replication and concomitant reduction in luminal *S. Typhimurium* [172]. Additionally, *Naip1-6* deficiency was sufficient to delay tissue pathology induced by *S. Typhimurium*, suggesting that a significant portion of the pathology is due to inflammasome activation. Notably, these investigators did not compare *Casp11<sup>-/-</sup>* mice to the *Naip1-6<sup>-/-</sup>* or *Casp1<sup>-/-</sup> Casp11<sup>-/-</sup>* mice. Therefore, from these experiments it is unclear whether CASP11 plays any role in *S. Typhimurium* infection.

A parallel study to the one discussed above investigated the role of noncanonical inflammasomes in a human colon cancer cell line, C2Bbe1 cells. Knock down of CASP4, but not CASP1 or CASP5, in C2Bbe1 cells led to decreased *S. Typhimurium*-induced IL-18 secretion, increased intracellular *S. Typhimurium* replication, and decreased cell extrusion [154]. Similar to the previous *in vivo* data hyper-replicating *S. Typhimurium* (>50 bacteria per cell) were present

in the C2Bbe1 cells, however this was found to be dependent on knock down of CASP4, not CASP1 [154]. To corroborate their findings in C2Bbe1 cells the investigators also explored the importance of CASP11 in mice using the streptomycin pretreated mouse model. *Casp11*<sup>-/-</sup> mice infected with *S. Typhimurium* exhibited decreased pathology and increased intraepithelial bacterial burden in the cecum compared to wild-type mice [154]. It is critical to note that *S. Typhimurium* infection of *Casp11*<sup>-/-</sup> mice was not compared to *Casp1*<sup>-/-</sup> *Casp11*<sup>-/-</sup> mice, thus it cannot be concluded that CASP11 is the dominant caspase without direct comparison to CASP1. Nonetheless, these results suggest that the noncanonical inflammasome plays a crucial role during *S. Typhimurium* infection of intestinal epithelial cells. The discrepancy in results between these two studies is likely due to use of different experimental designs for the mouse experiments (36 h vs 7 d post-infection) and *in vivo* vs *in vitro* experiments. Taken together these two studies underscore the importance of inflammasome activation in controlling *S. Typhimurium* infection and eliciting an immune response. Nevertheless, neither C2Bbe1 cells nor mice fully recapitulate the epithelial cellularity of the human gut. To better understand the role of canonical and noncanonical inflammasomes during *S. Typhimurium* infection of humans, it is imperative to study *S. Typhimurium* infection in a physiologically relevant cell culture system. Using human enteroids to study *S. Typhimurium*-induced inflammasome activation will likely provide key insights into the relative importance of the canonical and noncanonical inflammasomes in human intestinal epithelial cells during infection.

## Results

### Human enteroids express components of inflammasomes

Inflammasome activation in the human intestinal epithelium has been understudied, thus it is currently unknown which components of the inflammasome are expressed in untransformed intestinal epithelial cells. To determine whether human enteroids express genes involved in inflammasomes, we harvested RNA from human enteroids and C2Bbe1 cells and quantified relative gene expression of several inflammasome components. Human enteroids and C2Bbe1 cells express all three pro-inflammatory caspases at the transcriptional level (Fig. 10A and B). The downstream signaling molecules, *IL1B* and *IL18*, are also expressed in human enteroids. To determine whether caspase expression is detectable at the protein level, we immunoblotted for CASP1 and CASP4. Consistent with previous findings [154], C2Bbe1 cells express CASP4 and not CASP1 (Fig. 10C and D). Notably, human enteroids strongly express both CASP4 and CASP1 (Fig. 10C and D). Protein levels of CASP5 have yet to be evaluated in human enteroids.

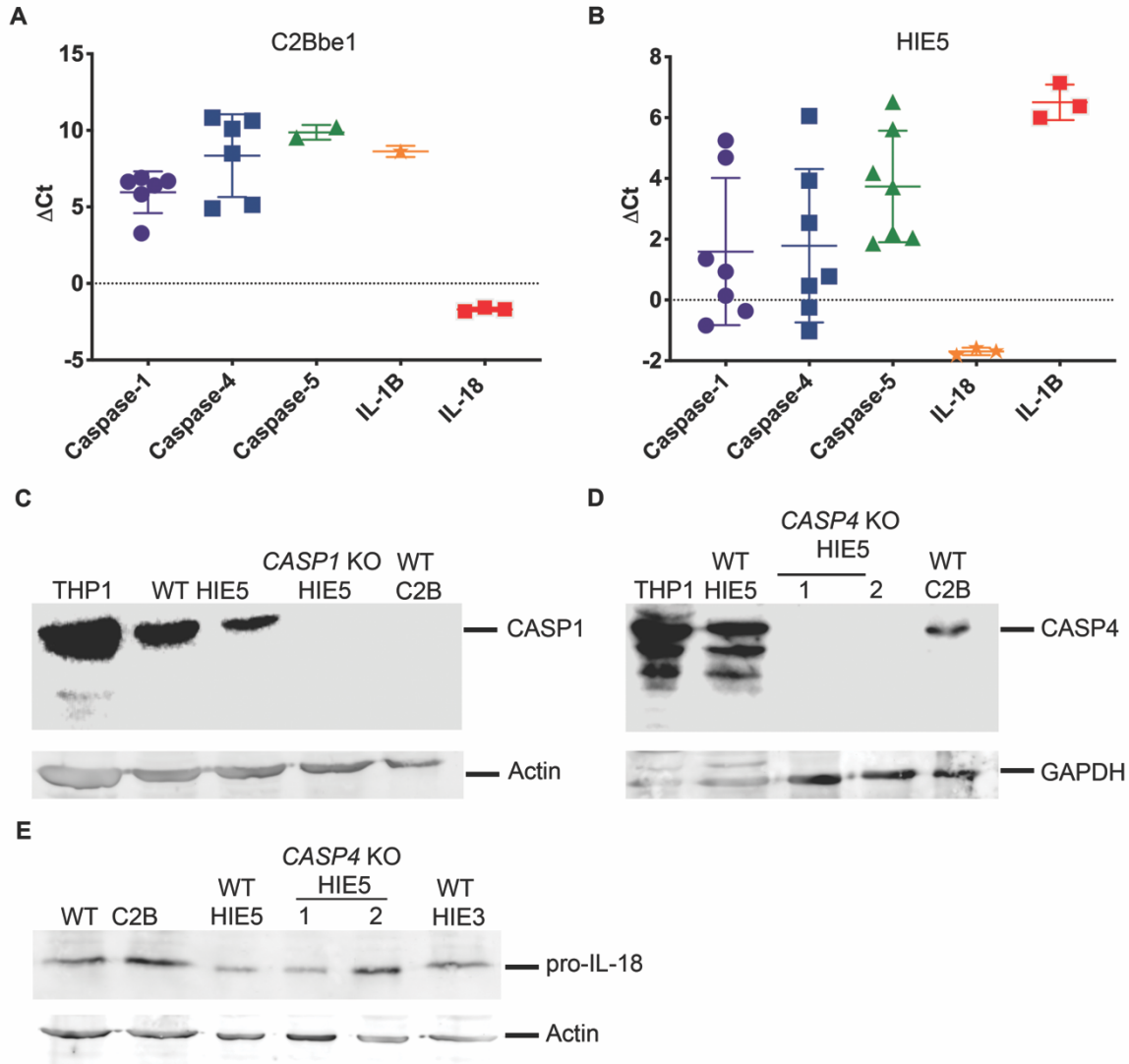


**Figure 10 Human enteroids express components of inflammasomes**

C2Bbe1 cells (A) and HIE5 (B) were harvested at day 4 and day 5 days post-plating, respectively, for gene expression analysis. Data are expressed as the  $\Delta C_t$  of the target of gene relative to a housekeeping gene (HPRT). C) Expression of CASP1 in THP-1 cells, WT HIE5 and *CASP1* KO HIE5 enteroids, and WT C2Bbe1 (C2B). D) Expression of CASP4 in THP-1 cells, WT HIE5 enteroids, *CASP4* KO HIE5 enteroid clones #1 and #2, and WT C2B. E) Expression of pro-IL-18 in THP-1 cells, WT C2B, WT HIE5 or HIE3 enteroids, and *CASP4* KO HIE5 enteroid clones. Protein expression levels were normalized either actin (C and E) or GAPDH (D).

### S. Typhimurium intracellular replication in intestinal epithelial cells

*S. Typhimurium* infection of human cell lines has been widely reported [153, 154, 166, 175, 176]; however, it is unknown how well *S. Typhimurium* infects untransformed human intestinal epithelial cells. Early studies of *S. Typhimurium* infection of mice suggested that *S. Typhimurium* primarily targets M cells overlying Peyer's patches in the intestinal epithelium [177]. However, mature enterocytes are also a target of *S. Typhimurium* during infection [154, 172], thus it is important to understand the replication kinetics in untransformed intestinal epithelial cells. We infected human enteroid monolayers and C2Bbe1 cells with *S. Typhimurium* and enumerated intracellular colony forming units (CFUs) at 1.5, 3, 5, and 7 h post-infection. As has been reported previously, *S. Typhimurium* readily infected C2Bbe1 cells and replicated steadily between 1.5 and 7 h post-infection (Fig. 11A). Intriguingly, human enteroid monolayers were not as susceptible to infection by *S. Typhimurium*, as there were fewer intracellular bacteria at early time points compared to C2Bbe1 cells (Fig. 11A). Interestingly, *S. Typhimurium* infection of human enteroid monolayers appeared to plateau after 3 h post-infection. It is unclear whether the plateau is due to equal rates of replication and death, or lack of replications after 3 h post-infection. Although, initial infection of human enteroid monolayers was less than C2Bbe1 cells, the fold increase in intracellular CFUs at 7 h was similar between the two cell culture systems (3.3- vs. 3.1-fold, respectively). Thus, *S. Typhimurium* can infect and replicate in human enteroid monolayers, but to a lesser extent than C2Bbe1 cells.

### S. Typhimurium infection of human enteroids elicits robust and rapid IL-18 secretion

IL-18 is a well documented downstream consequence of inflammasome activation and has been shown to recruit NK cells to the site of *S. Typhimurium* infection *in vivo* [148]. To evaluate the ability of *S. Typhimurium* to induce IL-18 secretion in untransformed intestinal

epithelial cells we infected human enteroid monolayers and C2Bbe1 cells with *S. Typhimurium*. IL-18 secretion in response to infection was quantified by ELISA at 1.5, 3, 5, and 7 h post-infection. C2Bbe1 cells began to secrete IL-18 at 3 h post-infection and gradually increased throughout the duration of the experiment (Fig. 11B). In contrast, human enteroids released significant levels of IL-18 by 1.5 h post-infection, which then plateaued out to 7 h post-infection (Fig. 11B).

A simple explanation for the discrepancy in the kinetics of IL-18 secretion and the amount of IL-18 secreted is a difference in basal pro-IL-18 levels in the two cell types. We quantified the amount of pro-IL-18 in uninfected cells by Western blot. C2Bbe1 cells and human enteroids contained similar quantities of pro-IL-18 (Fig. 10E), indicating that the difference in IL-18 secretion is not due to different levels of intracellular pro-IL-18. Therefore, the difference in kinetics of IL-18 release are potentially due to differential sensing of *S. Typhimurium* or differences in the physiology of the two cell types. These studies highlight the importance of studying host-pathogen interactions in untransformed cells, which likely more faithfully recapitulate cells *in vivo*.

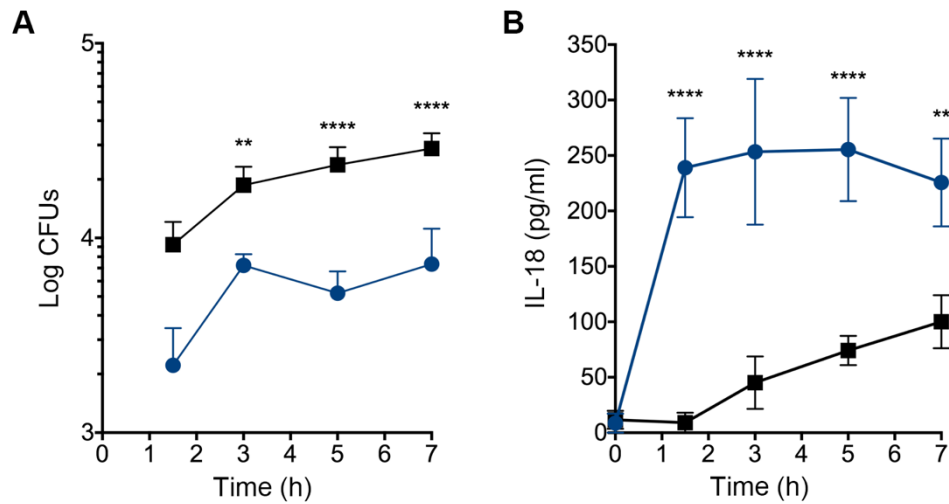


**Figure 11 S. Typhimurium replicates in and induces IL-18 secretion from intestinal epithelial cells**

(A) *S. Typhimurium* replicates in both C2Bbe1 cells (black squares) and human enteroid monolayers (blue circles). (B) Human enteroid monolayers and C2Bbe1 cells produce IL-18 in response to *S. Typhimurium* infection. Colored as in A. Data are mean  $\pm$  SD of intracellular CFUs (A) or IL-18 protein (B). Data were analyzed by one-way ANOVA. \*\*,  $P < 0.01$ ; \*\*\*\*,  $P < 0.001$ .

S. Typhimurium-induced IL-18 secretion can be partially inhibited by peptide inhibitors of pro-inflammatory caspases

Pro-IL-18 is processed to its mature form by CASP1 [157] (Fig. 10). To determine whether IL-18 secretion is dependent on proinflammatory caspase activity, we treated C2Bbe1 cells and human enteroid monolayers with two peptide inhibitors, Z-WEHD-FMK, which most potently inhibits CASP1, and Z-YVAD-FMK, which preferentially inhibits CASP4/5. However, both of these peptide inhibitors are able to inhibit all three pro-inflammatory caspases to different degrees [178]. Although IL-18 secretion was reduced by treatment with Z-YVAD-FMK or Z-WEHD-FMK inhibitor, it did not abolish IL-18 secretion entirely in either cell line (Fig. 12A). This was true whether the cells were treated for 3 h prior to infection or beginning 30 min post-infection. Additionally, treatment of cells with a combination of Z-WEHD-FMK and Z-YVAD-FMK at 30 min post-infection did not exhibit any synergistic or additive effects (Fig. 12A). Although the concentrations of inhibitors used in these studies exceed the inhibitory concentrations for all three pro-inflammatory caspases in *in vitro* enzymatic assays [178, 179], their inability, either alone or in combination, to completely inhibit IL-18 secretion could be due to poor diffusion of the peptide inhibitors within the cells or a pool of caspases that are inaccessible to the inhibitors.

Given that these inhibitors are able to inhibit all three enzymes to varying degrees [178], it is possible that their inhibitor capacities could be parsed. We treated cells at 30 min post-infection with different doses of either Z-WEHD-FMK or Z-YVAD-FMK. *S. Typhimurium* infected C2Bbe1 cells showed similar dose curves between the two inhibitors (Fig. 12B), consistent with expression of only one pro-inflammatory caspase, CASP4 [154], which can be

inhibited by both Z-WEHD-FMK and Z-YVAD-FMK. Interestingly, the dose curves for Z-WEHD-FMK and Z-YVAD-FMK in *S. Typhimurium*-infected human enteroid monolayers diverged. Z-YVAD-FMK more potently inhibited *S. Typhimurium*-induced IL-18 secretion from infected human enteroid monolayers than Z-WEHD-FMK (Fig. 12B). The different dose-dependent curves could indicate two potential explanations: 1) the two dose curves could represent the different  $K_d$  values for of Z-YVAD-FMK and Z-WEHD-FMK for the caspases or 2) functional redundancy of the pro-inflammatory caspases within enteroids, and 3) different caspases are dominant in the two cell systems.

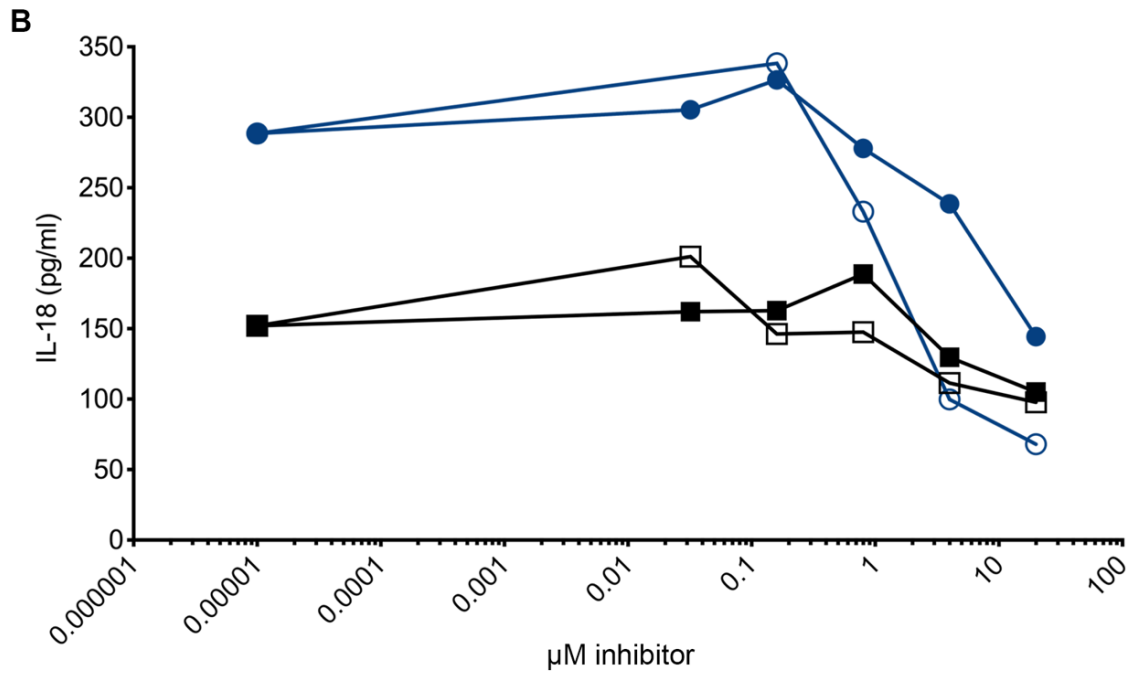
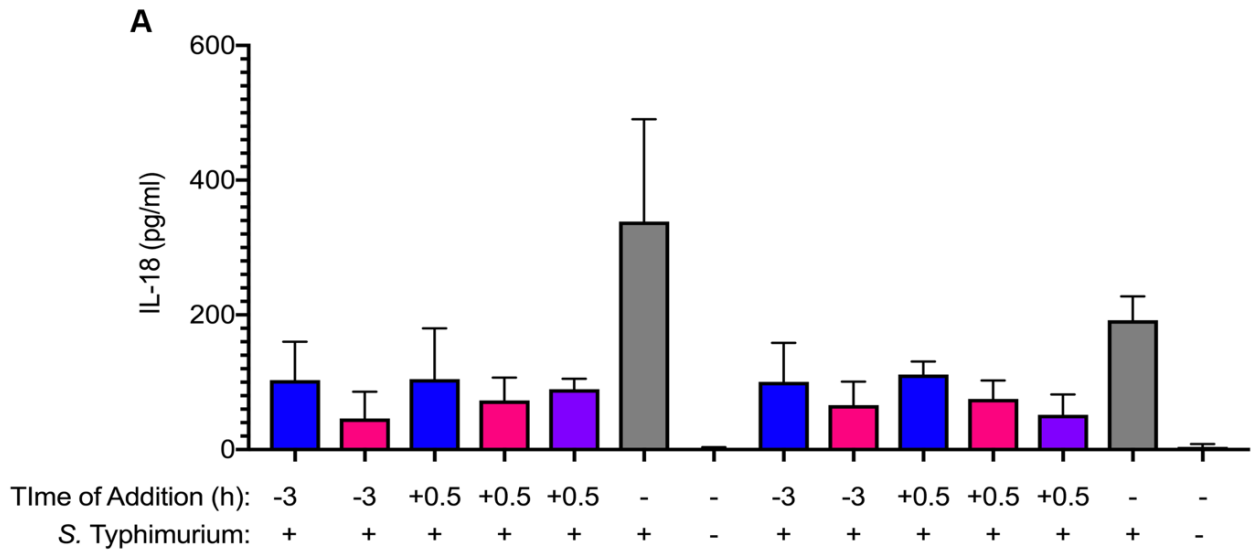


**Figure 12 IL-18 secretion is dependent on pro-inflammatory caspase activity**

(A) Human enteroid monolayers and C2Bbe1 cells were treated with 20  $\mu$ M Z-WEHD-FMK (blue) or 20  $\mu$ M Z-YVAD-FMK (pink) either 3 h prior to infection or 30 min post-infection, or 20  $\mu$ M Z-WEHD-FMK and 20  $\mu$ M Z-YVAD-FMK in combination (purple) 30 min post-infection. Data are mean  $\pm$  SD (n = 2). (B) Human enteroid monolayers (blue) and C2Bbe1 cells (black) were treated with different doses of Z-WEHD-FMK (closed symbols) and Z-YVAD-FMK (open symbols) 30 min post-infection. IL-18 secretion was quantified by ELISA at 10 h post-infection. Note untreated is graphed as 0.00001  $\mu$ M for simplified graphical representation only. Data from one representative experiment is shown.

IL-18 secretion by human epithelial cells in response to *Salmonella* Typhimurium is dependent on CASP4 activity

Due to the promiscuity of the caspase inhibitors, it is difficult to dissect which pro-inflammatory caspase is responsible for IL-18 secretion. Therefore, we used LentiCRISPR to knock out each proinflammatory caspase individually in human enteroids and C2Bbe1 cells. We generated clonal lines of each CRISPR target in both cell systems. It is important to note that generating clonal lines is difficult to achieve due to several factors: 1) human enteroids are difficult to transduce as single cells [85], and 2) 3D enteroids are capable of fusing together to form larger enteroids [180]. We generated one *CASP1* knock out (KO) enteroid clone, 2 *CASP4* KO enteroid clones, and 2 *CASP5* KO enteroid clones that appeared to be edited by both restriction fragment length polymorphism and Sanger sequencing. To identify the genetic lesions present and assess their clonality, we sequenced amplicons of the targeted genes in the populations using next generation sequencing. All 5 clones analyzed were composed of >2 alleles (Fig. 13A), indicating that the enteroid clones are likely made up of multiple edited cells. The vast majority of the alleles in the *CASP1* knockout enteroid clone were edited (4 different deletions), however a few reads of a WT allele were present in the population (Fig. 13A). To validate that the *CASP1* KO enteroid clone was functionally deleted for CASP1, we probed for CASP1 in this clone by Western blot (Fig. 10C). Even after multiple passages since isolation (>8 passages), the *CASP1* KO enteroids were deficient for CASP1 at the protein level, indicating these enteroids are knocked out for CASP1. For both *CASP4* knock out enteroid clone 1 and 2, all alleles were edited, manifesting primarily as deletions but some insertions were detected (Fig. 13A). To verify that the *CASP4* KO enteroid clones do not express any CASP4 at the protein level, we analyzed the clones by Western blot. Neither *CASP4* KO enteroid clone expressed

detectable CASP4 protein by immunoblot (Fig. 10D). Unlike the *CASP4* and *CASP1* KO enteroid clones, the *CASP5* KO enteroid clones 1 and 2 appear to be mixed populations of heterozygous cells with one edited allele and one wild-type allele (Fig. 13A).

To assess the effect of caspase deficiency on IL-18 secretion, we infected WT, *CASP1* KO, *CASP4* KO, and *CASP5* heterozygous (*CASP5* het) enteroid monolayers with *S. Typhimurium* and quantified IL-18 secretion at 7 h post-infection by ELISA. *CASP5* Het and *CASP1* KO enteroid monolayers secreted wild-type levels of IL-18 (Fig. 13B and D). Intriguingly, *CASP4* knock out enteroid monolayers did not secrete any IL-18 in response to *S. Typhimurium* infection (Fig. 13C). The lack of IL-18 secretion was not due to reduced pro-IL-18 levels in the *CASP4* KO enteroids (Fig. 10E), suggesting that CASP4 is responsible for IL-18 secretion in human enteroids, consistent with previous findings in C2Bbe1 cells [154].

#### *Salmonella Typhimurium* induced IL-8 expression is unaffected by CASP4 deficiency

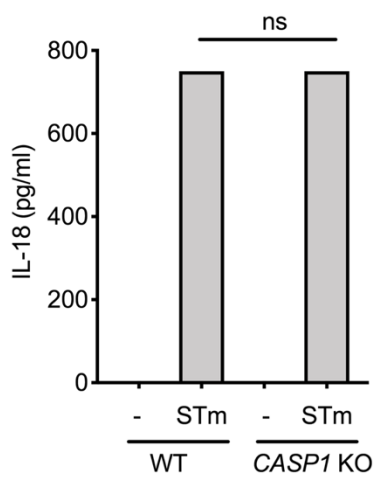
To verify that the lack of IL-18 secretion is not due to an inherent innate immune sensing and response defect in the *CASP4* knock out clone, we measured IL-8 expression in wild-type and *CASP4* knockout human enteroid monolayers and C2Bbe1 cells. IL-8 is regulated at the level of transcription [181], and is induced by toll-like receptor signaling and is independent of inflammasome activation [182]. IL-8 expression and secretion is a well-documented consequence of *S. Typhimurium* infection of epithelial cells [149]. *S. Typhimurium* infected C2Bbe1 cells, wild-type enteroid monolayers, and *CASP4* KO enteroid monolayers expressed similar amounts of IL-8 at 1.5 h post-infection (Fig. 13E). Moreover, wild-type and *CASP4* KO enteroid monolayers, and C2Bbe1 cells secreted similar levels of IL-8 into the supernatant (Fig.

13F). These data indicate that the effect on IL-18 secretion in *CASP4* KO enteroid monolayers is specific to the gene editing of *CASP4* and not due to a broad innate immune sensing defect.

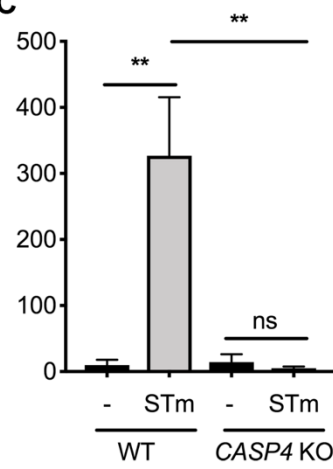
**A**

|                          | <i>CASP4</i> KO #1 | <i>CASP4</i> KO #2 | <i>CASP5</i> KO #1 | <i>CASP5</i> KO #2 | <i>CASP1</i> KO #1 |
|--------------------------|--------------------|--------------------|--------------------|--------------------|--------------------|
| <b>Complete Knockout</b> | Yes                | Yes                | No                 | No                 | Yes                |
| <b>Mixed Population</b>  | Yes                | Yes                | Yes                | Yes                | Yes                |
| <b># of alleles</b>      | 2                  | 7                  | 4                  | 4                  | 4                  |
| <b>Status</b>            | KO                 | KO                 | Heterozygous       | Heterozygous       | KO                 |

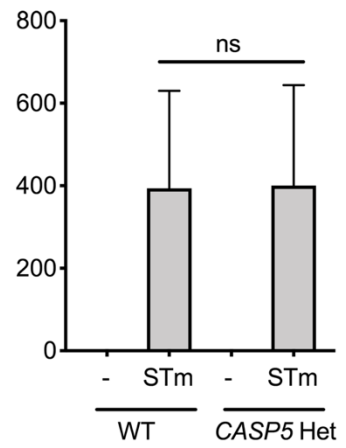
**B**



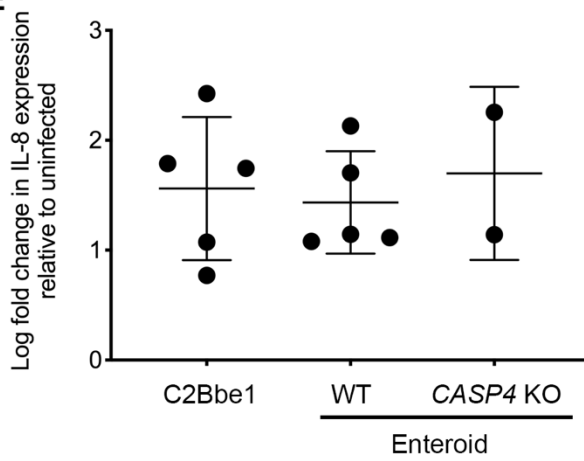
**C**



**D**



**E**



**F**

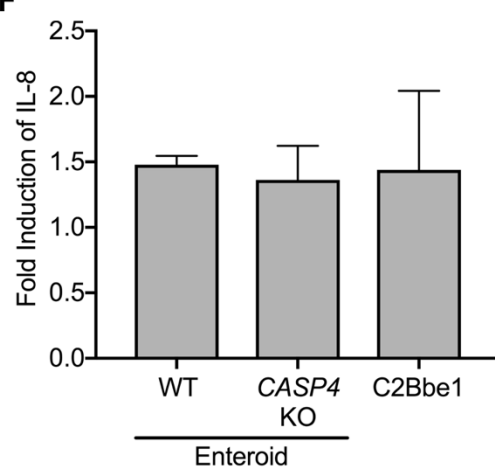


### Figure 13 IL-18 secretion is dependent on CASP4

(A) Status of caspase knock enteroids. Enteroids were knocked out for Caspase-1, Caspase-4, or Caspase-5 using LentiCRISPR. IL-18 secretion from wild-type and *CASP1* KO (B) *CASP4* KO (C) or *CASP5* KO (D) enteroid monolayers infected with *S. Typhimurium* (MOI = 150). Data are the mean  $\pm$  SD ( $n = 4$ ). Data were analyzed using one-way ANOVA. \*\*,  $P < 0.01$ ; ns, not significant. (E) C2Bbe1, wild-type enteroid monolayers and *CASP4* enteroid monolayers were infected with *S. Typhimurium* (MOI = 150). Cells were harvested at 8 h post-infection for gene expression analysis. Log fold increase in gene expression was calculated by comparing gene expression of infected cells to uninfected cells. Each dot is an independent biological replicate. (F) IL-8 secretion from wild-type and *CASP4* KO enteroid monolayers, and C2Bbe1 cells infected with *S. Typhimurium* (MOI = 150). Fold increase in IL-8 secretion was calculated by comparing IL-8 secretion from uninfected to *S. Typhimurium* infected supernatants. Data are the mean  $\pm$  SD ( $n = 2$ ).

*Salmonella* Typhimurium replicates to higher intracellular levels in CASP4 deficient enteroids than WT human enteroids

To determine the effect of caspase deficiency on intracellular bacteria levels, we infected wild-type, *CASP1* KO, *CASP4* KO, and *CASP5* het enteroid monolayers with *S. Typhimurium*. At 7 h post-infection *CASP5* het and *CASP1* KO enteroid monolayers had similar intracellular bacterial burdens to wild-type (Fig. 14A and C). In contrast, *CASP4* KO enteroid monolayers had modestly higher bacterial burdens than wild-type (Fig. 14B). These data suggest that *CASP4* plays an important role in restricting intracellular bacterial replication, possibly through reduced activation of inflammasomes and intestinal epithelial cell extrusion.

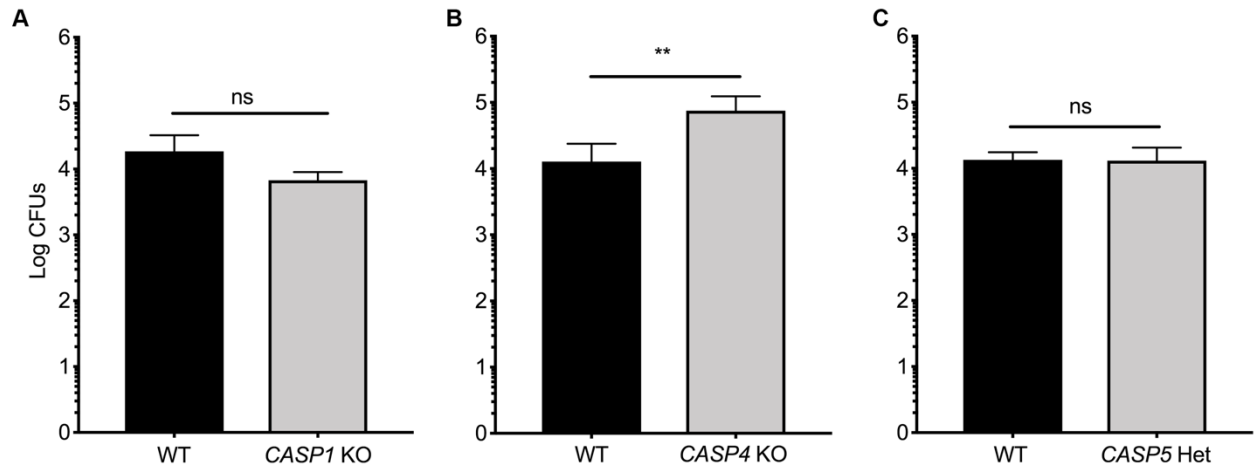


**Figure 14 S. Typhimurium replicates to higher intracellular CFUs in CASP4 KO enteroid monolayers.**

Wild-type and *CASP1* KO (A) *CASP4* KO (B) or *CASP5* het (B) enteroid monolayers were infected with *S. Typhimurium* (MOI 100-200). Intracellular CFUs were enumerated at 7 h post-infection. Data are the means  $\pm$  SD of *S. Typhimurium* CFUs (n=4). Data were analyzed using one-way ANOVA: \*\*,  $P < 0.01$ , ns, not significant.

### *S. Typhimurium* hyper-replication is absent in untransformed intestinal epithelial cells

Upon invasion of epithelial cells *S. Typhimurium* enters a cytosolic vacuole. *S. Typhimurium* can either remain in the vacuole and modify it to become an SCV or escape into the cytosol. Previous reports have shown that *S. Typhimurium* is capable of hyper-replicating in the cytosol of transformed cell lines (>50 bacteria/cell) [154, 174]. Rare cells with >20 bacteria have been found in the mouse intestinal epithelium, but most cells contained less than 10 bacteria per cell [172]. The physiological relevance of hyper-replication in human intestinal epithelial cells is unknown. To determine whether hyper-replication occurs in human enteroid monolayers, we infected wild-type human enteroid monolayers with *S. Typhimurium*. We quantified the number of *S. Typhimurium* per cell by fluorescence microscopy at 7 h post-infection. C2Bbe1 cells were infected with a wide range of *S. Typhimurium* per cell. The number of bacteria per cell ranged from 1 to 120 bacteria per cell, consistent with previous results (Fig. 15). In contrast, human enteroid monolayers were infected at a much lower level even though both C2Bbe1 cells and human enteroid monolayers received the same inoculum (Fig. 15). Interestingly, only a small proportion of infected cells contained greater than 5 bacteria per cell. This indicates that hyper-replication does not occur in untransformed epithelial cells and is potentially an artefact of transformed cells.

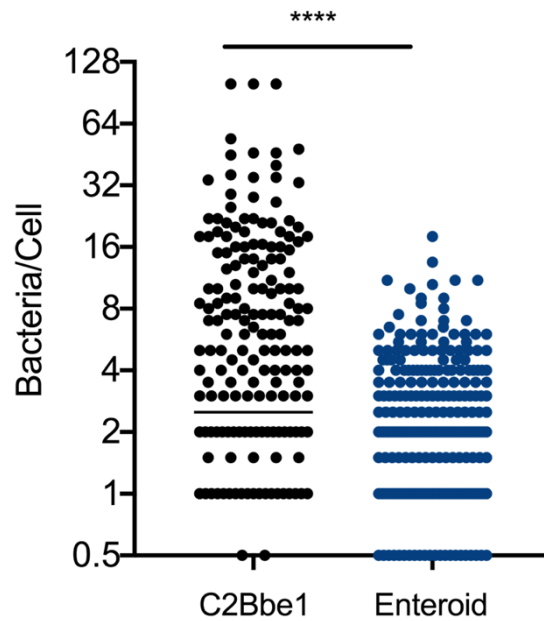


**Figure 15 Hyper-replication is absent in untransformed intestinal epithelial cells**

C2Bbe1 cells (black) and wild-type human enteroid monolayers (blue) were infected with *S. Typhimurium* (MOI 750). Cells were fixed at 7 h post-infection and number of bacteria per cell was quantified by fluorescence microscopy. Each symbol represents the number of intracellular bacteria in one cell and presented with mean  $\pm$  SD for the population (n=3). Data were analyzed with Mann-Whitney test: \*\*\*\*,  $p < 0.00001$ .

### CASP4 restricts *S. Typhimurium* from replicating to high numbers in untransformed epithelial cells.

The intestinal epithelium is turned over every 3-5 days, shedding  $\sim 10^{11}$  cells each day [1]. Mature intestinal epithelial cells differentiate from intestinal stem cells in the crypt base and transit up to the tip of the villi where they are extruded into the lumen (Fig. 1). The rapid turnover of mature intestinal epithelial cells can function as a defense mechanism to protect both the intestinal stem cells and the underlying lamina propria. Removal of infected cells via this process prevents spread of the infectious agent among neighboring uninfected cells. The process of homeostatic epithelial extrusion is initiated by increased pressure due to cell divisions within the crypt, leading to loss of cell junctions between the extruding cell and surrounding cells [183]. An actomyosin supracellular ring forms around the extruding cell and contracts to force the cell out of the epithelium [183]. Interestingly, these actomyosin supracellular rings were visible during extrusion of *S. Typhimurium* infected C2Bbe1 cells [153], suggesting similar processes during infection and homeostasis. Extruding infected C2Bbe1 cells were filled with hyper-replicating *S. Typhimurium* [153, 154, 172], which are likely replicating in the cytoplasm, and thus available for detection by CASP4 or CASP5.

To evaluate the effect of CASP4 deficiency on *S. Typhimurium* intracellular replication on a per cell basis we infected wild-type and *CASP4* KO human enteroid monolayers with *S. Typhimurium* and imaged infected monolayers at 7 h post-infection. Neither *CASP4* KO nor wild-type enteroid monolayers contained hyper-replicating bacteria (Fig. 16), however *CASP4* KO enteroid monolayers were infected with more *S. Typhimurium* than wild-type enteroid monolayers (Fig. 16). Moreover, more *CASP4* KO cells contained  $>6$  bacteria per cell ( $36.33\% \pm 32.65\%$ ) than wild-type cells ( $7.33\% \pm 4.93\%$ ) (Fig. 16A). These results suggest that CASP4 is

important for preventing *S. Typhimurium* from replicating to high numbers in human intestinal epithelial cells. We did not see actively extruding cells in either wild-type or *CASP4* KO enteroid monolayers, however based on previous findings [153, 154, 172, 174], it is likely that cells with large amounts of *S. Typhimurium* are being extruded in wild-type enteroid monoalyers and are not visible during confocal analysis or detectable when enumerating CFUs.

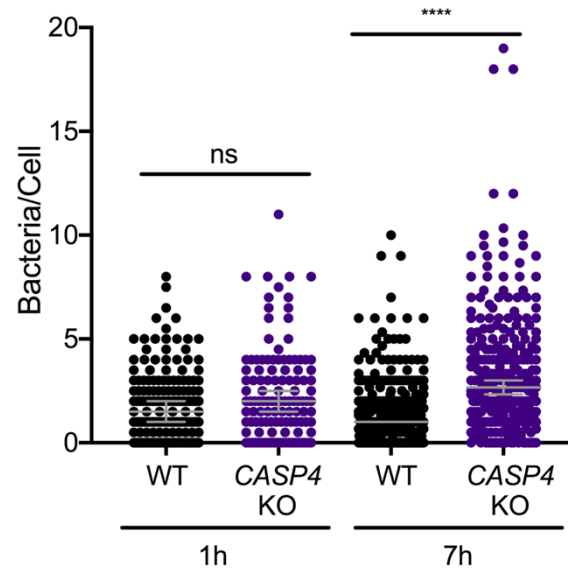


**Figure 16 CASP4 restricts intracellular replication**

Wild-type and *CASP4* KO enteroid monolayers were infected with *S. Typhimurium* expressing mCherry (MOI 750). Cells were fixed at 1 h and 7 h post-infection and the number of intracellular bacteria per cell was quantified by fluorescence microscopy. Each symbol represents the number of intracellular bacteria in one cell and presented with mean  $\pm$  SD for the population (n=2). Data were analyzed with Kruskal-Wallis test: \*\*\*\*,  $p < 0.00001$ .

## Discussion

Understanding the complex interaction between *S. Typhimurium* and human intestinal epithelial cells has been limited due to the lack of an untransformed cell culture system for many years. Human enteroids offer an opportunity to explore *S. Typhimurium* infection of and host-response to infection in untransformed intestinal epithelial cells that recapitulate the epithelial cellularity of the gut. It has been demonstrated by our group and others that human enteroids provide important information about host-pathogen interactions for both viral and bacterial pathogens that could not be appreciated in standard cell lines [87, 91, 93, 114, 140, 184].

To first evaluate whether human enteroids are a suitable *in vitro* system for studying *S. Typhimurium* infection, we measured the expression of inflammasome components in human enteroid monolayers and C2Bbe1 cells. Both human enteroid monolayers and C2Bbe1 cells expressed detectable levels of all three pro-inflammatory caspases (Fig. 10A and B). In contrast, the upstream sensors for the canonical inflammasome, NLRC4 and NLRP3 were not consistently detected in either cell culture system (Fig. 10A and B). To verify that the pro-inflammatory caspases CASP1 and CASP4 are expressed at the protein level, we assessed expression by immunoblot. Consistent with previous findings [154], C2Bbe1 cells express CASP4 but not CASP1 (Fig 10). In contrast, human enteroids expressed both CASP1 and CASP4 (Fig 10). These data demonstrate that human enteroids can be used to investigate inflammasome activation.

*S. Typhimurium* can infect many different cell lines [174] as well as mouse enteroids [185] and human intestinal organoids [186], however the ability of *S. Typhimurium* to infect

human intestinal epithelial cells derived from adult tissue has never been investigated. We showed that *S. Typhimurium* can infect human enteroid monolayers (Fig 11A). Interestingly, human enteroid monolayers were much less susceptible to *S. Typhimurium* infection than C2Bbe1 cells. Moreover, examination of the replication kinetics of intracellular *S. Typhimurium* revealed interesting differences between human enteroid monolayers and C2Bbe1 cells. *S. Typhimurium* gradually increased in intracellular CFUs in C2Bbe1 cells throughout the course of the experiment. In contrast, *S. Typhimurium* replication plateaued after 3 h post-infection in human enteroid monolayers. Although there were differences in kinetics and initial infection of C2Bbe1 cells and human enteroid monolayers, the fold increase in *S. Typhimurium* replication was similar between human enteroid monolayers (~3.3-fold) and C2Bbe1 cells (~3.1 fold). Since these experiments were done in parallel, it rules out any defects in components of the *S. Typhimurium* invasion machinery or differences in inocula between experiments. Therefore, these results could potentially reflect decreased binding of *S. Typhimurium* to the cells, reduced invasion of the untransformed intestinal epithelial cells, rapid cell death and extrusion of infected cells at early time points, or increased killing by gentamicin due to loss of membrane integrity in infected cells. It is important to note that more extensive experiments would be required to determine the cause of the reduced intracellular *S. Typhimurium* CFUs in human enteroid monolayers. Additionally, the plateau of *S. Typhimurium* replication in human enteroid monolayers, but not C2Bbe1 cells suggests potential differences in host cell sensing and response or altered intracellular life cycle of *S. Typhimurium*.

Upon invasion into cells, *S. Typhimurium* can either remain in the vacuole and modify it using the T3SS-2 or escape the vacuole and replicate in the cytosol. *S. Typhimurium* can stimulate inflammasome activation through a variety of pathways: NAIP sensing of T3SS needle

proteins, T3SS rod proteins (mouse only), or flagellin [187], NLRP3 sensing of membrane disruptions [167], or CASP4/5 binding intracellular LPS [163]. Upon activation of inflammasomes, pro-IL-18 is processed and secreted in its mature form to recruit immune cells to the site of infection. Monocytes and macrophages infected with *S. Typhimurium* secrete both IL-1 $\beta$  and IL-18; in contrast intestinal epithelial cells predominantly make IL-18 upon infection [154, 188, 189]. *S. Typhimurium* infection of human enteroid monolayers led to robust and rapid secretion of IL-18 by 1.5 h post-infection (Fig. 10B). This is notable because C2Bbe1 cells do not express detectable levels of IL-18 until 3 h post-infection. The difference in IL-18 secretion was not due to increased levels of intracellular pro-IL-18 in resting cells (Fig. 10E), but likely reflects differences in *S. Typhimurium* interaction with the host cells or difference in host sensing of *S. Typhimurium*. It is commonly thought that during pyroptosis IL-18 and IL-1 $\beta$  are released due to loss of membrane integrity and concomitant cell lysis, however both cytokines can also be released via autophagy associated vesicles [190]. The rapid induction of IL-18 secretion in human enteroid monolayers is not accompanied by overt epithelial cell death, as the monolayer remained intact throughout duration of the experiments, indicating the IL-18 is being secreted via some other mechanism than cell lysis. However, cell death needs to be quantified to fully rule out cell death as the route of IL-18 release from human enteroid monolayers. Recently it has been shown that cleavage of GSDMD by CASP4 promotes pore formation that likely allows IL-18 release prior to complete cell death [159]. Thus, unlike transformed cells, human enteroid monolayers are capable of responding rapidly to infection and potentiating an immune response through IL-18 secretion.

Maturation of IL-18 and IL-1 $\beta$  is carried out by CASP1 [157], however the relative dominance of CASP1, CASP4, and CASP5 in humans and CASP11 in mice is debatable. It has

been shown extensively in mice that CASP1 is the dominant player during *S. Typhimurium* infection of immune cells and intestinal epithelial cells [171, 172, 191], while CASP11 impacts immune responses and inflammation in mice by effecting macrophage cell death [171]. Although there is good agreement on separable roles of CASP1 and CASP11 in mice, results in human cells have varied significantly, largely due to different experimental set ups and cell types employed [154, 165, 166]. CASP4 and CASP5 have been shown to be important in human monocytes for mediating cell death and recruitment of the NLRP3/PYCARD/CASP1 inflammasome [166, 169]. Additionally, a one-step mechanism was recently described in which LPS treatment of human monocytes was sufficient to induce CASP5 cleavage, and CASP5 activity was required for IL-1 $\beta$  release [165]. In contrast, CASP1 is primarily responsible for maturation of IL-1 $\beta$  and IL-1 $\alpha$  [165, 166, 192], but can mediate GSDMD cleavage or recruitment of CASP8 to mediate cell death [157, 167]. Notably, many of the studies that inform this model were performed in immune cells, which differ significantly from intestinal epithelial cells, both in terms of physiology as well as mechanisms of interaction with bacterial pathogens. Experiments in human epithelial cells have been more limited. Using C2Bbe1 cells, it was found that CASP4 is critical for restricting intracellular replication of *S. Typhimurium*, IL-18 secretion, and mediating extrusion of infected cells [154]. Unfortunately, C2Bbe1 cells do not express detectable CASP1 or CASP5 [154] making it difficult to parse the relative importance of the different caspases during *S. Typhimurium* infection. However, this data would suggest that CASP4 inflammasome does not require recruitment of the NLRP3/PYCARD/CASP1 inflammasome to mediate secretion of IL-18. Given the discrepancy in the results, it underscores the need to investigate inflammasome activation in response during *S. Typhimurium* infection of

untransformed intestinal epithelial cells that express more than one pro-inflammatory caspases, such as enteroids.

Gene editing primary cells is a notoriously difficult problem to tackle. To circumvent the need to knockout caspases in human cells many researchers have used peptide inhibitors of caspases to evaluate the role of caspases during various cellular processes. It is important to note that the peptide inhibitors are relatively promiscuous amongst the different pro-inflammatory caspases. Z-WEHD-FMK is marketed as an inhibitor of CASP1 and Z-YVAD-FMK is marketed as an inhibitor of CASP4/5, however both of these inhibitors can inhibit all three pro-inflammatory caspases [178, 179]. Treatment of human enteroid monolayers and C2Bbe1 cells with either Z-WEHD-FMK or Z-YVAD-FMK 30 min post-infection reduced *S. Typhimurium*-induced IL-18 secretion, verifying that IL-18 secretion is dependent on pro-inflammatory caspase activity. Although not statistically significant, Z-YVAD-FMK appeared to inhibit IL-18 secretion to a greater extent than Z-WEHD-FMK, suggesting that CASP4/5 is more important for *S. Typhimurium*-induced IL-18 secretion. The cells were treated with concentrations of the inhibitors that far exceeded the saturation concentration for all three pro-inflammatory caspases [178, 179, 193], yet both human enteroid monolayers and C2Bbe1 cells still secreted low levels of IL-18. Moreover this residual IL-18 secretion was not abrogated by 3 h pre-treatment of human enteroid monolayers and C2Bbe1 cells with either Z-YVAD-FMK or Z-WEHD-FMK. This irreducible quantity of IL-18 secretion is potentially due to an inaccessible caspase pool or poor diffusion of the inhibitors across the cell membrane. The latter is likely the main contributor to the residual IL-18 secretion since both Z-YVAD-FMK and Z-WEHD-FMK are composed of hydrophobic residues and thus less likely to passively cross the cell membrane [194].

To clearly identify the critical caspase for sensing and responding to *S. Typhimurium* infection, we knocked out all three caspases in human enteroids using LentiCRISPR. Human enteroids can be genetically manipulated [85, 94, 135], but pose greater technical challenges than standard cell lines. First, human ileal enteroids grow slowly (~7 day doubling time) thus outgrowth of clonal lines takes weeks to months. Second, difficulties stably transducing human enteroid stem cells have been reported [85]. Third, human enteroids are capable of fusing with neighboring enteroids [195], creating a heterogenous population upon fusion. Fourth, unlike standard cell lines in which cloning discs or rings can be employed to isolate single colonies, individual human enteroids must be manually picked under a dissecting scope using a micropipette and transferred to individual wells. Fifth, human enteroids do not thrive in isolation and clonal selection results in a high attrition rate.

Provided the many technical challenges described above and the high improbability of achieving pure clonal populations we wanted to determine which alleles are present in the knock out enteroid clones. We analyzed the regions targeted by lentiCRISPR using next generation sequencing. For both *CASP4* KO enteroid clones, the cultures were composed of a mixed population but all of the alleles were edited, which was further supported by lack of *CASP4* protein expression in the clonal populations (Fig. 10D and 13A). The majority of the alleles in the *CASP1* KO enteroid clone were edited, but a very low frequency of one wild-type allele was found in the population (Fig. 13A). Western blot analysis of the *CASP1* KO enteroid clone demonstrated that this clone does not express detectable *CASP1* protein (Fig 10C), therefore we consider it to be knocked out for *CASP1*. Unlike the *CASP1* and *CASP4* KO enteroid clones, both *CASP5* KO clones had mixed populations of wild-type and edited alleles, indicating that

these clones are actually heterozygous for *CASP5*. Given that this occurred in both *CASP5* heterozygous enteroid cultures it is likely some epigenetic change prevented editing of one allele.

*CASP1* is the only definitively identified processor of pro-IL-18 [196]. It is thought that *CASP4* or *CASP5* cannot directly cleave pro-IL-18 but instead recruits the NLRP3 inflammasome [197]. Interestingly, IL-18 can be cleaved via a *CASP1*-independent mechanism [196]. IL-18 is potentially cleaved by another as yet unidentified cellular protein in C2Bbe1 cells given that they do not express detectable levels of *CASP1* protein [154]. Unlike C2Bbe1 cells, human enteroids express *CASP1* and *CASP4*, allowing for a more complete interrogation of caspase sufficiency following *S. Typhimurium* infection. *CASP5* het enteroid monolayers and *CASP1* KO enteroid monolayers secreted IL-18 in response to *S. Typhimurium* infection comparable to wild-type. Strikingly, *CASP4* KO enteroid monolayers did not secrete IL-18 following *S. Typhimurium* infection. Although *CASP4* KO enteroid monolayers lacked IL-18 secretion, they still had detectable levels of pro-IL-18 similar to wild-type, indicating that this phenotype is not due to a lack of pro-IL-18. Moreover, *CASP4* KO enteroid monolayers up-regulated expression of IL-8 and secrete IL-8 protein in response to infection, suggesting that the *CASP4* KO enteroid monolayers are still capable of sensing and responding to *S. Typhimurium* via an inflammasome-independent pathway. Taken together, these data suggest that *CASP4* is a critical component of the intestinal epithelial cell immune response during *S. Typhimurium* infection of untransformed human enteroid monolayers.

Previous work in mice and in C2Bbe1 cells has demonstrated that absence of inflammasome machinery leads to increased bacterial burden in the epithelium [154, 172, 174]. Caspases themselves are not directly antibacterial, but mediate processes that function to limit bacterial replication. In the intestinal epithelium caspases restrict intraepithelial bacterial loads

by initiating extrusion of infected cells from the monolayer [154, 172, 174]. In agreement with previous results in C2Bbe1 cells [154], *CASP4* KO enteroid monolayers had higher bacterial burdens than wild-type (Fig. 14B). In contrast, *CASP1* KO and *CASP5* het enteroid monolayers had similar levels of intracellular bacteria (Fig. 14A and C). The increase in bacterial burden of the *CASP4* deficient cells likely reflects a lack of activation of downstream mediators rather than direct antibacterial functions of the pro-inflammatory caspases. Activated *CASP11*, *CASP4*, and *CASP5* cleave Gasdermin-D (GSDMD) exposing the N-terminal domain [159, 167]. The expression of the GSDMD N-terminal domain alone is sufficient to induce cytotoxicity [167] through oligomerizes and forms pores in the inner leaflet of cellular membranes [159] (Fig. 9). Interestingly, cleaved GSDMD can kill bacteria in suspension, but it is currently unknown whether this direct bactericidal activity is physiologically relevant event. The elevated bacterial burden in *CASP4* KO enteroid monolayers is potentially due to absence of GSDMD activation. Another potential reason for lower bacterial burdens in wild-type human enteroid monolayers is due to the presence of gentamicin during the experiment. Cells undergoing pyroptotic cell death and extrusion from the monolayer lose membrane integrity [174], potentially leading to uptake of gentamicin in these cells. The diffusion of gentamicin into the cells could be killing bacteria contained within the extruding cells or cells with activated GSDMD. To offset this potential effect the concentration of gentamicin is lowered from the initially high concentration of 100 µg/ml at the beginning of the experiment to 10 µg/ml for the majority of the experiment. However, even this low concentration of gentamicin could likely killing some of the intracellular bacteria in cells with reduced membrane integrity.

Previous studies have identified two replication phenotypes within epithelial cells, slow replicating bacteria contained within the SCVs and hyper-replicating bacteria present in the cytosol

[153, 154, 172]. Hyper-replication has been noted in both transformed human cell lines and mouse intestinal epithelial cells *in vivo*, however, the extent to which the bacteria hyper-replicated varied. Hyper-replication appeared to be more extreme in the transformed human cell lines (>50 bacteria/cell) [153, 154, 174] than *in vivo* (>20 bacteria/cell) [172]. Furthermore, hyper-replication was a rare event in wild-type mice and only became evident when all six *Naip* genes were deleted [172]. This could be due to rapid extrusion of infected intestinal epithelial cells from the epithelium of wild-type mice compared to *Naip* deficient mice [172]. Thus, it is unclear whether hyper-replication occurs in untransformed human intestinal epithelial cells.

Human enteroid monolayers infected with *S. Typhimurium* did not show evidence of hyper-replication as defined by (>50 bacteria/cell) (Fig. 15). In wild-type human enteroid monolayers the number of bacteria per cell rarely exceeded 9. This not due to our infection conditions or protocol as we were able to recapitulate the data in C2Bbe1 cells (Fig. 15). Moreover, to achieve a quantifiable number of bacteria at 7 h post-infection, we had to increase the number of input *S. Typhimurium* from an MOI of 150 to an MOI of 750. This data corroborates our previous data from CFU enumeration; human enteroid monolayers are not as susceptible to *S. Typhimurium* infection as C2Bbe1 cells. These data suggest that they high amount of hyper-replication in C2Bbe1 cells is potentially an artefact of transformed cells.

We showed that *CASP4* KO enteroid monolayers contain higher numbers of intracellular bacteria at 7 h post-infection than wild-type (Fig 14). This data was collected by enumeration of intracellular CFUs, which is an average across the entire population. Previous reports have shown that knock down of *CASP4* in C2Bbe1 monolayers led to more cells with hyper-replicating bacteria [154]. Similarly, *CASP4* KO enteroid monolayers contained more cells with >6 bacteria per cell ( $36.33\% \pm 32.65\%$ ) than WT enteroid monolayers ( $7.33\% \pm 4.93\%$ ) (Fig.

16). Even with the absence of CASP4, only rare cells within the enteroid monolayers contained more than 20 bacteria. It is important to note that the hyper-replication phenotypes were determined in a cell line derived from colon cancer [154, 174] and cecal tissue in mice [172]. Although all are derived from the GI tract, colon cancer and cecal tissue are very different from the human small intestinal epithelium. These data support the findings in C2Bbe1 cells that CASP4 is important for restricting intracellular replication, but highlight the differences between transformed and untransformed cells, and cecal/colonic vs small intestinal epithelial cells.

The data presented here are not inconsistent with the findings from studies in mice in which NAIP/NLRC4/CASP1 inflammasome is critical for intestinal epithelial cell extrusion and restriction of intraepithelial bacterial replication [172]. Rather, it highlights the fact that mice and humans differ significantly in a variety of ways including repertoire of innate immune genes, antimicrobial peptides, and susceptibility to pathogens [25, 64, 77]. Human enteroids have illuminated interesting aspects of host-pathogen interactions that could not be appreciated in existing models [87, 114, 140]. Thus, using human enteroids to study other human pathogens, specifically human restricted pathogens, could reveal previously unappreciated aspects of host-pathogen interactions.

## **Chapter 5: Significance and Future Perspective**

### **Human enteroids as a platform for studying enteric pathogens**

The intestinal epithelium is the first cellular barrier to infection by fecal-orally transmitted pathogens; both enteric pathogens and those that cause systemic disease (i.e. poliovirus). Studying the interaction of pathogens with the human intestinal epithelium is key to further understanding pathogenesis of these diseases. Due to the absence of a reliable and sustainable cell culture system for untransformed human intestinal epithelial cells for many

years, much of our understanding of host-pathogen interactions in the gut has relied on models that do not fully recapitulate the human intestinal epithelium. It's been well noted that mice do not completely model human disease for many of these human pathogens. Human enteroids, composed of untransformed intestinal epithelial cells, are a valuable tool for investigating many questions related to gut physiology, drug screening, immune responses, susceptibility to infection, and effect of virulence factors on intestinal epithelial cells.

Human enteroids support replication of diverse enteric viruses including adenovirus, rotavirus, norovirus, and enterovirus [15, 87, 88, 114, 136]. Although these viruses replicate well *in vivo* and are excreted in high numbers from infected individuals, isolation of these enteric viruses has been difficult. We showed that clinical isolates of enteric adenovirus, which are highly fastidious, replicate in human enteroids. Thus, human enteroids are potentially a unified platform for culturing fastidious enteric viruses. Expanding upon their capacity to support enteric viral replication, enteroids could help to model other related diseases in the GI tract.

Hematopoietic stem cell transplant (HSCT) recipients are susceptible to reactivation of human adenoviruses in the intestine [107, 198] and intestinal graft-versus-host disease (GVHD) [199]. Reactivation of HAdV in the gut is a significant problem in HSCT patients because it often precedes systemic HAdV infection, a contributor to fatal outcomes. Additionally, pediatric small bowel transplant recipients are susceptible to adenovirus infection in the GI tract. Human enteroids have the potential to be a new means to understand molecular mechanisms driving the resurgence of latent adenovirus infection, development of GVHD, and drug screening to find drugs that inhibit adenovirus replication.

We and others have put significant effort into using human enteroids to study enteric viral replication, however human enteroids and intestinal organoids have also been used to study

enteric bacterial infection. Human enteroids can be infected by *Shigella* [90, 91] and enterohemorrhagic *E. coli* (EHEC) [93]. *Clostridium difficile* infection of 3D human intestinal organoids resulted in disruption of the epithelial paracellular barrier [200]. Because human intestinal organoids contained polarized cells with microvilli they allowed for visualization of the epithelial barrier disruption manifesting as disorganization of the epithelium and loss of the brush border. Previous studies with human intestinal organoids showed that polarized human intestinal epithelial cells are susceptible to *S. Typhimurium* infection [186]. We showed here that not only are human enteroids susceptible to *S. Typhimurium* infection, but that key differences in *S. Typhimurium* infection of untransformed intestinal epithelial cells and C2Bbe1 cells, a transformed cell line, exist. *S. Typhimurium* infection of human enteroids elicited robust and rapid IL-18 secretion compared to the standard colonic epithelial cell line used. Furthermore, human enteroids did not take up as many bacteria as C2Bbe1 cells. Based on these interesting findings in both human enteroids and human intestinal organoids, it is likely that human enteroids will illuminate new aspects of infection processes and host responses to other enteric bacterial pathogens.

### **Future perspectives**

The advent of tissue culture in the early 20<sup>th</sup> century led to the establishment of cells that could be cultured indefinitely *in vitro*. These cell cultures launched a revolution that gave rise to the polio vaccine, antivirals, and many more advancements in science. However, culturing cells in 2D is very different from how the cells exist *in vivo*. The desire to culture not only malignant, but primary cells, in a more physiologically relevant structure *in vitro* has been around for many years yet has struggled to come into fruition and broad usage. Recently, the Clevers group

developed 3D tissue culture structures derived from adult intestinal stem cells, termed enteroids [201]. Organoids have now been derived from esophagus, stomach, intestine, liver, pancreas, brain, kidney, endometrium, breast, and prostate, as well as from both primary and transformed tissues [201] [202]. With the development of enteroids/organoids, numerous questions can now be asked in more physiologically relevant structures.

Humans are susceptible to a wide variety of enteric bacterial pathogens, both broadly infectious and human-restricted pathogens (e.g. *Shigella*). Moreover, diarrheal diseases represent a significant morbidity and mortality world-wide, accounting for more childhood deaths than AIDS, measles and malaria combined [203]. Rotavirus, *Shigella spp.*, *Vibrio cholerae*, adenovirus, and non-Typhoidal *Salmonella spp.* are responsible for the greatest number of infectious diarrheal related deaths worldwide [204]. Although many of the enteric pathogens listed above and other enteric pathogens are excreted in high numbers from infected individuals, clinical isolates have been difficult to culture *in vitro* (rotavirus and adenovirus) [129] or we lack suitable animal models that do not require young mice, highly immunocompromised mice, extremely high doses, or alternative routes of infectious (*V. cholerae*, *Salmonella enterica* serovar Typhi, and *Shigella spp.*) [205-208], or a surrogate bacterial species is used *in vivo* (EHEC) [209].

Investigating how these pathogens interact with and infect intestinal epithelial cells is critical to understanding their pathogenesis. Many aspects of the intestine are not recapitulated *in vitro* in transformed cell lines but are present in enteroids. Enteroids have allowed us and others to study fastidious enteric viruses *in vitro*. We showed HAdV-5 preferentially infects goblet cells over non-goblet cells [87], a phenotype that could not have been demonstrated in a cell line. Moreover, we showed that HAdV is restricted by interferon pretreatment in enteroids, but not

A549 cells. Furthermore, we lacked a cell culture system for studying human norovirus for decades. However, the Estes lab recently demonstrated that human norovirus infects human enteroids in the presence of bile acid [88]. Interestingly, addition of bile acid to transformed cell lines is not sufficient to promote human norovirus replication, highlighting the value of using human enteroids. Thus, although enteroids are cultured *in vitro* they have properties that are absent in standard cell culture.

The field of non-Typhoidal *Salmonella spp.* is vast with huge amounts of knowledge on the basic physiology of the bacteria, infection of transformed epithelial cells, primary immune cells, transformed immune cells, and mice. However, for many years this immense database lacked information on how non-Typhoidal *Salmonella spp.* infects untransformed human intestinal epithelial cells. Here we show the importance of using enteroids to study enteric bacterial infections. Untransformed intestinal epithelial cells are less susceptible to *S. Typhimurium* infection and secrete IL-18 faster and to a greater degree than C2Bbe1 cells. Using human enteroids we substantiated the findings that CASP4 is the dominant caspase responsible for responding to and restricting intraepithelial growth of *S. Typhimurium* in human epithelial cells. Moreover, these data highlight the difference between mouse and human cells. Previous work showed that CASP1 is crucial for restriction of *S. Typhimurium* infection of mouse intestinal epithelial cells *in vivo*, whereas the mouse ortholog of CASP4, Casp11 is dispensable. Collectively, these data demonstrate the utility and power of using human enteroids to better understand enteric pathogens.

The work that has been done in enteroids to study enteric viruses and enteric bacteria is just the beginning. It will be important to corroborate what has been found in transformed cells and animal models with what occurs in untransformed human intestinal epithelial cells. Several

enteric pathogens are human restricted pathogens (*Shigella* and *S. Typhi*) making it difficult to study them *in vivo*. Studying *S. Typhi in vivo* requires generation of humanized mice in which the mouse bone marrow is replaced with human embryonic cord blood [208]. These mice have provided key insights into *S. Typhi* pathogenesis, however, other than the circulating immune cells, every other cell in the mouse, including the intestinal epithelium, is still of mouse origin. Thus, the results of any experiment is a mixture of human and mouse responses. Similarly studies on *Shigella*, the second leading cause of diarrheal death, has suffered from a lack for a suitable animal model, thus we have a limited understanding of what occurs in the GI tract. Although *Shigella* can infect humans with less than 500 colony forming units [210], guinea pigs require high doses to get a low level of infection [211]. This has been attributed to lack of traditional adhesins, however this does not seem to be a significant issue for human infections. Two recent studies demonstrated that human enteroids can be used to investigate *Shigella* infections *in vitro* [90, 91]. It will be interesting to see how enteroids can further inform our understanding of *Shigella* infection of intestinal epithelial cells and downstream pathogenesis.

There has been a significant push towards developing organs-on-a-chip to model cellular diversity, tissue architecture, and organ-organ interactions [212]. Organs-on-a-chip would be an *in vitro* system that more faithfully recapitulates *in vivo* physiology. Notably, in the context of the gut the flow of luminal contents is an important physiological feature that is absent in both standard 2D culture and enteroids/organoids. Intestine on a chip using cells derived from human enteroids and colonoids was recently developed [213], which allows for flow of fluids across the intestinal epithelial cells. This represents an opportunity to study the effect of luminal flow and sheer stress on different cellular processes. Pharmaceutical companies are keenly interested in this technology because it could offer better indicators of drug potencies and toxicities. In fact,

intestine-on-a-chip has been used to study the effects of microbiome-derived metabolites during EHEC infection of colonic epithelial cells [214]. EHEC infection in the presence of human microbiome-derived metabolites caused more damage and elicited a greater immune response in the intestinal epithelial cells than when in the presence of mouse microbiome-derived metabolites. It's possible that intestine-on-a-chip could potentially be a platform for reconstituting the human microbiome *in vitro* allowing for a multitude of studies on how the microbiome affects pathogens and drug metabolism. Organs-on-a-chip could also be extended to studying complex interactions among different organs. Connecting intestine-on-a-chip with livers- and kidneys-on-a-chip could offer a unique way to study the effects of antibiotics and antivirals on enteric infections with concomitant understanding of metabolites produced and their effect on connected organs. It is clear that organs-on-a-chip have the potential to be a powerful tool for studying host-pathogen interactions, physiology, and drug potencies. Human enteroids and organoids derived from other sites in the human body are transforming the fields of virology, bacterial pathogenesis, gut physiology, and many more. We have just scratched the surface of what questions can be answered using organoids. It will be interesting to see what is uncovered using these structures which more accurately model the *in vivo* architecture and cellular composition.

### **Supplement 1: Paneth cells**

#### **Location and secretory function of Paneth cells**

Paneth cells are located at the base of the crypts of Lieberkühn in the small intestine of various animals and are interspersed amongst the intestinal stem cells from which they differentiate [5, 6, 8, 215-219]. Unlike other differentiated epithelial cell types (goblet cells, enteroendocrine cells, tuft cells, and enterocytes), which migrate out of the intestinal crypt,

Paneth cells remain within the crypt base [9]. Also, unique to Paneth cells are their long lifespans ( $\approx 30$  days) compared to the other differentiated epithelial cell types ( $\approx 3\text{--}5$  days) [10, 11, 220]. Paneth cells are characterized by apically located, large, cytoplasmic, and electron-dense granules that contain a mixture of antimicrobial peptides and proteins, cytokines, scaffolding molecules, and proteases. Mature granules are surrounded by an acidic mucopolysaccharide complex, which is visible as a halo in electron micrographs [221]. Like many dedicated secretory cells that undergo regulated secretion, Paneth cells package only a subset of their secreted proteins into their cytoplasmic granules. They also utilize constitutive secretion mechanisms common to most epithelial cells. A series of studies have elucidated secreted products, both granule-dependent and independent, that are specific to Paneth cells through a variety of methods including laser capture microdissection and single cell transcriptomics [7, 215, 217, 222-227]. The most well-known and characterized granule contents are the antimicrobial peptides and proteins; however, other proteins have also been localized to these structures. (Adapted from [12])

### **Models for studying Paneth cells**

Mice, rats, chickens, equines, nonhuman primates, and humans have Paneth cells in their small intestines, although they are not found in all animals, such as sheep, cows, and seals [137, 217, 218, 228, 229]. The prevalence of Paneth cells in animals is not fully known due to both a lack of thorough investigation and the absence of uniform criteria for identifying Paneth cells in GI tracts. Moreover, there appears to be no clear evolutionary relationship that explains the presence or absence of Paneth cells among species. Most of what we know about Paneth cell development and function is derived from mouse studies. Until recently, with the exception of limited studies of short-lived intestinal explants or crypt preparations, Paneth cells could only be

studied *in vivo* due to a lack of a culture system. In 2009, pioneering work by the Clevers group established a new model for culturing primary intestinal epithelial cells *in vitro*, termed enteroids [82]. Enteroids are three-dimensional tissue culture structures that contain the diversity of intestinal epithelial cell types found in the small intestine or colon [230]. They are untransformed and can be derived from adult intestinal epithelial, embryonic, or induced pluripotent stem cells, and their method of derivation determines the nomenclature used to describe them [84]. They can also be genetically manipulated, cryopreserved, and cultured continuously for extended periods of time. The robust formation of Paneth cells in mouse enteroids allows the manipulation and investigation of these cells *in vitro* for the first time, and enteroids are being used extensively in recent studies of intestinal development. Paneth cells in enteroids secrete mature  $\alpha$ -defensins that maintain antimicrobial activity, and they can be used to model oral infection by microinjecting bacteria and viruses into the lumen of enteroids, which is topologically equivalent to the small intestinal lumen [126, 200, 231, 232]. Enteroids provide a unique opportunity to study the interaction of enteric viruses with primary, intestinal epithelial cells. They have been shown to support the replication of rotaviruses, noroviruses, enteroviruses, and adenoviruses [15, 87, 88, 114, 126]. Additionally, the utility of enteroids in investigating host-pathogen interactions has become well established.

Although Paneth cells form in mouse enteroids, differentiated human enteroids lack differentiation of Paneth cells. We have sporadically seen Paneth cells in human enteroids, but Paneth cell differentiation is a rare event [85]. It is unknown why Paneth cells form spontaneously in mouse enteroids, but not in human enteroids. The deficiency could be due to a variety of factors including absence of specific growth factors, lack of contact with cells in the

stroma, or absence of the necessary Wnt gradient between Paneth cells, stem cells, and stromal cells. (Adapted from [12])

### **Inducing Paneth cells in human enteroids**

#### *Expression of Wnt3 in human enteroids*

Many of the Paneth cell-specific gene products are controlled by Wnt signaling [27, 233, 234]. When Wnt is present, it binds to its receptor Frizzled, leading to an intracellular signaling cascade that culminates in translocation of  $\beta$ -catenin to the nucleus and association with specific members of the T cell factor (TCF) family to act in concert to turn on transcription of target genes [230, 235]. The promoters of enteric  $\alpha$ -defensin genes in mice, *DEFA5* (HD5) and *DEFA6* (HD6) in humans, and *Mmp7* in both species contain consensus sequences for  $\beta$ -catenin/TCF-binding sites [27, 234, 236, 237]. Co-transfection of luciferase reporters driven by mouse enteric  $\alpha$ -defensin, *DEFA5*, and *DEFA6* promoters with activated  $\beta$ -catenin and TCF4 constructs greatly increased luciferase activity over basal activity [27]. Additionally, mutation of the  $\beta$ -catenin/TCF-binding sites in the *DEFA6* promoter significantly reduced luciferase activity of these constructs. Furthermore, deletion of *Tcf4* in the embryonic mouse small intestine significantly reduced enteric  $\alpha$ -defensin expression [26]. Thus, the Wnt- $\beta$ -catenin/TCF axis is important in regulating expression of specific Paneth cell products. (Adapted from [12])

Wnt signaling is critical for Paneth cell formation in addition to Paneth cell-specific gene expression [238]. Ectopic expression of Wnt3 in mouse enteroids induces Paneth cell differentiation [239]. Conditional deletion of APC, a protein complex that prevents  $\beta$ -catenin translocation to the nucleus, in intestinal epithelial cells results in increased Paneth cell differentiation and mislocalization out of the crypt base in the small intestine and Paneth cell formation in the colon, which does not normally contain Paneth cells [233]. Conversely,

expression of a hypomorphic allele of the  $\beta$ -catenin gene led to reduced numbers of granular cells in intestinal crypts and an associated decrease in production of lysozyme and Ang4. Abnormal Paneth cell localization in these models may be due to disruption of the EphB receptor/B-type ephrin gradient. EphB receptors are TCF/ $\beta$ -catenin responsive receptors required to correctly position Paneth cells along the crypt/villus axis [236]. *EphB3* is normally expressed in the crypt up to the +4 LRC position. Cells expressing this receptor are positioned inversely to a gradient of the ligand ephrin-B1, expression of which is decreased by TCF/ $\beta$ -catenin signaling [236, 240]. Thus, deletion of *EphB3* also leads to mislocalization of Paneth cells outside of the crypt base [236]. Interestingly, these mislocalized Paneth cells lack nuclear  $\beta$ -catenin but express lysozyme, demonstrating that Paneth cell morphology and lysozyme expression can occur in the absence of  $\beta$ -catenin stabilization and translocation to the nucleus. (Adapted from [12])

Taken together these results demonstrate that Wnt signaling is essential for proper Paneth cell development. Mouse enteroids spontaneously differentiate and contain Paneth cells without the addition of exogenous Wnt. In contrast, human enteroids are propagated in an undifferentiated state in the presence Wnt3a to support division of the intestinal stem cells. Withdrawal of Wnt3a has been shown to lead to differentiation of the enteroids into mature enterocytes, goblet cells, and enteroendocrine cells but not into Paneth cells. Even though Wnt3a is highly similar to Wnt3, it is not expressed in the GI tract where Paneth cells are resident [239]. Additionally, Wnt3 produced by Paneth cells is tethered to the cell membrane and diffuses along the membrane towards the stem cells [241]. Thus, in the GI tract a directed Wnt3 gradient exists to allow for crosstalk between Paneth cells and stem cells that is not recapitulated *in vitro* by exogenous addition of Wnt3a.

To recreate this Wnt3 gradient in human enteroids we drove expression of Wnt3 off of the human defensin 5 promoter (HD5p) in a lentiviral vector. *DEFA5*, the gene that encodes HD5, is only expressed in Paneth cells in the small intestine, thus expression of Wnt3 should be restricted to cells within the enteroid that have been specified as Paneth cells. This approach has been shown to work *in vivo* with transgenic expression of *DEFA5* in the mouse GI tract being restricted to Paneth cells [59]. We transduced human enteroids with the lentivirus containing the HD5pWnt3 construct and selected the bulk population with puromycin. To assess whether the HD5pWnt3 enteroids had become Wnt independent, the enteroids were seeded into media without Wnt3a conditioned media and passaged every 7 days. Wild-type human enteroids gradually dwindled in numbers while HD5pWnt3 enteroids propagated in the absence of Wnt3a conditioned media (data not shown). The HD5pWnt3 enteroids are Wnt-independent, but Paneth cells were not evident by bright field microscopy. Wild-type and HD5pWnt3 enteroids were histologically sectioned and stained with hematoxylin and eosin to evaluate the differentiation status of the enteroids. Both wild-type and HD5pWnt3 enteroids were composed of single cell epithelium with polarized cells indicative of mature enterocytes (Fig 17A-B, D-E). No morphologically distinct Paneth cells present in the population, suggesting expression of Wnt3 in cells specified as Paneth cells is not sufficient for Paneth cell differentiation *in vitro*.

#### *Expression of Mist1 in human enteroids*

In addition to unique gene expression, secretory morphology is a defining feature of Paneth cells. The genetic factors that contribute to this characteristic are not completely known, and there is evidence that signaling pathways that specify Paneth cell secretory morphology are distinct from those that control the expression of Paneth cell secretory products. For example,

Wnt/ $\beta$ -catenin signaling is dysregulated in some tumors that express Paneth cell gene products without a secretory morphology [26]. Additionally, in mice, Paneth cell effectors are expressed prior to the development of mature Paneth cells, which begins 7 days after birth and reaches adult levels 30 days after birth [242-244]. (Adapted from [12])

Mist1/BHLHA15 is a transcription factor that is important for normal secretory cell morphology and function in pancreatic acinar cells and gastric chief cells [245-247]. Pancreatic acinar cells and chief cells, like Paneth cells, have apically located secretory granules that fuse with the plasma membrane to release their contents. Loss of Mist1 in mice results in mislocalization of the granules, loss of apical-basal polarity, and failure in cell-to-cell communications [246]. Additionally, chief cells lacking Mist1 developed secretory granules in early stages of differentiation similar to wild-type but failed to extend their apical cytoplasm to accommodate the granules and achieve full cellular differentiation [245]. Moreover, induced Mist1 expression in gastric parietal cells, which release acid through non-regulated secretion, is sufficient to cause enlargement of the apical cytoplasm and development of apical granules [248]. Mist1 is not the driver of granule biogenesis but is a critical transcription factor in the morphological development of secretory cells.

Mist1 is expressed in Paneth cells [249], suggesting that induced expression of Mist1 in enteroids could promote development of cells that have already specified as Paneth cells. We engineered a similar construct as above with the human defensin 5 promoter driving expression of Mist1 (HD5pMist1) in a lentiviral vector. Human enteroids were transduced with the HD5pMist1 construct and the bulk population was selected. To determine whether expression of Mist1 in a Paneth-cell specific manner had any effect on cellular morphology we histologically sectioned and stained HD5pMist1 human enteroids with H&E. Both wild-type and

HD5pMist1 enteroids contained single cell, polarized epithelia indicative of mature enterocytes (Fig 17A-B, D-E), however, no morphologically distinct Paneth cells present in the population. These data indicate that expression of Mist1 in a Paneth cell-specific manner is not sufficient for Paneth cell differentiation *in vitro*. Taken together, these data suggest that Paneth cell differentiation likely requires complex signals beyond overexpression of specific growth and transcription factors.

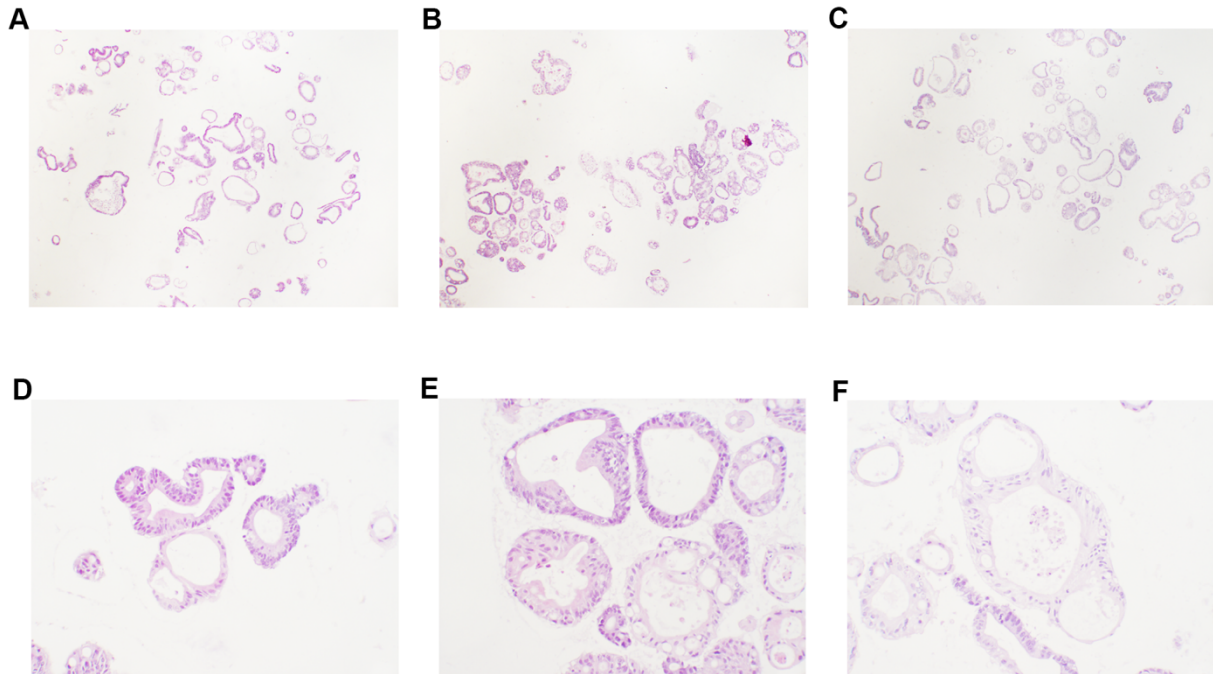


**Figure 17 Expression of Mist1 or Wnt3 is not sufficient to induce Paneth Cell differentiation**

Human enteroids were transduced with either (B) HD5 promoter-Wnt3 or (C) HD5 promoter-Mist1 lentiviral constructs. Differentiated wild-type (A,D), HD5 promoter-Wnt3 (B,E), and HD5 promoter-Mist1 (C,F) human enteroids stained with hematoxylin and eosin. A-C 20X objective and D-E 4X objective.

## **Chapter 6: Materials and Methods**

**Cells and cell culture.** 293 $\beta$ 5 [250], 293-SV5/V [120], A549 (ATCC), and C2Bbe1 cells (ATCC) were maintained in Dulbecco's modified Eagle's medium (DMEM) with 10% fetal bovine serum (FBS), penicillin, streptomycin, L-glutamine, and nonessential amino acids (NEAA). C2Bbe1 cells culture was supplemented with 10  $\mu$ g/ml human transferrin (Sigma).

**Viruses.** Prototype strains HAdV-5p (strain Adenoid 75), HAdV-16p (strain Ch. 79), and HAdV-41p (strain Tak) were acquired from ATCC. Large-scale cultures of these viruses from A549 (HAdV-5p and HAdV-16p) or 293 $\beta$ 5 or 293-SV5/V cells (HAdV-41p) were twice purified by CsCl density gradient ultracentrifugation as described in reference 250. The purified virus was dialyzed against three changes of 150 mM NaCl, 40 mM Tris, 10% glycerol, and 2 mM MgCl<sub>2</sub> (pH 8.1), snap-frozen in liquid nitrogen, and stored at -80°C. The purified stocks were quantified by disrupting the capsids in 1% SDS for 4 min at 100°C and then measuring the concentration of viral DNA by Qubit fluorometric quantitation (Thermo Fisher Scientific). All other inocula used in these studies were virus-containing cell lysates. Enteroids were inoculated directly with lysate containing HAdV-12p (strain Huie) from ATCC. HAdV-40p (strain Dugan) lysate from ATCC was passaged once on 293-SV5/V cells prior to use. HAdV-41 clinical isolates (NY/2010/4845, NY/2010/4849, and NY/2010/4851) were originally detected and identified as HAdV in the laboratory of Howard S. Faden, Division of Infectious Disease, Children's Hospital of Buffalo, and then typed and characterized in the laboratory of Kirsten St. George, Laboratory of Viral Diseases, Wadsworth Center, New York State Department of Health (NYSDOH). They were passaged once on A549 cells and once on 239T cells in the St. George

lab prior to our use. Clinical isolates of HAdV-2 V-2375-18 and HAdV-41 V-2161 were kindly provided by the Centers for Disease Control and Prevention (CDC). Prior to our use, HAdV-2 V2375-18 had been passaged twice on HepG2 cells and once on A549 cells, and HAdV-41 V-2161 was passaged once on 293 cells. To measure the amount of virus in lysates, total DNA was isolated using the GeneJET Viral DNA and RNA purification kit (Thermo Fisher Scientific), and viral DNA was quantified by qPCR using primers for a conserved region of *hexon* (Table 1) against a standard curve of HAdV-5p genomes. HAdV-12p was quantified using primers specific for a region of *hexon* conserved between HAdV-A and HAdV-5 (Table 1) against the same standard curve. qPCR was performed with Sso Advanced Sybr green Supermix or Sso Fast Sybr green Supermix (Bio-Rad) on a Bio-Rad CFX Connect thermocycler.

**Bacterial strains.** *Salmonella enterica* serovar Typhimurium SL1344 (*S. Typhimurium*) was the wild-type strain used in these studies. Strains and plasmids are listed in Table 1.

| <b>Table 1.</b> Strains and plasmids used in this study     |   |
|---|---|
| Genotype  | Source  |
| <i>S. Typhimurium</i> SL1344 pFPV-<br><i>PrpsM::mCherry</i> | Kelly Smith (University of Washington)            |
| <i>S. Typhimurium glmS::Ptrc-mCherryST::FRT</i>             | Leigh Knodler (Washington State University) [154] |

**Infection of cell lines.** HAdV-5p, HAdV-16p, and HAdV-41p were serially diluted on 293β5, 293- SV5/V, and A549 cells in 96-well black wall plates (Perkins-Elmer). Infected cells were quantified 24 h post-infection by staining fixed cells with anti-hexon antibody 8C4 (1:900; Fitzgerald Industries) and an Alexa Fluor 488-conjugated secondary antibody (1:1,000). Total well fluorescence in relative fluorescent units (RFU) was measured with a Typhoon 9400

scanner. Each sample was normalized to the maximal value for HAdV-5p for each individual experiment and plotted relative to log MOI (genomes/cell).

For the time course, parallel samples of 293β5 cells were infected with the same number of genomes of HAdV-5p, HAdV-16p, and HAdV-41p (MOI, 5 to 10 genomes/cell). Viruses were incubated with cells for 45 min at 4°C with rocking. The inoculum was removed and replaced with complete medium. Every day postinfection, supernatant and cells were harvested together. Total DNA was isolated using the GeneJET viral DNA and RNA purification kit. Viral DNA was quantified by qPCR, as described above. Cellular genomes were quantified by qPCR using a standard curve of A549 genomic DNA and primers for *HPRT* (Table 2). The ratio of viral genomes to cellular genomes was calculated for each sample.

**Wnt3a conditioned medium.** L-Wnt3a cells were obtained from ATCC and propagated in DMEM with 10% FBS. Once cells were ~95% confluent, the cells were pooled and seeded at

| <b>Table 2. qPCR Primers for Virus Quantitation</b> |                                 |
|---|---------------------------------|
| Primer  | Sequence                        |
| HAdV Hexon FWD1                                     | GCVCTVGCCTCGACATGACTTTTGAGGTGGA |
| HAdV Hexon REV1                                     | TCGATGACGCCGCGGTG               |
| HAdV-A Hexon FWD1                                   | GATGCCGCAGTGGTCTTACATG          |
| HAdV-A Hexon REV1                                   | GCCACMGTGGGRTTYCTAAACT          |
| HPRT gDNA qPCR FWD2                                 | GAAAGGGTGTTCCTCATG              |
| HPRT gDNA qPCR REV2                                 | CAGCTGCTGATGTTTGAAATTA          |

5x10<sup>7</sup> cells per 15-cm dish in 10% FBS, 10 mM HEPES, 1X NEAA and 1X Glutamax in DMEM, and the cells were incubated for 4 days. The resulting conditioned medium (CM) was harvested and filtered. Each batch of Wnt3a CM was assayed using a Wnt-sensitive reporter system as follows: M50 Super 8X TOPFlash (Addgene 12456) or M51 Super 8X FOPFlash (Addgene 12457) was transfected into 293β5 cells with pRL-TK (Promega). After 24 h, the medium was changed to Wnt3a CM, and the cells were incubated for an additional 24 h. Cells

were lysed, and luciferase activity was measured using the dual luciferase reporter assay system (Promega), per the manufacturer's instructions. The ratio of firefly luciferase activity in TOPFlash-transfected cells to that in the FOPFlash-transfected cells, both normalized to *Renilla* luciferase activity, was calculated. CM was considered usable if this ratio exceeded the value for an archived batch of Wnt3a CM known to support human enteroids.

**Rspondin-1 conditioned medium.** 293-Rspondin-1 cells were obtained from Calvin Kuo (Stanford University) and maintained in DMEM with 10% FBS. Once the cells reached ~95% confluence, the cells were pooled and seeded at  $6 \times 10^7$  cells per 15-cm dish in 10% FBS, 10 mM HEPES, 1X NEAA and 1X Glutamax in DMEM, and the cells were incubated for 4 days. Rspondin-1 CM was harvested and filtered. Each batch of Rspondin-1 CM was assayed using the Wnt-sensitive reporter system described above, except that a mixture of 10% Rspondin-1 CM and 10% Wnt3a CM in ADF with 10% FBS, 10 mM HEPES, and 1X Glutamax was added to transfected cells. CM was considered usable if the activity in this assay exceeded that of an archived batch of Rspondin-1 CM known to support human enteroids.

**Noggin conditioned medium.** 293-Noggin cells were a gift from Hans Clevers (Hubrecht Institute) and maintained in DMEM with 10% FBS. Once the cells reached ~95% confluence, the medium was changed to 10 mM HEPES and 1X Glutamax in Advanced DMEM/F12, and the cells were incubated for 7 days. Noggin CM was harvested and filtered. Serial dilutions of each batch of Noggin CM were analyzed by immunoblotting with an anti-Noggin antibody (1:1,000; Abcam). CM was considered usable if the concentration of Noggin was comparable to that of a batch of Noggin CM known to support human enteroids.

**Human enteroids.** Adult human ileal tissue was acquired through NW BioTrust and NW BioSpecimen from normal, healthy tissue during surgical resections. The University of Washington Institutional Review Board has determined that the deidentified ileal tissue specimens used in this study do not meet the federal regulatory definition of research on human subjects. Ileal tissue was placed in ADF containing 1X antibiotic-antimycotic, 1X penicillin-streptomycin, and 100 µg/ml gentamicin at room temperature for 15 min. Following antibiotic treatment, the tissue was cut into 1-cm square pieces and placed in dissociation solution (8 mM EDTA and 10 mM dithiothreitol [DTT] in 1X Dulbecco's phosphate-buffered saline [DPBS]) for 90 min at 4°C with gentle rocking. Crypts were dissociated from the intestinal tissue by shaking in ADF supplemented with 20 µM Y-27632 (Abcam) and 0.5 µM Jag-1 (Anaspec). Fractions containing crypts were centrifuged at 400 × g at 4°C for 5 min and then plated in Matrigel (growth factor reduced, phenol red free). For experiments in chapters 2 and 3 enteroids were cultured in complete crypt culture medium (CCCM): 50% Wnt3a CM, 10% Rspodin-1 CM, 10% Noggin CM, 1X B-27 supplement, 1X N-2 Supplement, 10 µM SB202190 (Sigma), 10 mM HEPES, 1X Glutamax, 1X antibiotic-antimycotic, 1 mM N-acetyl-L-cysteine (Sigma), 10 µM Y-27632, 500 nM A-8301 (Tocris), 50 ng/ml epidermal growth factor (EGF), 10 nM gastrin (Sigma), 50 ng/ml fibroblast growth factor-2/basic (Peprotech), 100 ng/ml insulin like growth factor-1 (BioLegend), and 10 mM nicotinamide. Jag-1 (0.5 µM) was added only for the initial crypt culture. For experiments in chapter 4 enteroids were cultured in IF media [85]: 50% Wnt3a CM, 10% Rspodin-1 CM, 10% Noggin CM, 1X B-27 supplement, 10 mM HEPES, 1X Glutamax, 1X antibiotic-antimycotic, 1 mM N-acetyl-L-cysteine (Sigma), 10 µM Y-27632, 500 nM A-8301 (Tocris), 50 ng/ml epidermal growth factor (EGF), 10 nM gastrin (Sigma), 50 ng/ml fibroblast growth factor-2/basic (Peprotech), and 100 ng/ml insulin like growth factor-1

(BioLegend). All medium components are from Thermo Fisher Scientific, except where noted. Enteroids derived from individual patients were sequentially numbered (e.g., HIE3 or HIE5). Except for gene expression analysis, histology, and pilot experiments, all experiments were performed with enteroids (HIE5) from a single donor. For differentiation experiments in Chapters 2 and 3, human enteroids were sheared with a 23-gauge needle and plated into differentiation medium (CCCM without nicotinamide or CHIR99021 and with SB202190 reduced to 2.5  $\mu$ M) for 5 days.

**Enteroid monolayers.** Human enteroid monolayers were generated as previously described [88]. Briefly, 96-well plates were coated with human placental collagen, type IV (10  $\mu$ g/cm<sup>2</sup>; Sigma), in water for 1.5 h at 37°C. Undifferentiated human enteroids were removed from Matrigel using cell recovery solution (Thermo Fisher Scientific), dissociated in 0.05% trypsin at 37°C for 5.5 min, quenched with ADF containing 10% FBS, 10 mM HEPES, and 1X Glutamax, and mechanically dissociated with a pipette. Cells were passed through a 40- $\mu$ m cell strainer, centrifuged at 400  $\times$  g for 5 min, resuspended in CCCM, and plated onto collagen-coated wells (300,000 cells/well). The cultures were incubated for 5 days prior to infection.

**LentiCRISPR.** CRISPR guide RNAs (gRNAs) were designed using the CRISPR design tool in Benchling [Biology Software]. (2017). Retrieved from <https://benchling.com>. gRNAs were cloned into plentiCRISPR v2.0 (Addgene) or pRRL lentiCRISPR (Dan Stetson, University of Washington). LentiCRISPR vectors were transfected into 293 $\beta$ 5 cells with p-VSV-g (envelope) and psPAX2 (packaging) using Lipofectamine 2000 (ThermoFisher Scientific). Lentivirus was harvested at 72 h post-transfected and filtered through a 0.45  $\mu$ m PES syringe filter.

**Lentiviral transduction.** Human enteroids were cultured in 2X infection media (modified CCCM with 20 mM nicotinamide and 80% Wnt3a conditioned media) for 3 days prior to transduction. Human enteroids were removed from Matrigel using cell recovery solution, dissociated in 0.05% trypsin at 37°C for 5.5 min, quenched with DMEM containing 10% FBS, 10 mM HEPES, and 1X Glutamax, and mechanically dissociated with a pipette. Dissociated cells were pelleted at 300 × g for 5 min at 4°C. The pellet was resuspended in 2X infection media with 16 µg/ml polybrene and 20 µM Y-27632, mixed with an equal volume of lentivirus, plated into a 48-well plate, and centrifuged at 600 × g for 60 min at room temperature (25°C). The plate was then transferred to 37°C + 5% CO<sub>2</sub> for an additional 6 h. Transduced enteroids were harvested and plated in Matrigel. Matrigel plugs were overlaid with 500 µl of 2X infection media and incubated at 37°C + 5% CO<sub>2</sub> for 2 days. After two days the media was changed on transduced enteroids to CCCM with 2 µg/ml of puromycin. Selection media was changed every 3-4 days until all cells in the untransduced cells died. C2Bbe1 cells were seeded at 2.5 x10<sup>5</sup> cells per well in a 6-well plate one day prior to lentivirus transduction. 2 ml of lentivirus was added to C2Bbe1 cells and centrifuged at 300 × g for 30 minutes then transferred to 37°C + 5% CO<sub>2</sub> for 24 h. One day post-transduction C2Bbe1 cells were transferred to a 10-cm dish and cultured for an additional 24 h. Transduced C2Bbe1 cells were selected with 20 µg/ml of puromycin and selection media was changed every 3-4 days until all cells in the untransduced sample died.

**Clonal Selection.** Puromycin-resistant enteroids were removed from Matrigel using cell recovery solution, centrifuged at 600 × g for 10 min at 4°C, and resuspended in with DMEM containing 10% FBS, 10 mM HEPES, 1X Glutamax, 10 µM Y-27632, and 0.67 µM Jag-1. Human enteroids were transferred to a 60-mm dish on ice. Individual enteroids were picked

using a pipette under a dissecting scope and transferred to individual tubes with Matrigel on ice. Isolated enteroids in Matrigel were plated into individual wells in a 96-well plate. Each well was overlaid with 500  $\mu$ l of CCCM. Media was changed every 3-4 days until enteroids were large enough to see by eye. Individual enteroids were expanded using a 25-g needle and a 1 ml syringe. C2Bbe1 colonies were picked using cloning discs (Bel-Art) and transferred to individual collagen coated wells in a 24-well plate. Media was changed every 3-4 days until cells became ~80% confluent. Clonal cell lines were expanded up to 10-cm dishes.

**Verification of CRISPR knock outs.** Genomic DNA from potential CRISPR knockout human enteroids and C2Bbe1 cells was isolated using the GeneJET Genomic DNA Purification Kit (Thermo Fisher Scientific). Target regions were amplified by PCR using primers listed in Table 3. PCR products were subsequently gel purified using QIAquick Gel Extraction Kit (Qiagen). Purified PCR products were digested with restriction enzymes (Table 3) that cut at the site of editing and run on a 3% MetaPhor Agarose gel (Thermo Fisher Scientific). Edited clones were identified by a shift in bands compared to wild-type. PCR products from potential knockout clones were sequenced by Sanger Sequencing (Genewiz).

| <b>Table 3. PCR Primers and Enzymes Used for Knockout Verificaton</b> |                               |                           |
|---|-------------------------------|---------------------------|
| <u>Primer</u>   | <u>Sequence</u>               | <u>Restriction Enzyme</u> |
| <u>CASP1 FWD</u>  | <u>GGGAGAGGGAGGAGAGAAGGAA</u> | <u>BsaJI</u>              |
| <u>CASP1 REV</u>  | <u>TGGTAACAGGCAACCAGGTGAT</u> |                           |
| <u>CASP4 FWD</u>  | <u>GGGAATCCACGGCCCCATAA</u>   | <u>BstNI</u>              |
| <u>CASP4 REV</u>  | <u>AGTCTCAGCACTCACCCACCTC</u> |                           |
| <u>CASP5 FWD</u>  | <u>ATGAAACTGGCACATGTGAGGC</u> | <u>DdeI</u>               |
| <u>CASP5 REV</u>  | <u>GACCCACACACATGCAAACACA</u> |                           |

**CRISPR Knockout Variant Analysis.** 350-450 bp target regions were amplified using PCR primers containing Illumina Nextera XT adapter sequences (Table 4). Amplicons were purified

and barcoded according to the Illumina 16S Metagenomic Sequencing Library Preparation protocol. Briefly, amplicons were purified using AMPure XP beads (Beckman Coulter Genomics). Illumina sequencing adapters were attached to purified amplicons using Nextera XT Index Kit (Illumina) and indexed amplicons were purified using AMPure XP beads. The resulting library was normalized to 4 nM and run on Illumina MiSeq. Data was analyzed using Illumina BaseSpace.

| <b>Table 4. PCR Primers for Illumina Nextera XT Kit</b> |   |
|---|---|
| CASP1 NGS<br>FWD  | tcgtcggcagcgtcagatgtgtataagagacagTGGAGACTATTGAGGGAAACAA |
| CASP1 NGS<br>REV  | gtctcgtgggctcggagatgtgtataagagacagccCTTTCGGAATAACGGAGT  |
| CASP4 NGS<br>FWD  | tcgtcggcagcgtcagatgtgtataagagacagGGCCCCATAAAGAAGGAAAA   |
| CASP4 NGS<br>REV  | gtctcgtgggctcggagatgtgtataagagacagccAAACATCACAATCCTCTGC |
| CASP5 NGS<br>FWD  | tcgtcggcagcgtcagatgtgtataagagacagCGCTCATGGTAAATCTAGGAGG |
| CASP5 NGS<br>REV  | gtctcgtgggctcggagatgtgtataagagacagccTCTGCATACACCTTCA    |

**Transgene expression.** The lentiviral vector for transgene expression (pRRL puro) was constructed by replacing GFP in pRRL MND GFP (Addgene 36247) with puromycin resistance gene. Human Wnt3 (BC112118) and Mist1/BHLHA15 cDNA (BC1133394) were obtained from GE Dharmacon. HD5 promoter fused to Wnt3 or Mist1 was achieved by splice overlap extension PCR. HD5 promoter-Wnt3 and HD5 promoter-Mist1 constructs were inserted into pRRL puro vector using In-Fusion HD Cloning Plus Kit (Clontech). Lentivirus transfection, transduction, and selection were performed as above.

**Gene expression.** RNA was extracted from enteroids using RNA-Bee (Tel-Test), and cDNA was synthesized (Promega GoScript). Target gene expression was quantified by qPCR using the primers listed in Table 5. The  $\Delta\Delta C_T$  method (where  $C_T$  is threshold cycle) was used to determine the fold increase in gene expression of day 5 differentiated enteroids relative to day 1 differentiated enteroids normalized to *HPRT* expression. For samples in which the target gene was undetectable (e.g., *DEFA5*), the maximum number of cycles was imputed (46 cycles).

| <b>Table 5. qPCR Primers for Gene Expression</b> |                                 |       |
|--|---------------------------------|-------|
| Primer   | Sequence                        | Ref   |
| DEF5 FWD   | AGG AAA TGG ACT CTC TGC TCT TAG | [93]  |
| DEFA5 REV  | TTG CAC TGC TTT GGT TTC TAT CTA | [93]  |
| Trefoil Factor 3 FWD                             | AGC TCT GCT GAG GAG TAC GTG     | [93]  |
| Trefoil Factor 3 REV                             | ACA GAA AAG CTG AGA TGA ACA GTG | [93]  |
| Chromagranin B FWD                               | CAG CCA ACG CTG CTT CTC         | [92]  |
| Chromagranin B REV                               | TGG CAT GGA ATT GAC AGC         | [92]  |
| SLC10A2 FWD                                      | GGG TTA CTC CCT GGG GTT TC      | [93]  |
| SLC10A2 REV                                      | CCA TGA CAT TTC TTG TAT GCC ACA | [93]  |
| OAS1 FWD   | CTGTGTGTGTGTCCAAGGTG            |       |
| OAS1 REV   | AGTGGTGAGAGGACTGAGGA            |       |
| ISG54 FWD  | ACGGTATGCTTGGAACGA              | [251] |
| ISG54 REV  | AACCCAGAGTGTGGCTGATG            | [251] |
| HPRT FWD   | TGA CCT TGA TTT ATT TTG CAT ACC | [92]  |
| HPRT REV   | CGA GCA AGA CGT TCA GTC CT      | [92]  |
| CASP4 qPCR FWD                                   | CAA GAG AAG CAA CGT ATG GCA     | [154] |
| CASP4 qPCR REV                                   | AGG CAG ATG GTC AAA CTC TGT A   | [154] |
| CASP1 qPCR FWD                                   | TTT CCG CAA GGT TCG ATT TTC A   | [154] |
| CASP1 qPCR REV                                   | GGC ATC TGC GCT CTA CCA TC      | [154] |
| CASP5 qPCR FWD                                   |                                 |       |
| CASP5 qPCR REV                                   |                                 |       |
| hIL-1 $\beta$ qPCR FWD                           |                                 |       |
| hIL-1 $\beta$ qPCR REV                           |                                 |       |

**Histology.** Differentiated human enteroids were removed from Matrigel using cell recovery solution, concentrated by centrifugation at  $400 \times g$ , and fixed in 4% paraformaldehyde (PFA).

Enteroids were then stained with hematoxylin (Gill's formula) to facilitate visualization, resuspended in Histogel (Thermo Scientific), stored overnight in 10% neutral buffered formalin, and embedded in paraffin. They were then sectioned at 4  $\mu$ m and stained with hematoxylin and eosin or periodic acid-Schiff stain using standard methods.

**Immunoblotting.** Human enteroids and cell lines were lysed using RIPA buffer with 1X Halt protease inhibitor for 30 minutes on ice. Lysates were centrifuged at 16,400 rpm for 10 min at 4°C to pellet insoluble debris. Supernatants were denatured by boiling in 1X SDS buffer and 0.1 M DTT. Proteins were separated using SDS-PAGE, transferred to a nitrocellulose membrane, and blocked in 3% BSA in 0.1% Tween-20/PBS for 1 h. Blots were probed with the following antibodies: goat polyclonal anti-caspase-1 (1:1000, R&D), mouse monoclonal anti-Caspase-4 (4B9) (1:2000, MBL International), rabbit polyclonal anti-human IL-18 antibody (1:1000, MBL International), mouse monoclonal anti- $\beta$ -actin (1:1000, OriGene) and Goat anti-GAPDH (1:1000, R&D). Caspase-1 and caspase-4 immunoblots were probed with a HRP conjugated secondary antibody, developed with Clarity Western ECL, and imaged on the Li-Cor Odyssey Fc. All other immunoblots were probed with fluorescently conjugated secondaries and imaged on the Typhoon 9400.

**Viral infection of enteroids.** The number of cells in each well of enteroids was estimated by counting dissociated enteroids from a representative well on a hemocytometer. Matrigel containing enteroids was sheared with a 23-gauge needle, and purified HAdV-5p, HAdV-16p, or HAdV-41p at an MOI of 3,000 genomes/cell in CCCM supplemented with 1  $\mu$ M Jag-1 was added. The sample was incubated for 45 min at 4°C with agitation. Enteroids were pelleted, the inoculum was removed, and the enteroids were replated in Matrigel. Each Matrigel plug was

overlaid with 500  $\mu$ l of CCCM or differentiation medium. The day 0 sample was harvested 2 h post-warming. One well of infected enteroids was then harvested every day for 5 days. Viral and cellular DNAs were isolated by GeneJET Viral DNA and RNA purification kit and quantified by qPCR as described above.

Infections with clinical isolates and with HAdV-12p and HAdV-40p were performed as described above with slight modifications: the inoculum consisted of lysate rather than purified virus, the enteroids were not sheared prior to infection, and the entire volume of enteroid-virus mixture was mixed with Matrigel and plated. Infected enteroids were passaged on days 7, 14, and 21, if needed, until greater than 80% of the enteroids showed signs of cytopathic effect (CPE), at which point a lysate was made and used to infect new enteroids. Each clinical isolate underwent two viral passages.

For Fig. 7A to D, human enteroid monolayers or A549 cells were treated with 1,000 IU/ml interferon- $\beta$  (IFN- $\beta$ ) or 500 ng/ml IFN- $\lambda$ 3 (R&D Systems) 24 h prior to infection. Human enteroid monolayers were infected at MOIs of 15 and 6 genomes/cell for HAdV-5p and HAdV-41p, respectively. A549 cells were infected at MOIs of 0.75 and 85 genomes/cell for HAdV-5p and HAdV-41p, respectively. Inocula were chosen to achieve similar levels of infection between serotypes at 2 h post-infection. Viral genomes and cellular genomes were quantified at 2, 24, and 48 h (HAdV-41p only) post-infection as described above. For Fig. 7E, human enteroid monolayers were infected at an MOI of 200 and 30 for HAdV-41p and HAdV-5p, respectively, for 24 h. Expression of *OAS1* and *ISG54* was quantified at 24 h post-infection relative to uninfected cells, as described above. For Fig. 6F, human enteroid monolayers and A549 cells

were treated with 1,000 IU/ml IFN- $\beta$  or 500 ng/ml IFN- $\lambda$ 3 for 24 h, and expression of *OAS1* and *ISG54* was quantified at 24 h posttreatment.

For Fig. 8, HAdV-41p and HAdV-5p were incubated in the presence or absence of 15  $\mu$ M HD5 for 45 min on ice. The virus was then added to human enteroid monolayers for 2 h at 37°C. The medium was then replaced. Human enteroid monolayers were infected at MOIs of 200 and 30 for HAdV-41p and HAdV-5p, respectively. Cells were trypsinized 48 h post-infection, fixed in 2% PFA, and stained with a mixture of 8C4 mouse anti-hexon antibody and rabbit anti-MUC2 (Santa Cruz H-300, 1:50) followed by a mixture of Alexa Fluor 488-conjugated anti-mouse and Alexa Fluor 647-conjugated anti-rabbit (1:200) secondary antibodies. Flow cytometry data were acquired on a Canto II (BD) and analyzed with FlowJo version 9.9.4 (BD) with doublet exclusion and using isotype controls for gating.

**Verification of clinical isolates.** Total DNA isolated by the GeneJET viral DNA and RNA purification kit from the lysates of HAdV-12p- and HAdV-40p-infected cells, lysates containing primary isolates from NYSDOH and CDC, and lysates from enteroid cultures at the end of the second passage of each virus were analyzed by PCR to determine HAdV species present in each sample as described previously [121]. Note that the PCRs for each HAdV species were performed separately rather than multiplexed, the melting temperatures ( $T_m$ ) for the HAdV-A, -B, and -C reactions were modified to 56°C, a new forward primer (5'-GGATAVGCDGT-NGTRCTKGGCAT-3') was designed for the HAdV-B reaction to match HAdV-16, and the extension temperature was lowered to 68°C per the manufacturer's instructions (Roche).

**Bacterial infections of human enteroid monolayers and C2Bbe1 cells.** For culturing C2Bbe1 cells, wells in a 96-well plate were coated with collagen as described above. C2Bbe1 cells were

seeded 4 days prior to infection at  $3.5 \times 10^5$  cells per well and media was changed every day. Bacteria were cultured in LB Miller for 3 h at 37°C (late log phase) then centrifuged at 2000xg for 3 min, washed 2x with DPBS, and concentrated 10x in DPBS. Bacteria were then diluted 200-fold into Sato IF media for infections. Media was removed from the epithelial cells, washed 1x with DPBS. Bacteria were added to the cells at an MOI of ~100-200. Bacteria were allowed to bind and internalize for 10 minutes, then unbound bacteria were washed away with DPBS. Fresh media was added to the cells and adherent bacteria were allowed to internalize for an additional 20 min. Media was then changed to media containing 100 µg/ml gentamicin and cells were then incubated for 1 h at 37°C to kill the extracellular bacteria. After 1 h the media was again changed to media containing 10 µg/ml gentamicin for the duration of the experiment. For confocal microscopy studies, human enteroid monolayers were seeded into µ-slide angiogenesis slides (Ibidi) at  $1.8 \times 10^5$  cells per well. For In Cell 2000 analysis, human enteroid monolayers and C2Bbe1 cells were seeded into 96-well black wall plates (Corning) at  $3.5 \times 10^5$  cells per well and  $2.5 \times 10^4$  cells per well, respectively. Infections were performed as above except cells were fixed in 2% PFA for 20 min at room temp at 1 h and 7 h post-infection.

**IL-18 measurements.** Culture supernatants were collected and were quantified using ELISA kits for human IL-18 (R&D Systems).

**Enumeration of intracellular bacteria.** Infected monolayers were washed once with DPBS, lysed in 200 µl of 1% (vol/vol) Triton-X 100 in water, and serially diluted in DPBS. Each serial dilution was plated in triplicate on LB agar plates and incubated at 37°C.

**Fluorescence Microscopy.** Enteroid monolayers were fixed in 2% PFA for 20 min, washed with PBS, permeabilized in 20mM glycine and 0.1% Triton-X 100 in PBS for 20 min at room

temperature. For enumeration of intracellular bacteria, enteroid monolayers and C2Bbe1 cells were stained with 10  $\mu\text{g/ml}$  Hoechst 33342 for 15 min at RT to stain the nuclei.

**Image analysis.** Bright-field images were acquired using a Nikon Eclipse Ti inverted microscope fitted with a 4X objective, a charge-coupled-device (CCD) camera, and image acquisition software ( $\mu\text{Manager}$ ; Open Imaging). Images of histology were acquired using a 40X objective. For quantification of intracellular bacteria images were acquired using either a Nikon A1R microscope or GE IN Cell Analyzer 2000.

**Statistical analysis.** All statistical analysis was performed using Prism 7.0c. For Fig. 2 and 7E and F, the log transformation of the fold increase in gene expression was compared to a theoretical value of zero using a one-sample *t* test. For Fig. 3, 4, and 5, curves and 95% confidence intervals were fitted by nonlinear regression to the mean data for three biological replicates. For Fig. 7A to D, we compared untreated to IFN-treated samples by one-way analysis of variance (ANOVA) with *post hoc* Tukey's test. For Fig. 8, we compared HAdV infection in the presence of HD5 to that in the absence of HD5 (as 100% infection) and HAdV infection of goblet cells and nongoblet cells using ratio paired *t* tests. For Fig. 11A and B, we compared each time point in enteroids to the corresponding time point in C2Bbe1 cells using 2-way ANOVA with *post hoc* Sidak's test. For Fig. 13B-D, we compared infected wild-type and caspase KO samples by one-way analysis of variance (ANOVA) with *post hoc* Tukey's test. For Fig. 14A-C, we compared CFUs from infected wild-type and caspase KO samples using ratio paired *t* tests. For Fig. 15, we compared the number of bacteria per cell in C2Bbe1 cells and wild-type human enteroid monolayers using the Mann-Whitney test. For Fig. 16, we compared the number of

bacteria in wild-type and *CASP4* KO enteroid monolayers at 1 and 7 h post-infection using Kruskal-Wallis test.

## **Copyright Permissions**

Gastrointestinal tract and Paneth cell background reprinted with permission from Viruses, Volume 10, Issue 5, Mayumi K Holly and Jason G Smith, Paneth Cells during Viral Infection and Pathogenesis, Copyright (2018).

Gastrointestinal tract background reprinted with permission from Annual Review of Virology, Volume 4, Issue 1, Mayumi K Holly, Karina Diaz and Jason G Smith, Defensins in Viral Infection and Pathogenesis, Copyright (2017).

## VITA

### EDUCATION

B.S. in Microbiology, 2013  
Washington State University  
Pullman, WA

### PUBLICATIONS

**Holly, M. K.** and Smith, J. G. Paneth cells during viral infection and pathogenesis. 2018. *Viruses* 10(5).

**Holly, M. K.** and Smith, J.G. Adenovirus infection of human enteroids reveals interferon sensitivity and preferential infection of goblet cells. 2018 *J Virol* 92(9): e00250-18

**Holly MK**, Diaz K, and Smith J. G. Defensins in viral infection and pathogenesis. 2017. *Annu Rev Virol* 4(1): 369-91.

Wilson SS, Bromme BB, **Holly MK**, Wiens ME, and Smith JG. 2017. Alpha-defensin enhancement of enteric viral infection. 2017. *PLOS Pathogens* 13(6).

Wilson SS, Wiens, ME, **Holly MK** and Smith JG. Defensins at the Mucosal Surface: Latest Insights into Defensin-Virus Interactions. 2016. *J Virol* 90(11): 5216-8.

Wilson SS, Tocchi A, **Holly MK**, Parks WC and J. G. Smith. A small intestinal organoid model of non-invasive enteric pathogen-epithelial cell interactions. *Mucosal Immunol* 8(2): 352-61.

Feng S, Eucker TP, **Holly MK**, Konkel M, Lu X, Wang S. Investigating the responses of *Cronobacter sakazakii* to garlic-derived organosulfur compounds: a systematic study of pathogenic-bacterium injury by use of high-throughput whole-transcriptome sequencing and confocal micro-Raman spectroscopy. 2014. *Appl Environ Microbiol.* 80(3): 959–71.

### ORAL PRESENTATIONS

Holly, M. K. and Smith, J. G. “Adenovirus infection of human enteroids reveals interferon sensitivity and preferential infection of goblet cells.” 13<sup>th</sup> International Adenovirus Conference, September 28<sup>th</sup> 2018. **Oral Presentation.**

Holly, M. K. and Smith, J. G. “Intestinal enteroids as a model for infectious disease.” Northwest branch meeting for the American Society for Microbiology, November 19<sup>th</sup> 2016. **Oral Presentation.**

## Bibliography

1. Barker, N., *Adult intestinal stem cells: critical drivers of epithelial homeostasis and regeneration*. Nat Rev Mol Cell Biol, 2014. **15**(1): p. 19-33.
2. Thompson, C.A., A. DeLaForest, and M.A. Battle, *Patterning the gastrointestinal epithelium to confer regional-specific functions*. Dev Biol, 2018. **435**(2): p. 97-108.
3. Middendorp, S., et al., *Adult stem cells in the small intestine are intrinsically programmed with their location-specific function*. Stem Cells, 2014. **32**(5): p. 1083-91.
4. Clevers, H. and E. Battle, *SnapShot: the intestinal crypt*. Cell, 2013. **152**(5): p. 1198-1198 e2.
5. Clevers, H.C. and C.L. Bevins, *Paneth cells: maestros of the small intestinal crypts*. Annu Rev Physiol, 2013. **75**: p. 289-311.
6. Bevins, C.L. and N.H. Salzman, *Paneth cells, antimicrobial peptides and maintenance of intestinal homeostasis*. Nat Rev Microbiol, 2011. **9**(5): p. 356-68.
7. Ouellette, A.J., *Paneth cells and innate mucosal immunity*. Curr Opin Gastroenterol, 2010. **26**(6): p. 547-53.
8. Klein, S., *On the nature of the granule cells of paneth in the intestinal glands of mammals*. American Journal of Anatomy, 1906. **5**(3): p. 315-330.
9. Tan, D.W. and N. Barker, *Intestinal stem cells and their defining niche*. Curr Top Dev Biol, 2014. **107**: p. 77-107.
10. Troughton, W.D. and J.S. Trier, *Paneth and Goblet Cell Renewal In Mouse Duodenal Crypts*. J Cell Biol, 1969. **41**: p. 251-268.
11. Cheng, H., J. Merzel, and C.P. Leblond, *Renewal of Paneth cells in the small intestine of the mouse*. Am J Anat, 1969. **126**(4): p. 507-25.
12. Holly, M.K. and J.G. Smith, *Paneth Cells during Viral Infection and Pathogenesis*. Viruses, 2018. **10**(5).
13. Steele, S.P., S.J. Melchor, and W.A. Petri, Jr., *Tuft Cells: New Players in Colitis*. Trends Mol Med, 2016. **22**(11): p. 921-924.
14. Ting, H.A. and J. von Moltke, *The Immune Function of Tuft Cells at Gut Mucosal Surfaces and Beyond*. J Immunol, 2019. **202**(5): p. 1321-1329.
15. Saxena, K., et al., *Human Intestinal Enteroids: a New Model To Study Human Rotavirus Infection, Host Restriction, and Pathophysiology*. J Virol, 2015. **90**(1): p. 43-56.
16. Blutt, S.E., et al., *Gastrointestinal microphysiological systems*. Exp Biol Med (Maywood), 2017. **242**(16): p. 1633-1642.
17. Johansson, M.E. and G.C. Hansson, *Immunological aspects of intestinal mucus and mucins*. Nat Rev Immunol, 2016. **16**(10): p. 639-49.
18. Johansson, M.E., J.M. Larsson, and G.C. Hansson, *The two mucus layers of colon are organized by the MUC2 mucin, whereas the outer layer is a legislator of host-microbial interactions*. Proc Natl Acad Sci U S A, 2011. **108 Suppl 1**: p. 4659-65.
19. Kluver, E., et al., *Structure-activity relation of human beta-defensin 3: influence of disulfide bonds and cysteine substitution on antimicrobial activity and cytotoxicity*. Biochemistry, 2005. **44**(28): p. 9804-16.
20. Pazgier, M., et al., *Human beta-defensins*. Cell Mol Life Sci, 2006. **63**(11): p. 1294-313.
21. Cunliffe, R.N. and Y.R. Mahida, *Expression and regulation of antimicrobial peptides in the gastrointestinal tract*. J Leukoc Biol, 2004. **75**(1): p. 49-58.

22. O'Neil, D.A., *Regulation of expression of beta-defensins: endogenous enteric peptide antibiotics*. Mol Immunol, 2003. **40**(7): p. 445-50.
23. Zaragoza, M.M., et al., *Persistence of gut mucosal innate immune defenses by enteric alpha-defensin expression in the simian immunodeficiency virus model of AIDS*. J Immunol, 2011. **186**(3): p. 1589-97.
24. Linzmeier, R.M. and T. Ganz, *Human defensin gene copy number polymorphisms: comprehensive analysis of independent variation in alpha- and beta-defensin regions at 8p22-p23*. Genomics, 2005. **86**(4): p. 423-30.
25. Holly, M.K., K. Diaz, and J.G. Smith, *Defensins in Viral Infection and Pathogenesis*. Annu Rev Virol, 2017. **4**(1): p. 369-391.
26. van Es, J.H., et al., *Wnt signalling induces maturation of Paneth cells in intestinal crypts*. Nat Cell Biol, 2005. **7**(4): p. 381-6.
27. Andreu, P., et al., *Crypt-restricted proliferation and commitment to the Paneth cell lineage following Apc loss in the mouse intestine*. Development, 2005. **132**(6): p. 1443-51.
28. Spencer, J.D., et al., *Human alpha defensin 5 expression in the human kidney and urinary tract*. PLoS One, 2012. **7**(2): p. e31712.
29. Klotman, M.E., et al., *Neisseria gonorrhoeae-induced human defensins 5 and 6 increase HIV infectivity: role in enhanced transmission*. J Immunol, 2008. **180**(9): p. 6176-85.
30. Porter, E., et al., *Distinct defensin profiles in Neisseria gonorrhoeae and Chlamydia trachomatis urethritis reveal novel epithelial cell-neutrophil interactions*. Infect Immun, 2005. **73**(8): p. 4823-33.
31. Grandjean, V., et al., *Antimicrobial protection of the mouse testis: synthesis of defensins of the cryptdin family*. Biol Reprod, 1997. **57**(5): p. 1115-22.
32. Com, E., et al., *Expression of antimicrobial defensins in the male reproductive tract of rats, mice, and humans*. Biol Reprod, 2003. **68**(1): p. 95-104.
33. Ayabe, T., et al., *Secretion of microbicidal alpha-defensins by intestinal Paneth cells in response to bacteria*. Nat Immunol, 2000. **1**(2): p. 113-118.
34. Farin, H.F., et al., *Paneth cell extrusion and release of antimicrobial products is directly controlled by immune cell-derived IFN-gamma*. J Exp Med, 2014. **211**(7): p. 1393-405.
35. Raetz, M., et al., *Parasite-induced TH1 cells and intestinal dysbiosis cooperate in IFN-gamma-dependent elimination of Paneth cells*. Nat Immunol, 2013. **14**(2): p. 136-42.
36. Aldred, P.M., E.J. Hollox, and J.A. Armour, *Copy number polymorphism and expression level variation of the human alpha-defensin genes DEFA1 and DEFA3*. Hum Mol Genet, 2005. **14**(14): p. 2045-52.
37. Amid, C., et al., *Manual annotation and analysis of the defensin gene cluster in the C57BL/6J mouse reference genome*. BMC Genomics, 2009. **10**: p. 606.
38. Hollox, E.J., *Copy number variation of beta-defensins and relevance to disease*. Cytogenet Genome Res, 2008. **123**(1-4): p. 148-55.
39. Martinez Rodriguez, N.R., et al., *Expansion of Paneth cell population in response to enteric Salmonella enterica serovar Typhimurium infection*. Infect Immun, 2012. **80**(1): p. 266-75.
40. Munch, J., et al., *Discovery and optimization of a natural HIV-1 entry inhibitor targeting the gp41 fusion peptide*. Cell, 2007. **129**(2): p. 263-75.
41. Ouellette, A.J. and M.E. Selsted, *Paneth cell defensins: Endogenous peptide components of intestinal host defense*. FASEB J, 1996. **10**(11): p. 1280-1289.

42. Zhou, Y.S., et al., *Partial deletion of chromosome 8 beta-defensin cluster confers sperm dysfunction and infertility in male mice*. PLoS Genet, 2013. **9**(10): p. e1003826.
43. Semple, C.A., M. Rolfe, and J.R. Dorin, *Duplication and selection in the evolution of primate beta-defensin genes*. Genome Biol, 2003. **4**(5): p. R31.
44. Beckloff, N. and G. Diamond, *Computational analysis suggests beta-defensins are processed to mature peptides by signal peptidase*. Protein Pept Lett, 2008. **15**(5): p. 536-40.
45. Schroeder, B.O., et al., *Reduction of disulphide bonds unmasks potent antimicrobial activity of human beta-defensin 1*. Nature, 2011. **469**(7330): p. 419-23.
46. Spencer, J., J.H.Y. Siu, and L. Montorsi, *Human intestinal lymphoid tissue in time and space*. Mucosal Immunol, 2019. **12**(2): p. 296-298.
47. Mowat, A.M. and W.W. Agace, *Regional specialization within the intestinal immune system*. Nat Rev Immunol, 2014. **14**(10): p. 667-85.
48. Jepson, M.A. and M.A. Clark, *The role of M cells in Salmonella infection*. Microbes Infect, 2001. **3**(14-15): p. 1183-90.
49. Schroeder, G.N. and H. Hilbi, *Molecular pathogenesis of Shigella spp.: controlling host cell signaling, invasion, and death by type III secretion*. Clin Microbiol Rev, 2008. **21**(1): p. 134-56.
50. Knoop, K.A. and R.D. Newberry, *Goblet cells: multifaceted players in immunity at mucosal surfaces*. Mucosal Immunol, 2018. **11**(6): p. 1551-1557.
51. Rescigno, M., et al., *Dendritic cells express tight junction proteins and penetrate gut epithelial monolayers to sample bacteria*. Nat Immunol, 2001. **2**(4): p. 361-7.
52. Kinnebrew, M.A. and E.G. Pamer, *Innate immune signaling in defense against intestinal microbes*. Immunol Rev, 2012. **245**(1): p. 113-31.
53. Vaishnava, S., et al., *Paneth cells directly sense gut commensals and maintain homeostasis at the intestinal host-microbial interface*. Proc Natl Acad Sci U S A, 2008. **105**(52): p. 20858-63.
54. Gong, J., et al., *Epithelial-specific blockade of MyD88-dependent pathway causes spontaneous small intestinal inflammation*. Clin Immunol, 2010. **136**(2): p. 245-56.
55. Kulkarni, D.H., et al., *Goblet cell associated antigen passages are inhibited during Salmonella typhimurium infection to prevent pathogen dissemination and limit responses to dietary antigens*. Mucosal Immunol, 2018. **11**(4): p. 1103-1113.
56. Lee, S., et al., *Norovirus Cell Tropism Is Determined by Combinatorial Action of a Viral Non-structural Protein and Host Cytokine*. Cell Host Microbe, 2017. **22**(4): p. 449-459 e4.
57. Zmora, N., J. Suez, and E. Elinav, *You are what you eat: diet, health and the gut microbiota*. Nature Reviews Gastroenterology & Hepatology, 2019. **16**(1): p. 35-56.
58. Maier, L., et al., *Extensive impact of non-antibiotic drugs on human gut bacteria*. Nature, 2018. **555**(7698): p. 623-628.
59. Salzman, N.H., et al., *Enteric defensins are essential regulators of intestinal microbial ecology*. Nat Immunol, 2010. **11**(1): p. 76-83.
60. Spanogiannopoulos, P., et al., *The microbial pharmacists within us: a metagenomic view of xenobiotic metabolism*. Nat Rev Microbiol, 2016. **14**(5): p. 273-87.
61. Rivera-Chavez, F., et al., *Depletion of Butyrate-Producing Clostridia from the Gut Microbiota Drives an Aerobic Luminal Expansion of Salmonella*. Cell Host Microbe, 2016. **19**(4): p. 443-54.

62. Goverse, G., et al., *Diet-Derived Short Chain Fatty Acids Stimulate Intestinal Epithelial Cells To Induce Mucosal Tolerogenic Dendritic Cells*. J Immunol, 2017. **198**(5): p. 2172-2181.
63. Canfora, E.E., et al., *Gut microbial metabolites in obesity, NAFLD and T2DM*. Nat Rev Endocrinol, 2019.
64. Hapfelmeier, S. and W.D. Hardt, *A mouse model for S. typhimurium-induced enterocolitis*. Trends Microbiol, 2005. **13**(10): p. 497-503.
65. Sorbara, M.T. and E.G. Pamer, *Interbacterial mechanisms of colonization resistance and the strategies pathogens use to overcome them*. Mucosal Immunol, 2019. **12**(1): p. 1-9.
66. Wilson, C.L., et al., *Regulation of intestinal alpha-defensin activation by the metalloproteinase matrilysin in innate host defense*. Science, 1999. **286**(5437): p. 113-7.
67. Mastroianni, J.R., et al., *Alternative luminal activation mechanisms for paneth cell alpha-defensins*. J Biol Chem, 2012. **287**(14): p. 11205-12.
68. Salzman, N.H., et al., *Enteric Salmonella Infection Inhibits Paneth Cell Antimicrobial Peptide Expression*. Infection and Immunity, 2003. **71**(3): p. 1109-1115.
69. Salzman, N.H., *Paneth cell defensins and the regulation of the microbiome: detente at mucosal surfaces*. Gut Microbes, 2010. **1**(6): p. 401-6.
70. Sano, T., et al., *An IL-23R/IL-22 Circuit Regulates Epithelial Serum Amyloid A to Promote Local Effector Th17 Responses*. Cell, 2015. **163**(2): p. 381-93.
71. Schnupf, P., et al., *Segmented filamentous bacteria, Th17 inducers and helpers in a hostile world*. Curr Opin Microbiol, 2017. **35**: p. 100-109.
72. Hurley, B.P. and B.A. McCormick, *Translating tissue culture results into animal models: the case of Salmonella typhimurium*. Trends in Microbiology, 2003. **11**(12): p. 562-569.
73. Randall, K.J., J. Turton, and J.R. Foster, *Explant culture of gastrointestinal tissue: a review of methods and applications*. Cell Biol Toxicol, 2011. **27**(4): p. 267-84.
74. Bradley, D.W., et al., *Transformed and nontransformed cells differ in stability and cell cycle regulation of a binding activity to the murine thymidine kinase promoter*. Proc Natl Acad Sci U S A, 1990. **87**(23): p. 9310-4.
75. Ahmed, D., et al., *Epigenetic and genetic features of 24 colon cancer cell lines*. Oncogenesis, 2013. **2**: p. e71.
76. Devriese, S., et al., *T84 monolayers are superior to Caco-2 as a model system of colonocytes*. Histochem Cell Biol, 2017. **148**(1): p. 85-93.
77. Donnelly, R.P. and S.V. Kotenko, *Interferon-lambda: a new addition to an old family*. J Interferon Cytokine Res, 2010. **30**(8): p. 555-64.
78. Hugenholtz, F. and W.M. de Vos, *Mouse models for human intestinal microbiota research: a critical evaluation*. Cell Mol Life Sci, 2018. **75**(1): p. 149-160.
79. Masopust, D., C.P. Sivula, and S.C. Jameson, *Of Mice, Dirty Mice, and Men: Using Mice To Understand Human Immunology*. J Immunol, 2017. **199**(2): p. 383-388.
80. Perlman, R.L., *Mouse models of human disease: An evolutionary perspective*. Evol Med Public Health, 2016. **2016**(1): p. 170-6.
81. Coers, J., M.N. Starnbach, and J.C. Howard, *Modeling infectious disease in mice: co-adaptation and the role of host-specific IFN-gamma responses*. PLoS Pathog, 2009. **5**(5): p. e1000333.
82. Sato, T., et al., *Single Lgr5 stem cells build crypt-villus structures in vitro without a mesenchymal niche*. Nature, 2009. **459**(7244): p. 262-5.

83. Spence, J.R., et al., *Directed differentiation of human pluripotent stem cells into intestinal tissue in vitro*. *Nature*, 2011. **470**(7332): p. 105-9.
84. Stelzner, M., et al., *A nomenclature for intestinal in vitro cultures*. *Am J Physiol Gastrointest Liver Physiol*, 2012. **302**(12): p. G1359-63.
85. Fujii, M., et al., *Human Intestinal Organoids Maintain Self-Renewal Capacity and Cellular Diversity in Niche-Inspired Culture Condition*. *Cell Stem Cell*, 2018. **23**(6): p. 787-793 e6.
86. Finkbeiner, S.R., et al., *Transcriptome-wide Analysis Reveals Hallmarks of Human Intestine Development and Maturation In Vitro and In Vivo*. *Stem Cell Reports*, 2015.
87. Holly, M.K. and J.G. Smith, *Adenovirus infection of human enteroids reveals interferon sensitivity and preferential infection of goblet cells*. *J Virol*, 2018.
88. Ettayebi, K., et al., *Replication of human noroviruses in stem cell-derived human enteroids*. *Science*, 2016. **353**(6306): p. 1387-1393.
89. Finkbeiner, S.R., et al., *Stem cell-derived human intestinal organoids as an infection model for rotaviruses*. *MBio*, 2012. **3**(4): p. e00159-12.
90. Ranganathan, S., et al., *Evaluating Shigella flexneri Pathogenesis in the Human Enteroid Model*. *Infect Immun*, 2019. **87**(4).
91. Koestler, B.J., et al., *Human intestinal enteroids as a model system of Shigella pathogenesis*. *Infect Immun*, 2019.
92. Sato, T., et al., *Long-term expansion of epithelial organoids from human colon, adenoma, adenocarcinoma, and Barrett's epithelium*. *Gastroenterology*, 2011. **141**(5): p. 1762-72.
93. VanDussen, K.L., et al., *Development of an enhanced human gastrointestinal epithelial culture system to facilitate patient-based assays*. *Gut*, 2015. **64**(6): p. 911-20.
94. Fujii, M., et al., *Efficient genetic engineering of human intestinal organoids using electroporation*. *Nat Protoc*, 2015. **10**(10): p. 1474-85.
95. Yin, X., et al., *Niche-independent high-purity cultures of Lgr5+ intestinal stem cells and their progeny*. *Nat Methods*, 2014. **11**(1): p. 106-12.
96. Das, S., et al., *Rab8a vesicles regulate Wnt ligand delivery and Paneth cell maturation at the intestinal stem cell niche*. *Development*, 2015. **142**(12): p. 2147-62.
97. Battle, E., et al., *Beta-catenin and TCF mediate cell positioning in the intestinal epithelium by controlling the expression of EphB/ephrinB*. *Cell*, 2002. **111**(2): p. 251-63.
98. Petersen, N., et al., *Generation of L cells in mouse and human small intestine organoids*. *Diabetes*, 2014. **63**(2): p. 410-20.
99. Wold, W.S.M. and M.G. Ison, *Adenoviruses*, in *Fields Virology*, B.N. Fields, D.M. Knipe, and P.M. Howley, Editors. 2013, Wolters Kluwer Health/Lippincott Williams & Wilkins: Philadelphia.
100. Uhnou, I., et al., *Importance of enteric adenoviruses 40 and 41 in acute gastroenteritis in infants and young children*. *J Clin Microbiol*, 1984. **20**(3): p. 365-72.
101. Stevenson, F. and V. Mautner, *Aspects of the molecular biology of enteric adenoviruses*, in *Viral Gastroenteritis*, U. Desselberger and J.J. Gray, Editors. 2003, Elsevier Science.
102. Tiemessen, C.T. and A.H. Kidd, *Adenovirus type 40 and 41 growth in vitro: host range diversity reflected by differences in patterns of DNA replication*. *J Virol*, 1994. **68**(2): p. 1239-44.
103. Berk, A., *Adenoviridae*, in *Fields Virology*, B.N. Fields, D.M. Knipe, and P.M. Howley, Editors. 2013, Wolters Kluwer Health/Lippincott Williams & Wilkins: Philadelphia.

104. Albinsson, B. and A.H. Kidd, *Adenovirus type 41 lacks an RGD alpha(v)-integrin binding motif on the penton base and undergoes delayed uptake in A549 cells*. *Virus Res*, 1999. **64**(2): p. 125-36.
105. de Jong, J.C., *Candidate Adenovirus 40 and 41: Fastidious adenoviruses from human infant stool*. *J Med Virol*, 1983. **11**(3).
106. Witt, D.J. and E.B. Bousquet, *Comparison of Enteric Adenovirus Infection in Various Human Cell-Lines*. *Journal of Virological Methods*, 1988. **20**(4): p. 295-308.
107. Kosulin, K., et al., *Persistence and reactivation of human adenoviruses in the gastrointestinal tract*. *Clin Microbiol Infect*, 2016. **22**(4): p. 381 e1-381 e8.
108. Fox, J.P., et al., *The virus watch program: a continuing surveillance of viral infections in metropolitan New York families. VI. Observations of adenovirus infections: virus excretion patterns, antibody response, efficiency of surveillance, patterns of infections, and relation to illness*. *Am J Epidemiol*, 1969. **89**(1): p. 25-50.
109. Fox, J.P., C.E. Hall, and M.K. Cooney, *The Seattle Virus Watch. VII. Observations of adenovirus infections*. *Am J Epidemiol*, 1977. **105**(4): p. 362-86.
110. De Jong, J.C., *Epidemiology of enteric adenoviruses 40 and 41 and other adenoviruses in immunocompetent and immunodeficient individuals*, in *Viral Gastroenteritis*, U. Desselberger and J.J. Gray, Editors. 2003, Elsevier Science.
111. Schmitz, H., R. Wigand, and W. Heinrich, *Worldwide epidemiology of human adenovirus infections*. *Am J Epidemiol*, 1983. **117**(4): p. 455-66.
112. Magwalivha, M., et al., *High prevalence of species D human adenoviruses in fecal specimens from Urban Kenyan children with diarrhea*. *J Med Virol*, 2010. **82**(1): p. 77-84.
113. Lyons, A., et al., *A double-blind, placebo-controlled study of the safety and immunogenicity of live, oral type 4 and type 7 adenovirus vaccines in adults*. *Vaccine*, 2008. **26**(23): p. 2890-8.
114. Drummond, C.G., et al., *Enteroviruses infect human enteroids and induce antiviral signaling in a cell lineage-specific manner*. *Proc Natl Acad Sci U S A*, 2017. **114**(7): p. 1672-1677.
115. Pieniazek, D., et al., *Enteric adenovirus 41 (Tak) requires low serum for growth in human primary cells*. *Virology*, 1990. **178**(1): p. 72-80.
116. Pieniazek, D., et al., *Differential growth of human enteric adenovirus 41 (TAK) in continuous cell lines*. *Virology*, 1990. **174**(1): p. 239-49.
117. Wickham, T.J., et al., *Integrins alpha v beta 3 and alpha v beta 5 promote adenovirus internalization but not virus attachment*. *Cell*, 1993. **73**(2): p. 309-19.
118. Gaggar, A., D.M. Shayakhmetov, and A. Lieber, *CD46 is a cellular receptor for group B adenoviruses*. *Nat Med*, 2003. **9**(11): p. 1408-12.
119. Bergelson, J.M., et al., *Isolation of a common receptor for Coxsackie B viruses and adenoviruses 2 and 5*. *Science*, 1997. **275**(5304): p. 1320-3.
120. Sherwood, V., et al., *Improved growth of enteric adenovirus type 40 in a modified cell line that can no longer respond to interferon stimulation*. *J Gen Virol*, 2007. **88**(Pt 1): p. 71-6.
121. Xu, W., M.C. McDonough, and D.D. Erdman, *Species-specific identification of human adenoviruses by a multiplex PCR assay*. *J Clin Microbiol*, 2000. **38**(11): p. 4114-20.

122. Zheng, Y., T. Stamminger, and P. Hearing, *E2F/Rb Family Proteins Mediate Interferon Induced Repression of Adenovirus Immediate Early Transcription to Promote Persistent Viral Infection*. PLoS Pathog, 2016. **12**(1): p. e1005415.
123. Julier, Z., et al., *Promoting tissue regeneration by modulating the immune system*. Acta Biomater, 2017. **53**: p. 13-28.
124. Smith, J.G., et al., *Insight into the mechanisms of adenovirus capsid disassembly from studies of defensin neutralization*. PLoS Pathog, 2010. **6**(6): p. e1000959.
125. Smith, J.G. and G.R. Nemerow, *Mechanism of adenovirus neutralization by Human alpha-defensins*. Cell Host Microbe, 2008. **3**(1): p. 11-9.
126. Wilson, S.S., et al., *Alpha-defensin-dependent enhancement of enteric viral infection*. PLoS Pathog, 2017. **13**(6): p. e1006446.
127. Gounder, A.P., et al., *Defensins Potentiate a Neutralizing Antibody Response to Enteric Viral Infection*. PLoS Pathog, 2016. **12**(3): p. e1005474.
128. Li, B., et al., *Drebrin restricts rotavirus entry by inhibiting dynamin-mediated endocytosis*. Proc Natl Acad Sci U S A, 2017. **114**(18): p. E3642-E3651.
129. Mautner, V., V. Steinthorsdottir, and A. Bailey, *Enteric Adenoviruses*, in *The Molecular Repertoire of Adenoviruses III*, W. Doerfler and P. Böhm, Editors. 1995, Springer: Berlin, Heidelberg, Germany.
130. Tiemessen, C.T., M. Ujfalusi, and A.H. Kidd, *Subgroup F adenovirus growth in foetal intestinal organ cultures*. Arch Virol, 1993. **132**(1-2): p. 193-200.
131. Hashimoto, S., et al., *Fastidious human adenovirus type 40 can propagate efficiently and produce plaques on a human cell line, A549, derived from lung carcinoma*. J Virol, 1991.
132. Tiemessen, C.T. and A.H. Kidd, *Sensitivity of subgroup F adenoviruses to interferon*. Arch Virol, 1992: p. 1-13.
133. Roelvink, P.W., et al., *The coxsackievirus-adenovirus receptor protein can function as a cellular attachment protein for adenovirus serotypes from subgroups A, C, D, E, and F*. Journal of Virology, 1998. **72**(10): p. 7909-7915.
134. Zhang, Y. and J.M. Bergelson, *Adenovirus receptors*. J Virol, 2005. **79**(19): p. 12125-31.
135. Matano, M., et al., *Modeling colorectal cancer using CRISPR-Cas9-mediated engineering of human intestinal organoids*. Nat Med, 2015. **21**(3): p. 256-62.
136. Good, C., A.I. Wells, and C.B. Coyne, *Type III interferon signaling restricts enterovirus 71 infection of goblet cells*. Sci Adv, 2019. **5**(3): p. eaau4255.
137. Takeuchi, A. and K. Hashimoto, *Electron microscope study of experimental enteric adenovirus infection in mice*. Infect Immun, 1976. **13**(2): p. 569-80.
138. Pott, J., et al., *IFN-lambda determines the intestinal epithelial antiviral host defense*. Proc Natl Acad Sci U S A, 2011. **108**(19): p. 7944-9.
139. Baldridge, M.T., et al., *Expression of Ifnlr1 on Intestinal Epithelial Cells Is Critical to the Antiviral Effects of Interferon Lambda against Norovirus and Reovirus*. J Virol, 2017. **91**(7).
140. Saxena, K., et al., *A paradox of transcriptional and functional innate interferon responses of human intestinal enteroids to enteric virus infection*. Proc Natl Acad Sci U S A, 2017. **114**(4): p. E570-E579.
141. Behnsen, J., et al., *Exploiting host immunity: the Salmonella paradigm*. Trends Immunol, 2015. **36**(2): p. 112-20.

142. Hurley, D., et al., *Salmonella-host interactions - modulation of the host innate immune system*. Front Immunol, 2014. **5**: p. 481.
143. Foley, S.L., et al., *Population dynamics of Salmonella enterica serotypes in commercial egg and poultry production*. Appl Environ Microbiol, 2011. **77**(13): p. 4273-9.
144. Alvarez-Ordóñez, A., et al., *Salmonella spp. survival strategies within the host gastrointestinal tract*. Microbiology, 2011. **157**(Pt 12): p. 3268-81.
145. LaRock, D.L., A. Chaudhary, and S.I. Miller, *Salmonellae interactions with host processes*. Nat Rev Microbiol, 2015. **13**(4): p. 191-205.
146. Brennan, M.A. and B.T. Cookson, *Salmonella induces macrophage death by caspase-1-dependent necrosis*. Mol Microbiol, 2000. **38**(1): p. 31-40.
147. Storek, K.M. and D.M. Monack, *Bacterial recognition pathways that lead to inflammasome activation*. Immunol Rev, 2015. **265**(1): p. 112-29.
148. Muller, A.A., et al., *An NK Cell Perforin Response Elicited via IL-18 Controls Mucosal Inflammation Kinetics during Salmonella Gut Infection*. PLoS Pathog, 2016. **12**(6): p. e1005723.
149. McCormick, B.A., et al., *Apical secretion of a pathogen-elicited epithelial chemoattractant activity in response to surface colonization of intestinal epithelia by Salmonella typhimurium*. J Immunol, 1998. **160**(1): p. 455-66.
150. Winter, S.E., et al., *Gut inflammation provides a respiratory electron acceptor for Salmonella*. Nature, 2010. **467**(7314): p. 426-9.
151. Muller, A.J., et al., *Salmonella gut invasion involves TTSS-2-dependent epithelial traversal, basolateral exit, and uptake by epithelium-sampling lamina propria phagocytes*. Cell Host Microbe, 2012. **11**(1): p. 19-32.
152. Bakowski, M.A., V. Braun, and J.H. Brumell, *Salmonella-containing vacuoles: directing traffic and nesting to grow*. Traffic, 2008. **9**(12): p. 2022-31.
153. Knodler, L.A., et al., *Dissemination of invasive Salmonella via bacterial-induced extrusion of mucosal epithelia*. Proc Natl Acad Sci U S A, 2010. **107**(41): p. 17733-8.
154. Knodler, Leigh A., et al., *Noncanonical Inflammasome Activation of Caspase-4/Caspase-11 Mediates Epithelial Defenses against Enteric Bacterial Pathogens*. Cell Host & Microbe, 2014. **16**(2): p. 249-256.
155. Delgado, M., et al., *Autophagy and pattern recognition receptors in innate immunity*. Immunol Rev, 2009. **227**(1): p. 189-202.
156. Takeuchi, O. and S. Akira, *Pattern recognition receptors and inflammation*. Cell, 2010. **140**(6): p. 805-20.
157. Man, S.M. and T.D. Kanneganti, *Regulation of inflammasome activation*. Immunol Rev, 2015. **265**(1): p. 6-21.
158. Rauch, I., et al., *NAIP-NLRC4 Inflammasomes Coordinate Intestinal Epithelial Cell Expulsion with Eicosanoid and IL-18 Release via Activation of Caspase-1 and -8*. Immunity, 2017. **46**(4): p. 649-659.
159. Liu, X., et al., *Inflammasome-activated gasdermin D causes pyroptosis by forming membrane pores*. Nature, 2016. **535**(7610): p. 153-8.
160. Kortmann, J., S.W. Brubaker, and D.M. Monack, *Cutting Edge: Inflammasome Activation in Primary Human Macrophages Is Dependent on Flagellin*. J Immunol, 2015. **195**(3): p. 815-9.
161. Zhao, Y., et al., *The NLRC4 inflammasome receptors for bacterial flagellin and type III secretion apparatus*. Nature, 2011. **477**(7366): p. 596-600.

162. Yang, J., et al., *Human NAIP and mouse NAIP1 recognize bacterial type III secretion needle protein for inflammasome activation*. Proc Natl Acad Sci U S A, 2013. **110**(35): p. 14408-13.
163. Kayagaki, N., et al., *Non-canonical inflammasome activation targets caspase-11*. Nature, 2011. **479**(7371): p. 117-21.
164. Shi, J., et al., *Inflammatory caspases are innate immune receptors for intracellular LPS*. Nature, 2014. **514**(7521): p. 187-92.
165. Vigano, E., et al., *Human caspase-4 and caspase-5 regulate the one-step non-canonical inflammasome activation in monocytes*. Nat Commun, 2015. **6**: p. 8761.
166. Casson, C.N., et al., *Human caspase-4 mediates noncanonical inflammasome activation against gram-negative bacterial pathogens*. Proc Natl Acad Sci U S A, 2015. **112**(21): p. 6688-93.
167. Kayagaki, N., et al., *Caspase-11 cleaves gasdermin D for non-canonical inflammasome signalling*. Nature, 2015. **526**(7575): p. 666-71.
168. Shi, J., et al., *Cleavage of GSDMD by inflammatory caspases determines pyroptotic cell death*. Nature, 2015. **526**(7575): p. 660-5.
169. Baker, P.J., et al., *NLRP3 inflammasome activation downstream of cytoplasmic LPS recognition by both caspase-4 and caspase-5*. Eur J Immunol, 2015. **45**(10): p. 2918-26.
170. Lagrange, B., et al., *Human caspase-4 detects tetra-acylated LPS and cytosolic Francisella and functions differently from murine caspase-11*. Nat Commun, 2018. **9**(1): p. 242.
171. Broz, P., et al., *Caspase-11 increases susceptibility to Salmonella infection in the absence of caspase-1*. Nature, 2012. **490**(7419): p. 288-91.
172. Sellin, M.E., et al., *Epithelium-intrinsic NAIP/NLRC4 inflammasome drives infected enterocyte expulsion to restrict Salmonella replication in the intestinal mucosa*. Cell Host Microbe, 2014. **16**(2): p. 237-248.
173. Blander, J.M., *Death in the intestinal epithelium-basic biology and implications for inflammatory bowel disease*. FEBS J, 2016. **283**(14): p. 2720-30.
174. Knodler, L.A., V. Nair, and O. Steele-Mortimer, *Quantitative assessment of cytosolic Salmonella in epithelial cells*. PLoS One, 2014. **9**(1): p. e84681.
175. Leung, K.Y. and B.B. Finlay, *Intracellular replication is essential for the virulence of Salmonella typhimurium*. Proc Natl Acad Sci U S A, 1991. **88**(24): p. 11470-4.
176. Raffatellu, M., et al., *SipA, SopA, SopB, SopD, and SopE2 contribute to Salmonella enterica serotype typhimurium invasion of epithelial cells*. Infect Immun, 2005. **73**(1): p. 146-54.
177. Jones, B.D., N. Ghori, and S. Falkow, *Salmonella typhimurium initiates murine infection by penetrating and destroying the specialized epithelial M cells of the Peyer's patches*. J Exp Med, 1994. **180**(1): p. 15-23.
178. Fassy, F., et al., *Enzymatic activity of two caspases related to interleukin-1beta-converting enzyme*. Eur J Biochem, 1998. **253**(1): p. 76-83.
179. Garcia-Calvo, M., et al., *Inhibition of Human Caspases by Peptide-based and Macromolecular Inhibitors*. J Biol Chem, 1998. **273**(49): p. 32608-32613.
180. Sachs, N., et al., *Intestinal epithelial organoids fuse to form self-organizing tubes in floating collagen gels*. Development, 2017. **144**(6): p. 1107-1112.
181. Roebuck, K., *Regulation of Interleukin-8 Gene Expression*. J Interferon Cytokine Res, 2004. **19**: p. 429-438.

182. Hoffmann, E., et al., *Multiple control of interleukin-8 gene expression*. J Leukoc Biol, 2002. **72**(5): p. 847-55.
183. Guillot, C. and T. Lecuit, *Mechanics of epithelial tissue homeostasis and morphogenesis*. Science, 2013. **340**(6137): p. 1185-9.
184. Pattison, A.M., et al., *Intestinal Enteroids Model Guanylate Cyclase C-Dependent Secretion Induced by Heat-Stable Enterotoxins*. Infect Immun, 2016. **84**(10): p. 3083-91.
185. Zhang, Y.G., et al., *Salmonella-infected crypt-derived intestinal organoid culture system for host-bacterial interactions*. Physiol Rep, 2014. **2**(9).
186. Forbester, J.L., et al., *Interaction of Salmonella enterica Serovar Typhimurium with Intestinal Organoids Derived from Human Induced Pluripotent Stem Cells*. Infect Immun, 2015. **83**(7): p. 2926-34.
187. Reyes Ruiz, V.M., et al., *Broad detection of bacterial type III secretion system and flagellin proteins by the human NAIP/NLRC4 inflammasome*. Proc Natl Acad Sci U S A, 2017. **114**(50): p. 13242-13247.
188. Thinwa, J., et al., *Integrin-mediated first signal for inflammasome activation in intestinal epithelial cells*. J Immunol, 2014. **193**(3): p. 1373-82.
189. Sellin, M.E., et al., *Inflammasomes of the intestinal epithelium*. Trends Immunol, 2015. **36**(8): p. 442-50.
190. Kim, J., H.Y. Gee, and M.G. Lee, *Unconventional protein secretion - new insights into the pathogenesis and therapeutic targets of human diseases*. J Cell Sci, 2018. **131**(12).
191. Monack, D.M., W.W. Navarre, and S. Falkow, *Salmonella-induced macrophage death: the role of caspase-1 in death and inflammation*. Microbes Infect, 2001. **3**(14-15): p. 1201-12.
192. Diamond, C.E., et al., *Salmonella typhimurium-induced IL-1 release from primary human monocytes requires NLRP3 and can occur in the absence of pyroptosis*. Sci Rep, 2017. **7**(1): p. 6861.
193. Margolin, N., et al., *Substrate and Inhibitor Specificity of Interleukin-1*. J Biol Chem, 1997. **272**(11): p. 7223-7228.
194. Callus, B.A. and D.L. Vaux, *Caspase inhibitors: viral, cellular and chemical*. Cell Death Differ, 2007. **14**(1): p. 73-8.
195. Snippert, H.J., et al., *Intestinal crypt homeostasis results from neutral competition between symmetrically dividing Lgr5 stem cells*. Cell, 2010. **143**(1): p. 134-44.
196. Afonina, I.S., et al., *Proteolytic Processing of Interleukin-1 Family Cytokines: Variations on a Common Theme*. Immunity, 2015. **42**(6): p. 991-1004.
197. Schmid-Burgk, J.L., et al., *Caspase-4 mediates non-canonical activation of the NLRP3 inflammasome in human myeloid cells*. Eur J Immunol, 2015. **45**(10): p. 2911-7.
198. Lion, T., *Adenovirus infections in immunocompetent and immunocompromised patients*. Clin Microbiol Rev, 2014. **27**(3): p. 441-62.
199. Takatsuka, H., et al., *Intestinal graft-versus-host disease: mechanisms and management*. Drugs, 2003. **63**(1): p. 1-15.
200. Leslie, J.L., et al., *Persistence and toxin production by Clostridium difficile within human intestinal organoids result in disruption of epithelial paracellular barrier function*. Infect Immun, 2015. **83**(1): p. 138-45.
201. Clevers, H., *Modeling Development and Disease with Organoids*. Cell, 2016. **165**(7): p. 1586-1597.

202. Drost, J. and H. Clevers, *Organoids in cancer research*. Nat Rev Cancer, 2018. **18**(7): p. 407-418.
203. Liu, L., et al., *Global, regional, and national causes of child mortality: an updated systematic analysis for 2010 with time trends since 2000*. Lancet, 2012. **379**(9832): p. 2151-61.
204. Troeger, C., et al., *Estimates of the global, regional, and national morbidity, mortality, and aetiologies of diarrhoea in 195 countries: a systematic analysis for the Global Burden of Disease Study 2016*. The Lancet Infectious Diseases, 2018. **18**(11): p. 1211-1228.
205. Shim, D.H., et al., *New animal model of shigellosis in the Guinea pig: its usefulness for protective efficacy studies*. J Immunol, 2007. **178**(4): p. 2476-82.
206. Matson, J.S., *Infant Mouse Model of Vibrio cholerae Infection and Colonization*. Methods Mol Biol, 2018. **1839**: p. 147-152.
207. Yang, J.Y., et al., *A mouse model of shigellosis by intraperitoneal infection*. J Infect Dis, 2014. **209**(2): p. 203-15.
208. Libby, S.J., et al., *Humanized nonobese diabetic-scid IL2rgammanull mice are susceptible to lethal Salmonella Typhi infection*. Proc Natl Acad Sci U S A, 2010. **107**(35): p. 15589-94.
209. Silberger, D.J., C.L. Zindl, and C.T. Weaver, *Citrobacter rodentium: a model enteropathogen for understanding the interplay of innate and adaptive components of type 3 immunity*. Mucosal Immunol, 2017. **10**(5): p. 1108-1117.
210. Kothary, M. and U. Babu, *Infective Dose of Foodborne Pathogens in Volunteers: A Review*. J Food Saf, 2001. **21**: p. 49-73.
211. Xu, D., et al., *Human Enteric alpha-Defensin 5 Promotes Shigella Infection by Enhancing Bacterial Adhesion and Invasion*. Immunity, 2018. **48**(6): p. 1233-1244 e6.
212. Zhang, B., et al., *Advances in organ-on-a-chip engineering*. Nature Reviews Materials, 2018. **3**(8): p. 257-278.
213. Kasendra, M., et al., *Development of a primary human Small Intestine-on-a-Chip using biopsy-derived organoids*. Sci Rep, 2018. **8**(1): p. 2871.
214. Tovaglieri, A., et al., *Species-specific enhancement of enterohemorrhagic E. coli pathogenesis mediated by microbiome metabolites*. Microbiome, 2019. **7**(1): p. 43.
215. Porter, E.M., et al., *Localization of human intestinal defensin in Paneth cell granules*. Infect Immun, 1997. **65**(6): p. 2389-2395.
216. Satoh, Y., et al., *Ultrastructure Paneth cells in the intestine of various mammals*. J Electron Microscop Tech, 1990. **16**(1): p. 69-80.
217. Porter, E.M., et al., *The multifaceted Paneth cell*. Cell Mol Life Sci, 2002. **59**(1): p. 156-70.
218. Takehana, K., et al., *Fine Structural and Histochemical Study of Equine Paneth Cells*. Anat Histol Embryol, 1998. **27**(1250129).
219. Ouellette, A.J. and C.L. Bevins, *Paneth Cell Defensins and Innate Immunity of the Small Bowel*. Inflamm Bowel Dis, 2001. **7**(1): p. 43-50.
220. Ireland, H., et al., *Cellular inheritance of a Cre-activated reporter gene to determine Paneth cell longevity in the murine small intestine*. Dev Dyn, 2005. **233**(4): p. 1332-6.
221. Selzman, H.M. and R.A. Liebelt, *Paneth Cell Granule of Mouse Intestine*. J Cell Biol, 1962.

222. Stappenbeck, T.S., J.C. Mills, and J.I. Gordon, *Molecular features of adult mouse small intestinal epithelial progenitors*. Proc Natl Acad Sci U S A, 2003. **100**(3): p. 1004-9.
223. Haber, A.L., et al., *A single-cell survey of the small intestinal epithelium*. Nature, 2017. **551**(7680): p. 333-339.
224. Takahashi, N., et al., *IL-17 produced by Paneth cells drives TNF-induced shock*. J Exp Med, 2008. **205**(8): p. 1755-61.
225. Hooper, L.V., et al., *Angiogenins: a new class of microbicidal proteins involved in innate immunity*. Nat Immunol, 2003. **4**(3): p. 269-73.
226. Cash, H.L., et al., *Symbiotic bacteria direct expression of an intestinal bactericidal lectin*. Science, 2006. **313**(5790): p. 1126-30.
227. Cadwell, K., et al., *A key role for autophagy and the autophagy gene Atg16l1 in mouse and human intestinal Paneth cells*. Nature, 2008. **456**(7219): p. 259-63.
228. Satoh, Y. and L. Vollrath, *Quantitative electron microscopic observations on Paneth cells of germfree and ex-germfree Wistar rats*. Anat Embryol, 1986. **173**(3): p. 317-322.
229. Wang, L., et al., *Identification of the Paneth cells in chicken small intestine*. Poult Sci, 2016. **95**(7): p. 1631-5.
230. Date, S. and T. Sato, *Mini-gut organoids: reconstitution of the stem cell niche*. Annu Rev Cell Dev Biol, 2015. **31**: p. 269-89.
231. Wilson, S.S., et al., *A small intestinal organoid model of non-invasive enteric pathogen-epithelial cell interactions*. Mucosal Immunol, 2015. **8**(2): p. 352-61.
232. Bartfeld, S., et al., *In vitro expansion of human gastric epithelial stem cells and their responses to bacterial infection*. Gastroenterology, 2015. **148**(1): p. 126-136 e6.
233. Andreu, P., et al., *A genetic study of the role of the Wnt/beta-catenin signalling in Paneth cell differentiation*. Dev Biol, 2008. **324**(2): p. 288-96.
234. Crawford, H.C., et al., *The metalloproteinase matrilysin is a target of beta-catenin transactivation in intestinal tumors*. Oncogene, 1999. **18**(18): p. 2883-91.
235. Nusse, R. and H. Clevers, *Wnt/beta-Catenin Signaling, Disease, and Emerging Therapeutic Modalities*. Cell, 2017. **169**(6): p. 985-999.
236. Batlle, E., et al., *Beta-Catenin and TCF Mediate Cell Positioning in the Intestinal Epithelium by Controlling the Expression of EphB/EphrinB*. Cell, 2002. **111**: p. 251-263.
237. Brabletz, T., et al., *beta-catenin regulates the expression of the matrix metalloproteinase-7 in human colorectal cancer*. Am J Pathol, 1999. **155**(4): p. 1033-8.
238. van der Flier, L.G. and H. Clevers, *Stem cells, self-renewal, and differentiation in the intestinal epithelium*. Annu Rev Physiol, 2009. **71**: p. 241-60.
239. Farin, H.F., J.H. Van Es, and H. Clevers, *Redundant sources of Wnt regulate intestinal stem cells and promote formation of Paneth cells*. Gastroenterology, 2012. **143**(6): p. 1518-1529 e7.
240. Clevers, H., *The intestinal crypt, a prototype stem cell compartment*. Cell, 2013. **154**(2): p. 274-84.
241. Farin, H.F., et al., *Visualization of a short-range Wnt gradient in the intestinal stem-cell niche*. Nature, 2016. **530**(7590): p. 340-3.
242. Bry, L., et al., *Paneth Cell differentiation in the developing intestine of normal and transgenic mice*. Proc Natl Acad Sci U S A, 1994. **91**: p. 10335-10339.
243. Darmoul, D., et al., *Cryptdin gene expression in developing mouse small intestine*. Am J Physiol, 1997. **272**(1): p. G197-G206.

244. Inoue, R., et al., *Postnatal changes in the expression of genes for cryptdins 1-6 and the role of luminal bacteria in cryptdin gene expression in mouse small intestine*. FEMS Immunol Med Microbiol, 2008. **52**(3): p. 407-16.
245. Ramsey, V.G., et al., *The maturation of mucus-secreting gastric epithelial progenitors into digestive-enzyme secreting zymogenic cells requires Mist1*. Development, 2007. **134**(1): p. 211-22.
246. Direnzo, D., et al., *Induced Mist1 expression promotes remodeling of mouse pancreatic acinar cells*. Gastroenterology, 2012. **143**(2): p. 469-80.
247. Johnson, C.L., et al., *Mist1 is necessary for the establishment of granule organization in serous exocrine cells of the gastrointestinal tract*. Mech Dev, 2004. **121**(3): p. 261-72.
248. Lo, H.G., et al., *A single transcription factor is sufficient to induce and maintain secretory cell architecture*. Genes Dev, 2017. **31**(2): p. 154-171.
249. King, S.L., J.J. Mohiuddin, and C.M. Dekaney, *Paneth cells expand from newly created and preexisting cells during repair after doxorubicin-induced damage*. Am J Physiol Gastrointest Liver Physiol, 2013. **305**(2): p. G151-62.
250. Nguyen, E.K., G.R. Nemerow, and J.G. Smith, *Direct evidence from single-cell analysis that human  $\{\alpha\}$ -defensins block adenovirus uncoating to neutralize infection*. J Virol, 2010. **84**(8): p. 4041-9.
251. Orzalli, M.H., et al., *cGAS-mediated stabilization of IFI16 promotes innate signaling during herpes simplex virus infection*. Proc Natl Acad Sci U S A, 2015. **112**(14): p. E1773-81.